UNIVERSIDAD DE CÁDIZ
FACULTAD DE CIENCIAS DEL MAR Y AMBIENTALES

VARIABILIDAD ESPACIO-TEMPORAL DEL SISTEMA DEL CARBONO INORGANICO EN ZONAS COSTERAS

Mercedes de la Paz Arándiga

Cádiz, 2007

Esta Tesis Doctoral ha sido realizada dentro del Grupo de Investigación consolidado del Plan Andaluz de Investigación *Oceanografía y Contaminación Litoral* (RNM 0144). La presente Tesis ha sido realizada gracias a la concesión de una Beca de Formación del Personal Investigador de la Universidad de Cádiz. El trabajo experimental ha sido financiado a través de los siguientes proyectos: CTM 2005-01364MAR, REN2001-3577/MAR y por el convenio de investigación nº 8 del PICOVER.

Memoria presentada por Mercedes de la Paz Arándiga para optar al grado de Doctor por la Universidad de Cádiz

Mercedes de la Paz Arándiga

D. JESÚS M. FORJA PAJARES, Profesor Titular del Departamento de Química Física de la Universidad de Cádiz y D. ABELARDO GÓMEZ PARRA, Catedrático del Departamento de Química-Física de la Universidad de Cádiz, como sus directores

HACEN CONSTAR:

Que esta Memoria, titulada **"Variabilidad espacio-temporal del sistema del carbono inorgánico en zonas costeras"**, presentada por Dª. Mercedes de la Paz Arándiga, resume su trabajo de Tesis y, considerando que reúne todos los requisitos legales, autorizan su presentación y defensa para optar al grado de Doctor en Ciencias del Mar por la Universidad de Cádiz

Cádiz, Julio de 2007

Dr. Jesús M. Forja Pajares

Dr. Abelardo Gómez Parra

Índice

Capitulo 1

Introducción, objetivos, zonas de estudio y organización de la tesis

1. Introducción

1.1. Los océanos y el calentamiento global

El dióxido de carbono (CO_2), el oxido nitroso (N_2O) y el metano (CH_4) son gases presentes en la atmósfera a nivel de trazas y contribuyen a la situación actual del clima en la Tierra (IPCC, 2001; WMO, 2003), ya que suponen el 88% de la capacidad de absorción de radiación en la atmósfera (Houghton et al, 1990). Este conjunto de gases se conoce comúnmente por "gases invernadero", ya que tienen la capacidad de absorber y radiar energía en la franja infrarroja del espectro electromagnético. Sin la presencia de estos gases en la atmósfera, la temperatura del planeta Tierra oscilaría en un intervalo comprendido entre -18 y -33 ºC (Mackenzie 1999, Houghton 2005). Sin embargo, a partir del siglo XVIII existe un paulatino incremento en la atmósfera de la concentración de estos gases invernadero (especialmente CO_2 y CH_4) como consecuencia del impacto derivado de actividades del hombre. El efecto mas notorio del fenómeno conocido como "calentamiento global" es el aumento en la temperatura media del planeta Tierra (~0.6 ºC en los últimos 30 años, IPCC 2001).

Desde comienzos de la revolución industrial ha existido un aumento dramático de la concentración de CO_2 en la atmósfera. A este periodo de tiempo se conoce con el nombre de Antropoceno, precisamente por la influencia que la actividad humana esta teniendo sobre los ciclos biogeoquímicos y el clima. Esta evolución puede observarse en la figura 1.1. Los valores experimentales de los últimos 50 años corresponden a medidas directas de la concentración de CO_2 en distintas estaciones de observación (e.g., Mauna Loa), y puede observarse la existencia de un aumento general de aproximadamente 1.4 ppm de CO_2 al año. Los valores anteriores a 1950 se han obtenido a partir del análisis de las burbujas de aire atrapadas en testigos de hielo, fundamentalmente tomados en la Antártida y Groenlandia (Petit et al., 1999). Este aumento es consecuencia de la actividad humana, principalmente la utilización de combustibles fósiles, aunque también contribuye la disminución de la masa forestal y de la extensión de zonas vírgenes en relación con las prácticas agrícolas. Como consecuencia de este impacto, la concentración de CO_2 atmosférico ha aumentado unos 100 ppm, desde los 280 ppm en la época

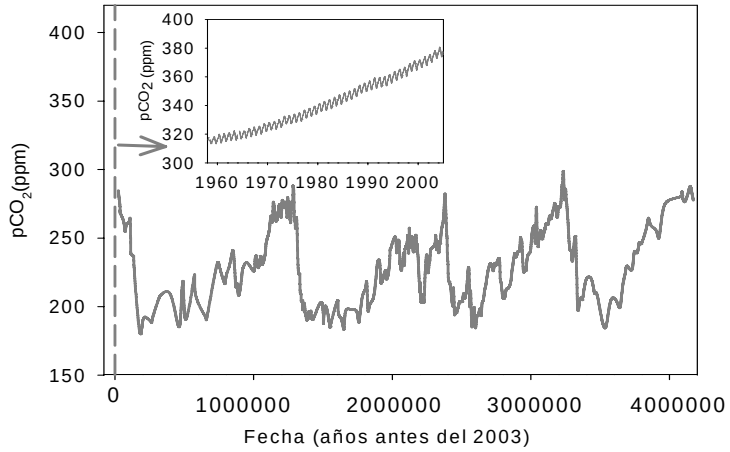

Figura 1.1. Evolución de la concentración de CO_2 en la atmósfera en tiempo geológico (datos CO_2 del testigo de hielo de Vostock, Polo Antártico. En la figura reducida, evolución de CO_2 en la atmósfera en el Observatorio de Mauna Loa (Hawaii, EEUU) desde el 1958 hasta 2004.

preindustrial hasta los 380 ppm registrados en la actualidad. Esto supone una tasa de crecimiento entre 10 y 100 veces mayor que en los últimos 420000 años. (Fig 1.1)

A pesar de que las series temporales de valores experimentales son cruciales para confirmar cualquier cambio relacionado con la actividad humana, en la actualidad existen evidencias notables, reflejadas en la cada vez más abundante literatura sobre el impacto del calentamiento global en el funcionamiento de diversos ecosistemas. Se está empezando a hacer un esfuerzo internacional por intentar disminuir las emisiones de CO_2 y otros gases con efecto invernadero a la atmósfera. Sin embargo, los combustibles fósiles constituyen la fuente primaria de energía y calor en el mundo industrial, y una reducción en las emisiones de CO_2 está acoplada necesariamente a importantes inversiones económicas en la optimización del uso de estos combustibles y en el desarrollo de otras energías menos contaminantes.

Los océanos en su conjunto regulan el clima del Planeta mediante un intercambio continuo con la atmósfera de calor y gases con efecto invernadero. En la actualidad, estos procesos de intercambio se conocen solamente de una forma aproximada. La cantidad de carbono inorgánico contenida en los océanos es aproximadamente unas 50 veces mayor que la existente en la atmósfera, mientras que la superficie terrestre, incluyendo la biota y el carbono fósil, posee unas tres veces más carbono inorgánico que la atmósfera. Por esta razón, la concentración de CO_2 en la atmósfera se encuentra fuertemente controlada por el intercambio con estos depósitos activos. De hecho, la concentración de CO_2 en la atmósfera aumenta a una velocidad anual de 3×10^9 t C, que corresponde solamente a la mitad de las emisiones producidas en la utilización de combustibles fósiles.

En la biosfera terrestre, el principal mecanismo que se encarga de bombear CO_2 es la producción neta del ecosistema, sin embargo, es el mas difícil de cuantificar debido a la gran heterogeneidad de las superficie terrestre.

La capacidad de los océanos en su conjunto para capturar parte de las emisiones antropogénicas de CO_2 estas controlada fundamentalmente por tres mecanismos que contribuyen a captar y transportar CO_2 desde la superficie a aguas profundas, y así alejarlos de un retorno a corto plazo a la atmósfera. Estos mecanismos son:

- *La bomba química:* se basa en la interacción del CO_2 atmosférico con el ión HCO_3^- y con el CO_3^{2-}, y la capacidad tampón del océano, que puede ser evaluada mediante el factor de Revelle (Zeebe y Wolf-Gladrow, 2001)
- *La bomba de solubilidad*: controlada por la temperatura, y que muestra su mayor eficiencia en la captación de CO_2 atmosférico en latitudes altas. Esta tiene sus efectos a escala local y regional; por ejemplo la pCO_2 en las aguas superficiales disminuye en invierno, debido a que el descenso de 1 ºC provoca un aumento medio del 4% en el coeficiente de solubilidad del CO_2.

Estos dos procesos están acoplados y en la literatura relativa al papel de los océanos reciben el nombre de *bomba física*.

- *La bomba biológica*: se basa en la actividad fotosintética del fitoplancton, que fija CO_2 atmosférico en la capa fótica y entra a formar parte de la cadena trófica. Existe por tanto una conversión de carbono inorgánico a carbono orgánico particulado. A medida que este carbono particulado cae por la columna de agua, se libera de nuevo carbono inorgánico en las aguas intermedias y profundas, bien debido a la oxidación bacteriana de los tejidos orgánicos, o a la disolución del carbonato cálcico biogénico. Estos procesos de regeneración de carbono continúan en los sedimentos superficiales, y finalmente parte del carbono

particulado, tanto orgánico como inorgánico, queda preservado en los sedimentos marinos.

Sabine et al. (2004) propone un balance global de CO_2 antropogénico donde se estima la capacidad de captación del océano, desarrollado a partir de la recopilación de 9618 medidas experimentales de CID en el océano. La actividad humana (consumo de combustibles fósiles, producción de cemento y cambios en los usos del suelo) suponen un fuente de 7.10 Pg C $año^{-1}$, de los que 3.25 Pg C $año^{-1}$ se acumulan en la atmósfera, 1.85 Gt C $año^{-1}$ se almacena en el océano, y se cierra el balance con un sumidero de 1.95 Gt C $año^{-1}$ por parte de la biosfera terrestre (Tabla 1.1).

Tabla 1.1 Balance de CO_2 antropogénico entre 1980 y 1999. Adaptado de Sabine et al. (2004). Los flujos se han sumado para el periodo 1980 y 1999, expresados en PgC (10^{15} gC).

Fuentes y sumideros de CO_2	**1980-1999**
(1) Emisiones procedentes del consumo de combustibles fósiles y producción de cemento	117 (±5)
(2) Emisiones derivadas de la deforestación	24 (±9)
(3) Almacenamiento en la atmósfera	-65 (±1)
(4) Captación y acumulación en el océano	-37 (±8)
Balance terrestre neto inferido	
(5) Captación de la biosfera terrestre = - (1) – (2) – (3) – (4)	-39 (±18)

Hay que resaltar que en la mayoría de los balances globales de carbono, las zonas costeras no se tienen en cuenta debido a su complejidad y heterogeneidad. La variabilidad espacial y temporal de los flujos de CO_2 en las aguas superficiales costeras es muy elevada, haciendo difícil su integración en los modelos globales

1.2. Química del carbono inorgánico en el agua de mar

El dióxido de carbono, a diferencia de los otros gases atmosféricos mayoritarios, no sólo se disuelve sino que reacciona con el agua dando lugar a cuatro especies distintas: CO_2 en su forma acuosa ($CO_{2\ (aq)}$), acido carbónico (H_2CO_3), bicarbonato (HCO_3^-) y carbonato (CO_3^{2-}). De todas ellas, los iones bicarbonato y carbonato son los mas abundantes, y constituyen el 99% del carbono inorgánico presente en los océanos (Wanninkhof y Feely, 1998).

El estudio termodinámico del sistema del carbono inorgánico en el agua de mar permite establecer la distribución de especies en el equilibrio y predecir sus cambios en función de la temperatura, presión y composición química de la disolución.
Las reacciones en las que interviene el dióxido de carbono en el agua de mar se pueden representar por el siguiente conjunto de equilibrios:

$$CO_{2(g)} \xleftrightarrow{K_0} CO_{2(ac)} \tag{1.1}$$

$$CO_{2(ac)} + H_2O \xleftrightarrow{K_H} H_2CO_3 \tag{1.2}$$

$$H_2CO_3 \xleftrightarrow{K_1} HCO_3^- + H^+ \tag{1.3}$$

$$HCO_3^- \xleftrightarrow{K_2} CO_3^{2-} + H^+ \tag{1.4}$$

La constante de hidratación del acido carbónico (K_H) tiene un valor relativamente bajo, del orden de 10^{-3}, y por lo tanto menos del 0.3 % del dióxido de carbono disuelto se encuentra como acido carbónico a la salinidad y pH del agua de mar. En la determinación de la constantes de disociación, no se puede diferenciar analíticamente entre y $CO_{2(ac)}$ y H_2CO_3, con lo cual se usa la suma sus concentraciones, y que de aquí en adelante nombraremos $CO_{2(ac)}$. De esta forma los equilibrios 1.2 y 1.3 se pueden reformular como:

$$CO_{2(ac)} + H_2O \xleftrightarrow{K1L} HCO_3^- + H^+ \tag{1.5}$$

Las constantes de equilibrio de las anteriores reacciones son las siguientes:

$$K_0 = [CO_{2(ac)}] / pCO_2 \quad (1.6)$$

$$K_{1L} = [HCO_3^-] [H^+] / [CO_2] \quad (1.7)$$

$$K_2 = [CO_3^{2-}] [H^+] / [HCO_3^-] \quad (1.8)$$

donde K_0 es la solubilidad del CO_2, y K_1 y K_2 la primera y segunda constante de disociación del carbónico, respectivamente. Estas tres constantes "aparentes" se definen como cociente de concentraciones y dependen de la salinidad, la temperatura y la presión.

La expresión mas usada de la solubilidad del dióxido de carbono en el agua de mar es la propuesta por Weiss (1974):

$$\text{Ln } K_0 = -60.241 + 93.452\,(100/T) + 23.359 \ln (T/100) + \quad (1.9)$$
$$+ S\,[0.0235 - 0.0237(T/100) + 0.00470\,(T/100)^2]$$

donde K_0 está expresado en moles kg^{-1} atm^{-1}, T es la temperatura absoluta y S la salinidad.

Existen un considerable numero de expresiones empíricas para el calculo de las constantes de disociación del acido carbónico en el agua mar, determinadas en diferentes medios (agua de mar artificial o natural) y en distintas escalas de pH. Se puede encontrar una relación detallada de sus expresiones matemáticas en DOE (1994) o en Zeebe y Wolf-Gladrow (2001). A pesar de que las diferencias entre los valores de las distintas constantes propuestas por diferentes autores no son muy grandes, la utilización de unas u otras produce grandes variaciones en los valores de los distintos parámetros del CO_2. Así pues, en la presente Tesis han sido utilizadas diversos set de constantes (Lueker et al., 2000 y Cai y Wang, 1998) en función de la escala de pH, y de la naturaleza del medio acuoso.

La expresión propuesta por Cai y Wang (1998) y específica para aguas estuáricas se define como:

$$\log_{10} K_1 \text{ Cai} = - 0.071692 (200.1 / T + 0.3220) S^{0.5} + 0.0021487 (200.1/ T + 0.3220) S +3404.71 / T +0.032786 T - 14.8435 \quad (1.10)$$

$$\log_{10} K_2 \text{ Cai} = - 0.3191 (-129.24/T + 1.4381) S^{0.5} + 0.0198 S + 2902.39/T + 0.02379 * T - 6.4980 \quad (1.11)$$

La expresión para K_1 y K_2 prepuestas por Luecker et al. (2000) son una reformulación para la escala Total basada en las constantes propuestas por Mehrbach et al. (1973). Se expresan como:

$$\log_{10} K_1 = 3633.86. / T - 61.2172 + 9.6777 \ln T - 0.011555 S + 0.0001152 S^2 \quad (1.12)$$

$$\log_{10} K_2 = 471.78 / T + 25.9290 - 3.16967 \ln T - 0.01781 S + 0.0001122 S^2 \quad (1.13)$$

donde S es la salinidad y T es la temperatura en ºk, tanto para las expresiones propuestas por Cai y Wang (1998), como para las de Luecker et al. (2000).

1.2.1. Parámetros experimentales para el estudio del sistema del carbónico

El conjunto de ecuaciones 1.1 a 1.13 constituyen la base para el cálculo de la especiación del sistema del carbono inorgánico. Las concentraciones de las distintas especies del sistema del carbónico (CO_2, HCO_3^-, CO_3^{2-}) no se pueden medir directamente. Sin embargo, se pueden obtener a partir de los valores de parámetros experimentales (pH, pCO_2, CID y AT) y la utilización de constantes aparentes de equilibrio. Para caracterizar el sistema del carbónico son necesarios al menos dos de estos cuatro parámetros.

a) El carbono inorgánico disuelto (CID) se define como:

$$CID = [CO_2] + [HCO_3^-] + [CO_3^{2-}] \quad (1.14)$$

La contribución relativa de cada una de las especies es 90:9:1 para $[HCO_3^-]$, $[CO_3^{2-}]$ y $[CO_2]$ respectivamente. Por esto, el CO_2 que se ve envuelto en el intercambio agua-atmósfera es una parte minoritaria del CID total. La determinación del CID se realiza por medio de técnicas culombimétricas (Jhonson, 1993; DOE, 1994).

b) La alcalinidad total (AT) se define como "el numero de moles de ión hidrogeno equivalentes al exceso de aceptores de protones (bases formadas a partir de ácidos débiles con una constante de disociación $K < 10^{-4.5}$ a 25 ºC) sobre donadores de protones (ácidos con $K > 10^{-4.5}$) en un kilogramo de muestra" (Dickson, 1981). En el agua de mar, considerando los principales equilibrios acido-base presentes, la AT se puede formular como:

$$\begin{aligned} AT = {} & \left[HCO_3^-\right] + 2\left[CO_3^{2-}\right] + \left[B(OH)_4^-\right] + \left[HPO_4^{2-}\right] + 2\left[PO_4^{3-}\right] + \left[SiO(OH)_3^-\right] + \\ & + \left[NH_3\right] + \left[HS^-\right] + 2\left[S^{2-}\right] + \left[OH^-\right] - \left[HSO_4^-\right] - [HF] - \left[H_3PO_4\right] - \left[H^+\right] \end{aligned} \quad (1.15)$$

La alcalinidad total es una magnitud experimental, que ha sido utilizada ampliamente junto con el pH para establecer la especiación del carbono inorgánico disuelto en aguas oceánicas.

La alcalinidad total es un parámetro que tradicionalmente se ha considerado conservativo en los estudios de mezcla de las masas de agua oceánicas (Goyet y Brewer, 1993). Sin embargo, en ambientes costeros y especialmente en estuarios, pueden ocurrir numerosas reacciones que afectan a la AT, debido a la producción o consumo de ácidos o bases. La amonificación, la desnitrificación, la reducción de Mn^{4+}, Fe^{3+} y SO_4^{2-}, son algunas de las reacciones que aumentan la alcalinidad total mediante un consumo de protones, mientras que otros procesos, como le nitrificación producen una disminución de la AT.

tras reacciones como la fotosíntesis/respiración o la disolución/precipitación de carbonato cálcico, también afectan al valor de la AT.

En la actualidad el método mas recomendado para la medida de la alcalinidad total es la valoración potenciométrica (DOE, 1994). En la presente Tesis, el método utilizado para la obtención del punto de equivalencia se basa en la aplicación de la función de Gran a la parte ácida de la curva de valoración.

c) El pH de las aguas naturales constituye una variable maestra para la descripción de los distintos sistemas ácido-base presentes en el medio. A pesar de su relevancia, es uno de los conceptos más confusos en el área de la Química Marina debido a que en la actualidad se usan simultáneamente tres escalas de pH en agua de mar: la escala "Libre", la escala de "Concentración Total del Ion Hidrógeno", y la escala del "Agua de Mar" (SWS). La diferencia entre las escalas se debe fundamentalmente a la naturaleza de las disoluciones reguladoras usadas para la calibración (principalmente en sulfato y fluoruro). Además, la escala NBS (National Boureau of Standars), definida para medios con baja fuerza iónica, es la mas apropiada para medidas en aguas estuáricas, fluviales y subterráneas. Para el agua de mar, la escala que actualmente tiene un mayor consenso internacional es la "Total". Con objeto de evitar errores asociados la deriva de los electrodos y a las variaciones en los potenciales de difusión, cada vez son más los oceanógrafos que utilizan métodos espectrofotométricos para la medida del pH (Clayton y Byrne, 1993).

d) Presión parcial del dióxido de carbono (pCO_2) en el agua de mar:

$$pCO_2 = K_0 \cdot [\, CO_{2\,(ac)}] \qquad (1.16)$$

donde K_0 es la constante de solubilidad.

Dado el comportamiento no ideal del CO_2, se debe usar la fugacidad en lugar de la presión parcial, así:

$$fCO_2 = f \cdot pCO_2 \qquad (1.17)$$

donde f es un coeficiente que tiene en cuenta la no-idealidad del CO_2. Sin embargo, generalmente se suele asumir que el CO_2 se comporta como un gas ideal, pues el error que se comete en las condiciones usuales de operación (presion total ~1 atm, pCO_2 entre 200 y 1500 μatm y temperatura de 0 a 30 ºC) es inferior al 0.5% (Murphy, 1996).

El principio de la medida del CO_2 se basa en equilibrar una fase gaseosa con el agua de mar, y la posterior determinación de la fracción molar de la fase gaseosa. Como el equilibrio agua-atmósfera del dióxido de carbono, depende de la temperatura y la presión a la que se realiza, es necesario conocer el valor de estas variables en el proceso de equilibración. En oceanografía suelen utilizarse equipos de medida de pCO_2 en continuo que se basan en diseños diferentes (Takahashi, 1961; Goyet y Peltzer, 1994; Kortzinger et al., 1996). Para el trabajo de campo desarrollado en esta tesis, se construyó un equipo a semejanza del desarrollado por el grupo de Oceanología del Instituto de Investigaciones Marinas (CSIC, Vigo) y similar al descrito por Koertzinger et al. (1996).

1.2.2. Precipitación /disolución del $CaCO_3$

Generalmente el agua de mar esta sobresaturada con respecto a la formación de carbonato cálcico (calcita o aragonito). El grado de saturación del $CaCO_3$ (Ω) se define como:

$$\Omega = ([Ca^{2+}] [CO_3^{2-}])/ K_{sp} \qquad (1.18)$$

donde K_s es el producto de solubilidad del $CaCO_3$, y $[Ca^{2+}]$ y $[CO_3^{2-}]$ son las concentraciones del ión calcio y carbonato respectivamente. Valores de Ω >1

corresponde a la sobresaturación (implica que la precipitación espontánea esta favorecida termodinámicamente) y por el contrario valores de $\Omega < 1$ representa condiciones de subsaturación de $CaCO_3$ (se ve favorecida termodinámicamente la disolución). El producto de solubilidad (K_{sp}) en este estudio se obtuvo a partir de la expresión propuesta por Mucci (1983) para la calcita y aragonito respectivamente:

$$\log K_{calcita} = -171.9065 - 0.077993\,T + 2839.319 / T + 71.595 \log T + (-0.77712 + 0.0028426\,T + 178.34 / T)\,S^{0.5} - 0.07711\,S + 0.0041249\,S^{1.5} \quad (1.19)$$

$$\log K_{aragonito} = -171.945 - 0.077993\,T + 2903.293 / T + 71.595 \log T + (-0.068393 + 0.0017276\,T + 88.135 / T)\,S^{0.5} - 0.10018\,S + 0.0059415\,S^{1.5} \quad (1.20)$$

La precipitación puede estar inducida por organismos planctónicos marinos (cocolitoforidos, foraminíferos, pteropodos) o bien por organismos bentónicos. (foraminiferos, corales, moluscos). Por cada mol de $CaCO_3$ que precipita, un mol de CO_2 es liberado en aguas continentales. En agua de mar depende de la capacidad buffer del sistema, y en promedio tiene un valor de 0.6 (Frankignoulle et al., 1995), lo que significa, que por cada mol de $CaCO_3$ que precipita, 0.6 moles de CO_2 son liberados al medio. Sin embargo en muchas zonas, la liberación de protones producida por la degradación aerobia de la materia orgánica induce a la disolución de carbonatos según la reacción:

$$CaCO_3 + CO_2 + H_2O \Leftrightarrow Ca^{2+} + 2\,HCO_3^- \quad (1.21)$$

1.3. Las zonas costeras

1.3.1. Características de las zonas costeras

Las zonas costeras son el nexo de unión entre el continente y el océano abierto. Además, soportan un intenso intercambio de nutrientes, materia orgánica disuelta y

particulada, contaminantes y sólidos en suspensión con los compartimentos adyacentes. La definición mas usada establece que el límite entre la zona costera y el océano está marcado por el cambio batimétrico que se produce entre la plataforma y el talud continental, y actualmente se ha fijado arbitrariamente en una profundidad de 200 m.

El intenso debate científico a cerca del papel de los márgenes continentales en el ciclo global del carbono, se debe en parte a las incongruencias en la definición de sus límites. Dadas las especiales características de las zonas costeras, se han sucedido en el tiempo numerosos intentos de establecer una definición precisa de su extensión. Una de las definiciones mas amplias es la propuesta por el grupo internacional de trabajo del IMBER (*Integrated Marine Biogeochemistry and Ecosystem Research*) y que considera a las zonas costeras: "...la región que está dominada por los procesos que resultan de la interacción entre las fronteras continente-océano. Por tanto su dimensión exacta varía en función de la disciplina de estudio o del elemento químico de interés", Hall et al. (2004). Este concepto de zonas costeras hace que su extensión se pueda ampliar significativamente hacia mar abierto en casos de estudio como el de los jets o filamentos costeros.

Otros autores, como Rabouille et al. (2001), decidieron abordar el estudio de las zonas costeras subdividiéndola en dos partes, para así poder caracterizar mejor los procesos biogeoquímicos en cada una de las regiones. Estas fueron definidas como: "zona costera próxima" que incluye bahías, parte externa de los estuarios, deltas, mares interiores y marismas, con una superficie total de $1.8\ 10^6$ km^2, y una profundidad media de 20 m. Esta zona se considera como un compartimento único y homogéneo donde producción y respiración tienen lugar simultáneamente. La otra región es la "zona costera distal" que incluye la plataforma continental hasta 200 m de profundidad y con una superficie total de $27\ 10^6$ km^2, y una profundidad media de 130 m. Esta zona esta dividida en dos compartimentos, la zona superficial de la columna de agua, dominada por

la producción primaria y la zona mas profunda la columna de agua, dominada por los procesos de remineralización. La tasa de sedimentación en la zona costera distal es 10 veces menor que en la zona costera próxima. A pesar de todo, en cualquiera de sus definiciones, las zonas costeras son el lugar donde continente, atmósfera y océano convergen e interaccionan.

A pesar de que las zonas costeras constituyen sólo un 7 % de la superficie de los océanos, en ellas se almacenan un 70-75 % de los aportes terrígenos al océano. Además, entre el 30-50% del carbono inorgánico y el 80% del carbono orgánico que accede a los sistemas costeros, y entre el 10y el 30 % de la productividad primaria del océano se acumula en estas zonas (Mackenzie et al., 2004)

Por otra parte, estos sistemas están sujetos a una fuerte presión humana, en especial los estuarios y la plataforma continental más próxima a tierra. Esto tiene que ver con la alta densidad de población que soporta (60% de la población mundial), junto con los vertidos industriales y de la agricultura, y las actividades de recreo. El fuerte aumento de estas actividades en el último siglo provoca una degradación severa de la calidad del agua, alteraciones en la estructura de las cadenas tróficas y en la composición de las comunidades. En los últimos 50 años, los aportes de materiales tanto naturales como sintéticos desde ambientes terrestres hacia las zonas costeras han aumentado en un factor de 1.5 a 2 como consecuencia de la actividad humana (Meybeck y Ragu, 1995). Sin embargo, se espera que los mecanismos naturales de control de los sistemas litorales sean lo suficientemente efectivos para dispersar los efectos de estas perturbaciones y prevenir la acumulación de “contaminantes”. Pero, la cuestión es hasta qué punto y escala de tiempo serán capaces las zonas de litorales de asimilar estas perturbaciones antes de que se sobrepase esa capacidad natural de regulación del sistema?. En la actualidad el método mas factible para evaluar esta cuestión a nivel global quizás sea el

uso de simulaciones numéricas (Rabouille et al., 2001), para las cuales será necesario disponer de amplias bases de datos de experimentales en estas zonas.

1.3.2. El ciclo del carbono en las zonas costeras

La modelización de los flujos de carbono inorgánico entre compartimentos ambientales es fundamental para la comprensión del ciclo biogeoquímico del C en las zonas litorales. La principal dificultad que existe para establecer el ciclo del C en estas zonas es la enorme variabilidad que presentan. A diferencia del océano, donde pueden aplicarse distintas aproximaciones debido a su comportamiento más homogéneo, los principales flujos de C que intervienen en las zonas litorales sólo se han estimado, de forma muy aproximada. En la figura 1.2 se muestra el ciclo propuesto por Ver et al. (1999), que incluye los principales procesos que constituyen el ciclo del carbono en las zonas costeras.

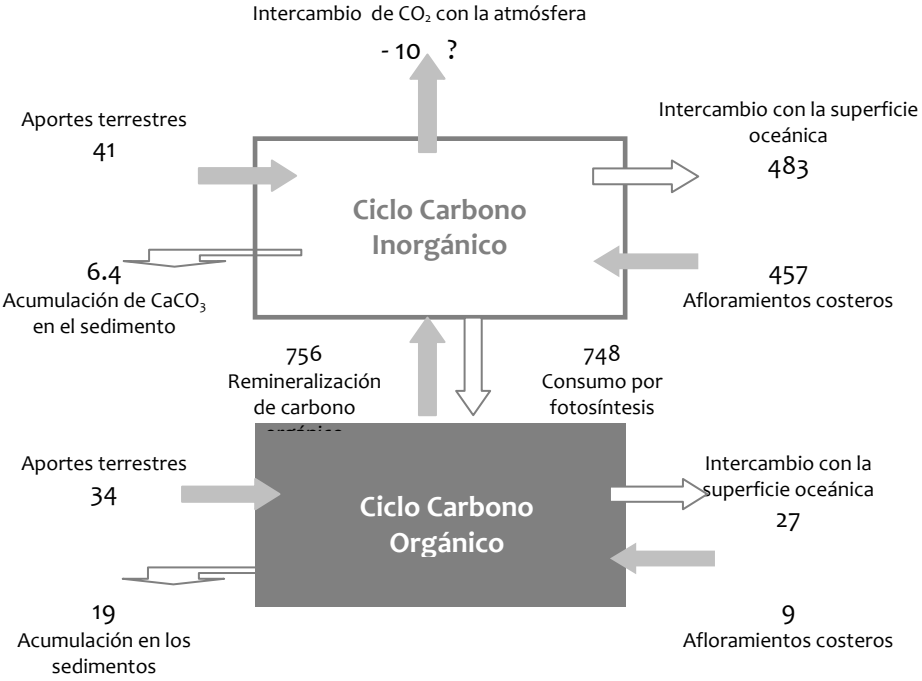

Figura 1.2. Ciclo del carbono en las zonas costeras propuesto para el año 1995 por Ver et al. (1999). Las unidades de los flujos son 10^{12} mol C $año^{-1}$.

Las principales entradas de carbono inorgánico a las zonas costeras son los aportes continentales de C inorgánico a través de los ríos, aguas subterráneas o escorrentías, así como la entrada de aguas profundas en los afloramientos costeros. Los principales flujos de salida de C inorgánico corresponden al transporte neto de agua desde las zonas costeras, la deposición y acúmulo de carbonato cálcico biogénico en los sedimentos y el consumo de CO_2 por fotosíntesis. Los principales flujos que existen en el ciclo del C en las zonas litorales son el consumo de C por fotosíntesis y la mineralización del carbono orgánico. Estos dos procesos constituyen a su vez los puntos de acoplamiento entre los ciclos del C inorgánico y orgánico. De manera análoga al C inorgánico, las principales entradas de C orgánico a los sistemas costeros son vía aportes continentales y afloramientos.

Los sistemas litorales intercambian carbono inorgánico y orgánico con los océanos a través de los afloramientos costeros y al intercambio con la superficie de los océanos inducidos por las mareas. Las salidas de C netas hacia el océano son superiores a las entradas (figura 1.2), ya que los sistemas litorales además de una zona de acumulación de carbono actúan como zona de tránsito entre los continentes y los océanos para todos los elementos que tienen un origen continental.

En la figura 1.2. se puede observar como la magnitud relativa de aportes continentales, la fotosíntesis, el almacenamiento en los sedimentos y el intercambio con el océano determinan fundamentalmente el balance de carbono en las zonas costeras, y por tanto el papel que éstas desempeñan como fuente o sumidero de CO_2 a la atmósfera.

En la actualidad, el debate a cerca del ciclo del carbono en las zonas costeras se centra en el estado trófico (balance producción / respiración en el ecosistema) y en el papel de las zonas costeras como fuente o sumidero de CO_2 a la atmósfera.

Llegados a este punto es conveniente considerar el concepto de producción neta del ecosistema: Un ecosistema se define autotrófico cuando la producción neta del ecosistema es positiva, es decir que la producción primaria bruta es mayor que respiración. Asimismo, un ecosistema será heterotrófico cuando la respiración sobrepase a la producción (Odum, 1956). Sin embargo, a pesar de que la literatura puede a veces ser confusa, el hecho de que un sistema sea autotrófico no implica necesariamente que se comporte como sumidero de CO_2, ya que el flujo neto de CO_2 depende principalmente del gradiente de concentraciones entre la superficie del agua y la atmósfera. Así por ejemplo, las zonas de afloramiento costeros son autotróficas y sin embargo son fuentes de CO_2 a la atmósfera debido a las altas concentraciones de CO_2 en las aguas profundas que emergen. Gattuso et al. (1998), a partir de una recopilación de los datos disponibles concluyeron que las zonas costeras mas próximas al continente, que están directamente influenciadas por los aportes de C orgánico, son fundamentalmente heterotróficas, y por tanto actúan como fuente de CO_2 a la atmósfera. Sin embargo, la plataforma continental se comporta como autotrófica debido a que sufren una menor influencia de los aportes continentales y una mayor exportación de C a los sedimentos. Esta hipótesis fue confirmada posteriormente por Tsunogai et al. (1999) y Chen et al. (2003) con una base de datos mayor, mostrando así que la plataforma continental a nivel global actúa como un sumidero de CO_2 atmosférico.

Además de la bomba biológica y la bomba de física como mecanismos de captación de CO_2 en aguas oceánicas y costeras, Tsunogai et al. (1999) observó la existencia de un mecanismo de captación de CO_2 exclusivo de la plataforma continental. Este mecanismo ha sido observado en sistemas que presentan una estratificación estacional. Este fenómeno consiste en que el enfriamiento del agua superficial favorece la formación de aguas más densas, que junto con un aumento de la solubilidad del CO_2 y la actividad fotosintética aceleran la absorción de CO_2 en estas zonas. Este CO_2 transformado en materia orgánica es transportado a aguas más profundas, donde es degradado a carbono

inorgánico y posteriormente exportado hacia el océano abierto. Este mecanismo es de gran relevancia como sumidero de CO_2 cuando se extrapola a la extensión total de la plataforma continental mundial.

Sin embargo los sistemas costeros más próximos al continente presentan generalmente un comportamiento opuesto. Los estuarios son sistemas heterotróficos (Gattuso et al., 1998) con capacidad de emitir grandes cantidades de CO_2 a la atmósfera, llegando a presentar concentraciones de hasta 9425 μatm, como es el caso del estuario del río Escalda (en inglés Scheldt), que es uno de los mas eutrofizados de Europa (Borges, 2005). Recientemente han sido publicadas varias recopilaciones de datos de CO_2 en diversos sistemas costeros (Ducklow y McAllister, 2004; Borges, 2005; Borges et al., 2006, que inciden en la gran heterogeneidad de sistemas existentes, y la desproporcionada magnitud que alcanzan las emisiones de CO_2 en ciertos sistemas, especialmente en estuarios, manglares y marismas.

1.3.3. Las zonas costeras: ¿fuente o sumidero de CO_2 atmosférico?

El estudio de la química del CO_2 en el agua de mar comenzó hace unos 70 años (Buch et al., 1932; Greenberg et al., 1932), asimismo la medida de la pCO_2 en la superficie del océano despegó en el "Año Geofísico Internacional" (1957-1958). Desde entonces, la base de datos disponible se aproxima a un millón de medidas experimentales (Takahashi et al, 2002). Esto hace que los mecanismos de control del intercambio de CO_2 agua-atmósfera en el océano están relativamente bien delimitados. Por el contrario, el interés por el ciclo del carbono en las zonas costeras es relativamente reciente (20 años si tomamos como referencia los estudios de Smith y Mackenzie, 1987).

El océano en la época preindustrial se comportaba como una fuente moderada de CO_2 a la atmósfera (0.2-0.4 PgC año^{-1}; 1 Pg = 10^{15} g), si se consideran las estimaciones elaboradas por Smith y Mackenzie (1987) y Mackenzie et al. (2004). Sin embargo, el

océano en la actualidad actúa como un sumidero de CO_2 atmosférico a nivel global (3.25 PgC $año^{-1}$) debido al progresivo incremento en la concentración de CO_2 atmosférico desde el siglo XVIII, lo que ha producido un aumento en el gradiente de concentraciones de CO_2 océano-atmósfera (Sabine et al., 2004). No obstante, la identidad de las zonas costeras como fuente o sumidero de CO_2 atmosférico es una cuestión todavía sin resolver.

Para intentar resolver esta cuestión, se han llevado a cabo diversos intentos para integrar los flujos de CO_2 en zonas costeras basándose en medidas experimentales de CO_2:

A escala europea, Borges et al. (2006) estimó que la plataforma continental, excluyendo a los estuarios de este balance, actúan como un sumidero de CO_2, con un flujo del orden de -1.9 mol C m^{-2} $año^{-1}$, que supone 68.1 Tg C $año^{-1}$ (1Tg = 10^{12}g), cantidad próxima a la captación por parte de la biosfera terrestre (66.1 Tg C $año^{-1}$). Por otra parte, los estuarios actúan como una fuente de CO_2 a la atmósfera, con una emisión del orden de 67 Tg C $año^{-1}$, cercana al valor de la captación de las plataformas continentales. El principal inconveniente de esta estimación procede de la gran incertidumbre del área ocupada por los estuarios necesaria para la extrapolación.

A escala global, Borges (2005) estimó que las zonas costeras, excluyendo estuarios y marismas, actúan como un sumidero cercano a -1.2 mol C m^{-2} $año^{-1}$. Esto supondría un aumento del 24% de la capacidad de captación de los océanos. Pero si la parte interna de los estuarios y las marismas son incluidas en el balance, las zonas costeras actúan como una fuente de CO_2 a la atmósfera (0.38 mol C m^{-2} $año^{-1}$) y la capacidad de captación del océano a nivel global disminuiría en un 12 %. No obstante, Borges (2005) resalta que estas estimaciones hay que tomarlas con cautela y señaló las principales fuentes de incertidumbre que afectan sobremanera a la integración de los flujos de CO_2 en zonas costeras. Como ejemplo se pueden citar:

- La alta variabilidad espacial y estacional de la parte interna de los estuarios así como la gran incertidumbre en la superficie que ocupan.
- La gran imprecisión asociada a la velocidad de transferencia del CO_2 en las zonas costeras. En la actualidad esta velocidad de transferencia es parametrizada en función de la velocidad del viento, sin embargo en estuarios la velocidad de la corriente puede contribuir de forma significativa a la velocidad de transferencia y por tanto a los flujos de CO_2 (Zappa et al., 2003).
- El papel de las plumas estuáricas en el ciclo del C, debido fundamentalmente a la escasez de datos disponibles en estas zonas
- Escasez o ausencia de datos de CO_2 en ecosistemas muy activos desde el punto de vista biogeoquímico, como son los lagunas costeras, marismas o praderas de fanerógamas marinas

2. Objetivos

El objetivo general de esta Tesis es definir el ciclo del carbono inorgánico en distintos sistemas costeros del golfo de Cádiz, identificando en ellos los procesos que determinan principalmente su variación espacial y temporal y midiendo, en cada caso, el intercambio de carbono inorgánico con la atmósfera y con el entorno marino más próximo. Se pretendía con ello contribuir al aumento de la base de datos actualmente disponible sobre el funcionamiento de la zona costera, de manera que se consiga en su día integrarla en un modelo global que explique el ciclo del carbono inorgánico a escala oceánica.

De manera específica, este objetivo general puede desglosarse en los siguientes más específicos:

1º) Delimitar las variaciones espaciales de la concentración de carbono inorgánico en cada sistema con objeto de conocer su heterogeneidad y de localizar las fuentes de carbono al medio.

2º) Establecer la importancia de las variaciones temporales –mareales y estacionales- en la estructura del ciclo del carbono inorgánico.

3º) Cuantificar los intercambios de carbono inorgánico con las zonas marinas adyacentes y los flujos de dióxido de carbono a través de la interfase agua-atmósfera.

3. Zonas de estudio y toma de muestra

Se han seleccionados tres sistemas costeros de diferentes características hidrodinámicas y grado de confinamiento y que a su vez están afectados en grado muy diferente por aportes terrígenos de carbono inorgánico y materia orgánica, cuyas características se describen brevemente a continuación.

Estuario del Río Guadalquivir: Constituye la frontera geográfica entre las provincias de Huelva y Cádiz, es uno de los más importantes de la vertiente atlántica de la península Ibérica, con 108 km de longitud. La geología de su cuenca de drenaje es el principal responsable de la distribución de carbono inorgánico en el estuario, así como de su exportación hacia el océano Atlántico, que depende principalmente de las variaciones en la descarga del río.

Caño de marea del Río San Pedro: Aunque en la antigüedad era una de las bocas por las que desembocaba al mar el Río Guadalete, en la actualidad es un caño de marea en el que el principal mecanismo de intercambio de agua con ésta es la acción de las mareas. Aunque forma parte del Parque Natural de la Bahía de Cádiz, a lo largo de sus 12 km de

longitud, se distribuyen en sus márgenes diversas actividades del sector primario como son la acuicultura y la extracción de sal, así de naturaleza recreativa. Todas estas actividades hacen que la zona se encuentre en un continuo proceso de cambio.

Estrecho de Gibraltar: es el único punto de conexión entre el Mar Mediterráneo y el Océano Atlántico. Se caracteriza por la salida del agua mediterránea en profundidad, más densa y fría que la masa de agua Atlántica en superficie, la cual presenta un flujo neto hacia el Mediterráneo. A diferencia de la mayor parte de la plataforma continental del Golfo de Cádiz, en el que las mareas son un mecanismo secundario en el patrón general de circulación, en el Estrecho de Gibraltar, la escala de tiempo mareal es la que presenta una mayor variabilidad, debido a la coexistencia de diversos fenómenos ondulatorios, como son ondas internas o el salto hidráulico a consecuencia de la interacción de los flujos con la topografía del fondo del Estrecho. Estos fenómenos ondulatorios que en mareas vivas pueden alcanzar gran intensidad, tienen grandes implicaciones en los ciclos biogeoquímicos del Estrecho y en las aguas adyacentes del Mar de Alborán.

Tabla 1.2: Periodo de estudio de cada uno de los sistemas estudiados en la presente memoria así como los parámetros de análisis en cada uno: alcalinidad total (AT), carbono inorgánico disuelto (CID), oxigeno disuelto (OD), carbono orgánico disuelto (COD), Clorofila *a*, materia particulada en suspensión (MPS).

Zona de estudio	**Periodo**	**Variables medidas**
Estuario del Río Guadalquivir	2000-2003	AT, CID, pCO_2, pH OD, Chl-a, COD, MPS.
Caño del Río San Pedro	2004	AT, CID, pCO_2, pH OD, Chl-a, MPS.
Estrecho de Gibraltar	2003; 2005-2006	AT, CID, pCO_2, pH OD, Chl-a.

4. Estructura de la Tesis:

Esta Tesis se ha estructurado en cinco capítulos, un primero de introducción general y de acercamiento al tema de estudio, objetivos de la tesis y se presentan las zonas de estudio (1), tres capítulos donde se presentan el grueso de resultados y discusión (2-4), y un capitulo final de conclusiones (5). Cada uno de los capítulos de resultados y discusión (del 2 al 4) está compuesto por uno o dos trabajos de investigación y que han sido, bien publicados o están en revisión en revistas internacionales incluidas en el "Science Citation Index". Asimismo, para facilitar la lectura de los resultados obtenidos, en cada uno de los capítulos correspondientes se ha incluido una introducción y una breve descripción en español de los resultados obtenidos. los resultados obtenidos.

Bibliografía

Borges, A. V., 2005. Do We Have Enough Pieces of the Jigsaw to Integrate CO_2 Fluxes in the Coastal Ocean? Estuaries, 28 (1): 3–27.

Borges, A.V., Schiettecatte L.-S., Abril G., Delille B. and Gazeau F., 2006. Carbon dioxide in European coastal waters. Estuar. Coast. Shelf Sci., 70(3): 375-387.

Cai, W.-J., Wang, Y., 1998. The chemistry, fluxes, and sources of carbon dioxide in the estuarine waters of the Satilla and Altamaha Rivers, Georgia. Limnology and Oceanography 43 (4), 657 - 668.

Buch, K., Harvey, H. W., Wattenberg and Grinpberg, 1932. Uber das Kohlensauresystem im Meerwasser. Conseil Permanent International pour la Explration de la Mer, Repports et Proces- Verbaux, 79, 1-70.

Chen, C.T.A., Liu, K.K., Macdonald, R., 2003. Continental margin exchanges. In: Fasham, M.J.R. (Ed.), Ocean Biogeochemistry: A Synthesis of the Joint Global Ocean Flux Study (JGOFS). Springer-Verlag, Berlin, pp. 53e97.

Clayton, T.D. and R.H. Byrne. 1993. Spectrophotometric seawater pH measurements: total hydrogen ion concentration scale concentration scale calibration of m-cresol purple and at-sea results. Deep-sea research I, Vol. 40, 10, 2115-2129.

Dickson AG (1981) An exact definition of total alkalinity and a procedure for the estimation of alkalinity and total inorganic carbon from titration data. Deep-Sea Research 28A:609-623

DOE, 1994. In: Dickson, A.G., Goyet, C. (Eds.), Handbook of Methods for the Analysis of the Various Parameters of the Carbon Dioxide System in Seawater, Ver.2, ORNL/CDIAC-74.

Ducklow, H.W. y S. L. Mcallister. 2004. The biogeochemistry of carbon dioxide in the coastal oceans, in press, *En* K. H. Brink and A. R. Robinson (eds.), The Global Coastal Ocean—Multiscale Interdisciplinary Processes, Volume 13. Harvard University Press, Cambridge, Massachusetts.

Gattuso, J.-P., Frankignoulle, M. and Wollast, R., 1998. Carbon and carbonate metabolism in coastal aquatic ecosystems. Annual Review Ecology Systematics, 29: 405-433.

Goyet, C. y Brewer, P.G., 1993. Biochemical Properties of the Oceanic Carbon Cycle. En: Modeling Oceanic Carbon Interaction (J. Willebrand y D.L.T. Anderson, Eds.) NATO ASI Series, Springer Verlag, vol. I: 271-297.

Greenberg, D. M., Moberg, E.G. Allen, E., 1932. Determination of carbon dioxide and tritable base in sea water. Industrial and Engineering Chemistry Analytical Edition, 4, 309-313.

Houghton RA (2005) The contemporary carbon cycle. In: Schlesinger WH (ed) Biogeochemistry. Elsevier-Pergamon, Oxford, p 473-513

Houghton, J. T., G. J. Jenkins, and J. J. Ephraums, 1990 Climate Change, The IPCC Scientific Assessment, Cambridge University Press, New York.

Johnson, K.M., Wills, K.D., Butler, D.B., Johnson, W.K. y Wong, C.S., 1993. Coulometric total carbon dioxide analysis for marine studies: maximizing the performance of an automated gas extraction system and coulometric detector. Mar. Chem., 44: 167-187.

Körtzinger, A., Thomas, H., Schneider, B., Gronau, N., Mintrop, L., Duinker, J.C., 1996. At-sea intercomparison of two newly designed underway pCO_2 systems - Encouraging results. Mar. Chem., 52:133-145.

Lueker, T.J., Dickson, A.G. and. Keeling, C.D., 2000. Ocean pCO_2 calculated from dissolved inorganic carbon, alkalinity, and equations for K_1 and K_2 : validation based on laboratory measurements of CO_2 in gas and seawater at equilibrium. Marine Chemistry., 90 (105-119)

Mackenzie, F.T., Lerman, A., Andersson, A.J., 2004. Past and present of sediment and carbon biogeochemical cycling models. Biogeosciences 1 (1), 11-32.

Mehrbach, C., Culberson, C.H., Hawley, J.E. y Pytkowicz, R.M., 1973. Measurement of the apparent dissociation constant of carbonid acid in seawater at atmospheric pressure. Limnol. Oceanogr., 18: 897-907.

Meybeck M. and Ragu A. (1995) *Water Quality of World River Basins*. UNEP GEMS Collaborating Centre for Fresh Water Quality Monitoring and Assessment, United Nations Environment Programme.

Millero, F.J., 1995. Thermodynamics of the carbon dioxide system in the oceans. Geochim. Cosmochim. Acta 59, 661–667.

Mucci, A., 1983. The solubility of calcite and aragonite in seawater at various salinities, temperatures and one atmosphere total pressure. Am. J. Sci. 283, 780–799.

Murphy, P., 1996. The carbonate system in seawater: laboratory and field studies. PhD thesis, University of Washington.

Odum, H.T., 1956. Primary production in flowing waters. Limnology and Oceanography 1, 102–117.

Petit, J. R., J. Jouzel, D. Raynaud, N. I. Barkov, J.-M. Barnola, I. Basile, M. Bender, J. Chappellaz, M. Davis, G. Delaygue, M. Delmotte, V. M. Kotlyakov, M. Legrand, V. Y. Lipenkov, C. Lorius, L. Pépin, C. Ritz, E. Saltzman, and M. Stievenard, 1999, Climate and atmospheric history of the past 420,000 years from Vostok ice core, Antarctica, Nature, 399, 429-436.

Rabouille, C., Mackenzie, F.T. and Ver, L.M., 2001. Influence of the human perturbation of carbon, nitrogen, and oxygen biochemical cycles in the global coastal ocean. Geoquimica et Cosmoquimica Acta, Vol 65 (21), 3615-3641.

Sabine, C.L., Feely, R.A., Key, R.M., Lee, K., Bullister, J.L., Wanninkhof, R., Wong, C.S., Wallace, D.W.R., Tilbrook, B., Millero, F.J., Peng, T.H., Kozyr, A., Ono, T., Rios, A.F., 2004. The oceanic sink for anthropogenic CO_2. Science 305 (5682), 367 -371.

Smith SV, Mackenzie FT (1987) The ocean as a net heterotrophic system: implications from the carbon biogeochemical cycle. Global Biogeochemical Cycles 1:187-198

Takahashi, T., 1961. Carbon dioxide in the atmosphere and in the Atlantic ocean water. J. Geophys. Res., 66: 477-494.

Takahashi, T., Sutherland, S.C., Sweeney, C., Poisson, A.,Metzl, N., Tilbrook, B., Bates, N., Wanninkhof, R., Feely, R.A., Sabine, C., Olafsson, J., Nojiri, Y., 2002. Global sea–air CO2 flux based on climatological surface ocean pCO2, and seasonal biological and temperature effects. Deep-Sea Research II 49, 1601–1622.

Tsunogai, S.,Watanabe, S., Sato, T., 1999. Is there a ‘‘continental shelf pump’’ for the absorption of atmospheric CO_2? Tellus Series B 5 (3), 701-712.

Ver LMB, Mackenzie FT, Lerman A (1999) Biogeochemical responses of the carbon cycle to natural and human perturbations: Past, present, and future. American Journal of Science 299:762- 801

Wanninkhof, R. y Feely, R.A., 1998. fCO_2 dynamics in the Atlantic South Pacific and South Indian Ocean. Mar. Chem., 60: 15-31.

Weiss, R.F., 1974. Carbon dioxide in water and seawater, the solubility of a non-ideal gas. Mar. Chem. 2, 203–215.

Zeebe, R. E., and D. A. Wolf-Gladrow, CO_2 in Seawater: Equilibrium, Kinetics, Isotopes, 346 pp., Elsevier Sci., New York, 2001.

Capitulo 2

Sistema del carbono inorgánico en el estuario del Guadalquivir

Los estuarios son zonas de transición entre el océano y los continentes en los que el agua dulce procedente del drenaje terrestre, se mezcla con el agua de mar, lo que provoca importantes gradientes de las propiedades físico-químicas del medio. Reciben grandes cantidades de materia tanto disuelta como particulada, en la que es muy significativa el contenido de carbono orgánico e inorgánico, así como de nutrientes procedentes del drenaje terrestre. Los estuarios, se caracterizan por constituir sistemas altamente dinámicos, con una intensa actividad biológica y una elevada tasa de sedimentación y resuspension. En sus aguas, los aportes continentales pueden sufrir profundas transformaciones antes de alcanzar las zonas costeras adyacentes. A pesar de que la intensidad de los procesos biogeoquímicos señala a los estuarios como importantes focos de emisión de gases, el estudio de su interacción con la atmósfera es relativamente reciente ya que comienza a realizarse en la década de los 80.

Dada la especiales características de estos sistemas y, también por la trascendencia administrativa y económica que tiene el conocer sus limites (Elliot y McLusky, 2002), se han sucedido en el tiempo numerosos intentos de establecer una definición precisa de lo que debe entenderse por un estuario y hasta que lugar del cauce del río se extiende.

Una de las definiciones más amplias es la que propusieron Cameron y Pritchard (1936): *"Un estuario es un cuerpo de agua semicerrado en libre conexión con el mar abierto y, dentro del cual, el agua de mar está diluida de modo apreciable con agua dulce procedente del drenaje terrestre"*. El principal inconveniente de esta definición radica en que no precisa cual es límite superior, o fluvial del estuario. Este limite superior del estuario se define hasta donde llega la influencia mareal (Fairbridge, 1980), donde el régimen hidrodinámico y los procesos sedimentarios presentan diferencias drásticas a las que se encuentran aguas arriba en el río. El límite aguas abajo del estuario lo establece la forma que tiene la costa en la desembocadura.

Los estuarios presentan una gran diversidad en términos geomorfológicos, geoquímicos, superficie de su cuenca de drenaje, descarga fluvial, influencia mareal, todos ellos atributos físicos que afectan enormemente a los ciclos biogeoquímicos de nutrientes y carbono, así como a su gradiente longitudinal y al tiempo de residencia del agua en el estuario. Los aportes continentales a través de los ríos son una de las mayores fuentes de alcalinidad al mar y uno de los mecanismos fundamentales que controlan el estado de saturación del $CaCO_3$ en el océano (Sundquist, 1993). Una de las principales fuentes de alcalinidad y carbono inorgánico al agua de río es la erosión química del suelo, reacción que a nivel global supone una importante captación de CO_2 desde la atmósfera. Meybeck (1993), en una revisión bibliográfica acerca del transporte fluvial de carbono inorgánico, estimó que del total exportado al océano - 381 TgC $año^{-1}$ - el 65 % tienen un origen atmosférico. En cualquier caso, la cantidad total de C exportada por los ríos será una función de la litología cuenca de drenaje y del régimen de descarga del río.

Además de los aportes de alcalinidad procedentes del río, en el propio estuario existen dos mecanismos fundamentales que pueden actuar como una fuente de alcalinidad: 1) la disolución de carbonatos: que se produce cuando el CO_2 disuelto reacciona con las partículas de $CaCO_3$ generando HCO_3^- y Ca^{2+}; y 2) los procesos

diagenéticos de la materia orgánica en la zona anóxica de los sedimentos (especialmente reacciones de reducción del nitrato, sulfato, hierro o manganeso) (Abril y Borges, 2004). En el mismo sentido influye el hecho de que generalmente los estuarios sean sistemas heterotróficos, debido fundamentalmente a los continuos aportes de materia orgánica que reciben, ya sean procedentes de las actividades humanas en sus márgenes o de los aportes naturales generados en marismas colindantes (Gattuso, 1998, Abril y Borges, 2004).

Recientemente, diversos autores han realizado un esfuerzo de integración y recopilación de datos de concentraciones de CO_2 medidas en estuarios así como las emisiones de CO_2 a la atmósfera (e.g.: Ducklow y Mccallister, 2004; Borges, 2005, Borges et al., 2006). Se desprende de estas revisiones que todos los estuarios estudiados son una fuente de CO_2 a la atmósfera, por lo que este comportamiento parece ser un patrón general de estos sistemas. Sin embargo, la magnitud de estas emisiones a la atmósfera varía dentro un amplio intervalo de valores, que van desde los 4.4 mol C m^{-2} $año^{-1}$ en el fiordo danés Randers, hasta los 76 mol C m^{-2} $año^{-1}$ observados en el estuario del río Duero (Borges, 2005). No obstante, estos sistemas que marcan el límite superior e inferior en cuanto a las emisiones a la atmósfera, no se corresponden con aquellos en los que se ha observado las concentraciones máximas y mínimas de CO_2. Esta circunstancia se debe principalmente a los diferentes valores del coeficiente de transferencia (k) usados para el cálculo de los flujos, que es una de las principales fuentes de incertidumbre en el cálculo del intercambio de gases agua-atmósfera. El valor de k para gases poco solubles como el CO_2 depende del grado de turbulencia en la fase líquida de la interfase agua-aire (Wannikhof, 1992). En el océano y lagos, el principal mecanismo impulsor de esta turbulencia es el viento, sin embargo, en estuarios existen fuentes adicionales como son la velocidad de la corriente, mareas, etc (Zappa et al., 2003). Algunas de las parametrizaciones para k han sido hechas en base a datos experimentales

en estuarios, (Carini, et al. 1996; Borges et al., 2004), sin embargo a pesar del gran debate que existe hoy en día alrededor del valor de k, algunos autores opinan que en el caso de estuarios lo mejor sería la integración de los efectos del viento, las corrientes y la profundidad de la columna de agua profundidad, por lo que la formulación para estimar k sería especifica para cada estuario.

El numero de estudios del sistema del carbono inorgánico en estuarios, y de sus emisiones a la atmósfera es todavía mas limitado en lo que respecta a la Península Ibérica, hallándose disponibles los estudios de Ortega et al., (2005) en tres estuarios del norte, Gago et al., (2003) y Alvarez et al. (1999) en la Ría de Vigo y otros estudios en la vertiente portuguesa como son los del Duero y el Sado (Frankignoulle et al., 1998).

En este capitulo, se aborda el estudio del estuario del Guadalquivir desde el punto de vista del sistema del carbono inorgánico: así, se ha estudiado su distribución longitudinal, su tipo de comportamiento y los principales procesos metabólicos involucrados en su variabilidad. Asimismo, se ha evaluado la exportación de CID hacia el Océano Atlántico y el papel del estuario como fuente de CO_2 a la atmósfera. Estos datos han permitido posteriormente hacer un balance global del CID en el estuario del Guadalquivir.

El río Guadalquivir y los afluentes que recibe en el tramo final de su cauce constituyen el sistema estuárico mas importante del sur de la Península Ibérica, con una longitud de 108 km desde la desembocadura del río hasta su límite fluvial, es decir hasta donde la acción del hombre ha limitado la influencia de las mareas. Su cuenca de drenaje tiene una extensión de 58000 km^2, que se encuentra dividida en dos cuencas: una de origen silíceo al norte y otra de origen carbonatado al sur. Esta composición contribuye a la alta concentración de sólidos en suspensión y carbonatos disueltos característicos del estuario del Río Guadalquivir. Respecto al régimen de mezcla, y de acuerdo a la

clasificación de los estuarios propuesta por Beer (1983), el estuario del Guadalquivir se aproxima mucho a un estuario verticalmente homogéneo.

La parte experimental de este trabajo se llevó a cabo entre los años 2000 y 2003 y consistió en la realización de transectos para establecer el gradiente longitudinal, así como la observación en tres estaciones fijas durante ciclos mareales de las concentraciones de carbono inorgánico. En estas campañas, las variables medidas fueron la alcalinidad total (AT), el pH, el oxígeno disuelto (OD), la Clorofila-a (Chl-a), la presión parcial de CO_2 (pCO_2), los sólidos en suspensión, así como el carbono orgánico disuelto (COD).

Los resultados obtenidos mostraron que la concentración de CID en el estuario crece hacia su extremo fluvial, poniendo de manifiesto que el origen de la AT y del CID en el estuario son los aportes del río, como consecuencia principalmente de la composición de la cuenca de drenaje. Además, el AT y el CID mostraron en la mayor parte de las campañas un comportamiento conservativo.

Las concentraciones mayores de TA y CID en el extremo fluvial del estuario han sido observadas en invierno, a consecuencia de que el descenso de la temperatura del agua favorece los procesos de disolución de carbonatos. Sin embargo, esta variación entre invierno y verano es poco importante en el extremo marino, en comparación con el importante gradiente longitudinal de concentraciones de CID y AT que se aprecia a lo largo del estuario.

Los valores de pCO_2 en el estuario se encuentran siempre por encima de las concentraciones de equilibrio con la atmósfera. El CO_2 también muestra una relación casi lineal con la salinidad en la mayor parte de los muestreos longitudinales, con las máximas concentraciones en la cabecera del estuario (entre 1029 y 3605 μatm), a consecuencia de

los altos valores de CID del agua de río. Estas concentraciones de sobresaturación de CO_2 provocan unos flujos medios de CO_2 a la atmósfera de 85.2 mmol m^{-2} d^{-1}.

Las variaciones de CID, AT, y OD con las mareas están asociadas principalmente a la advección y mezcla del agua de mar y el agua río con distintas concentraciones, poniendo de manifiesto el comportamiento conservativo del carbono inorgánico. La amplitud de las variaciones mareales es mucho menor en la estación más fluvial respecto a la más marina, debido a la menor influencia de la onda de marea aguas arriba en el estuario. Además de la mezcla de aguas, se han estudiado otros procesos adicionales capaces de modificar las concentraciones de CID, como son la degradación de la materia orgánica y la disolución de carbonatos, procesos ambos que aumentan la concentración de CO_2 en la columna de agua. Sin embargo, ninguna de las dos reacciones anteriores parece afectar de forma significativa al gradiente de concentraciones de DIC en el estuario, de forma que se han propuesto como los mecanismos que contrarrestan los elevados flujos de CO_2 a la atmósfera observados. El proceso de ventilación del CO_2 de origen fluvial en estuarios en muy variable, en el caso del Guadalquivir se ha estimado el 34% del total del carbono inorgánico exportado se emite a la atmósfera.

Bibliografía:

Abril G. y Borges A.V., 2004. Carbon dioxide and metahne emissions from estuaries. In: Trembaly, A., Varfalvy, L., Roehm, C., Garneau, M. (eds). Greenhouse gases emissions from natural environments and hydroelectric reservoirs: fluxes and processes. Springer, Berlin, Heidelberg, New York: 187-212.

Álvarez, M., Fernandez, E., Pérez, F.F., 1999. Air –sea CO2 fluxes in a coastal embayment affected by upwelling: physical vs. biological control. Oceanol. Acta 22, 499–515.

Beer, T. 1983. Environmental Oceanography: An Introduction to the Behavior of Coastal Waters. Pergamon Press, Oxford. 226 pp.

Borges, A. V., Delille, B., Schiettecatte, L.-S., Gazeau, F., Abril, G. and Frankignoulle, M., 2004a. Gas transfer velocities of CO_2 in three European estuaries (Randers Fjord, Scheldt, and Thames). Limnol. Oceanogr., 49:1630–1641.

Borges, A.V., Schiettecatte L.-S., Abril G., Delille B. and Gazeau F., 2006. Carbon dioxide in European coastal waters. Estuar. Coast. Shelf Sci., 70(3): 375-387.

Borges, A. V.,2005. Do We Have Enough Pieces of the Jigsaw to Integrate CO_2 Fluxes in the Coastal Ocean? Estuaries, 28 (1): 3–27.

Cameron, W. M. y D. W. Pritchard. 1963. Estuaries, p. 306–324. *En* M. N. Hill (ed.), The Sea, Volume 2. John Wiley &Sons, New York.

Carini, S., Weston, N., Hopkinson, C., Tucker, J., Giblin, A., and Vallino, J., 1996. Gas exchange rates in the Parker River estuary, Massachusetts. Biol. Bull., 191:333–334.

Ducklow, H.W. y S. L. Mcallister. 2004. The biogeochemistry of carbon dioxide in the coastal oceans, in press, *En* K. H. Brink and A. R. Robinson (eds.), The Global Coastal Ocean—Multiscale Interdisciplinary Processes, Volume 13. Harvard University Press, Cambridge, Massachusetts.

Elliot M. y McLusky, D.S:, 2002. The needs for definitions in understanding estuaries. Estuarine, Coastal and Shelf Science, 55:815-827.

Fairbridge, R.W., 1980. The estuary: its definition and geodynamics cycle. En: E. Olausson, e I. Cato (eds). Chemistry and biogeochemistry of estuaries. Jhon Wiley adn Sons, Chichester, pp:1-35.

Frankignoulle, M., Abril, G., Borges, A., Bourge, I., Canon, C., Delille, B. Liebert, E., and Theate, J.-M., 1998. Carbon dioxide emission from European estuaries. Science, 282:434–436.

Gago, J., M. Gilcoto, F.F. Perez, A.F. Rios, 2003. Short-term variability of fCO2 in seawater and air–sea CO2 fluxes in a coastal upwelling system (Ría de Vigo, NW Spain)

Gattuso, J.-P., M. Frankignoulle, y R. Wollast. 1998a. Carbon and carbonate metabolism in coastal aquatic ecosystems. *Annual Review Ecology Systematics* 29:405–433.

Meybeck, M., 1993. Riverine transport of atmosferic carbon: sources, global typology and budgets. Water, Air and Soil Pollution, 70: 443-463.

Ortega, T., Ponce, R. Forja, J. Gómez-Parra, A., 2005. Fluxes of dissolved inorganic carbon in three estuarine systems of the Cantabrian Sea (north of Spain). Journal of marine systems, 53:125-142.

Sundquist, ET., 1993. The global carbon dioxide budget. Science, 259: 934-41.

Wanninnkhof, R., 1992. Relationship between wind speed and gas exchange over the ocean. J. Geophys. Res., 97 (C5): 7373-7382.

Zappa, C. J., Raymond, P. A., Terray, E. A. and Mcguillis, W. R., 2003. Variation in surface turbulence and the gas transfer velocity over a tidal cycle in a macro-tidal estuary. Estuaries, 26: 1401–1415.

Inorganic carbon dynamic and air –water CO2 exchange in the Guadalquivir Estuary (SW Iberian Peninsula)[1].

de la Paz[*], M., Gómez-Parra, A. and Forja, J. M.

Departamento de Química-Física, Facultad de Ciencias del Mar y Ambientales, Universidad de Cádiz, Campus Río San Pedro s/n, Puerto Real (Cádiz) 11510, Spain

Abstract

The inorganic carbon distribution and the atmosphere-water CO_2 exchange along the Guadalquivir Estuary (SW Iberian Peninsula) have been evaluated on the basis of the field observation performed from 2000 to 2003. The study consisted of the measurement of total alkalinity (TAlk), pH, continuous underway CO_2 partial pressure (pCO_2), dissolved oxygen and chlorophyll measurements. The Guadalquivir river water is rich in TAlk and DIC and its behaviour is mainly conservative along the salinity gradient. Estuarine waters were CO_2 oversaturated in all the samplings in space and time. It have been suggested some biogeochemical processes affecting the water pCO_2 such as the CO_2 flux to the atmosphere, the organic matter aerobic respiration and the carbonate dissolution. The average CO_2 flux to the atmosphere is 85.2 mmol m^{-2} d^{-1} and the total CO_2 emission to the atmosphere is 3.2 mol C 10^6 d^{-1}. Ventilation of riverine CO_2 can contribute to the emission of the CO_2 from inner estuaries although it seems highly variable among European estuaries. It have been estimated than in the Guadalquivir Estuary 34% of the carbon exported is emitted to the atmosphere.

Keywords: Estuaries, carbon dioxide, dissolved inorganic carbon, air-water fluxes, river export, Guadalquivir River.

1. Introduction

The difference between the sources (7.1 ± 0.9 Pg C yr^{-1}, fossil fuel combustion and cement production) and sinks (5.1 ± 0.5 Pg C yr^{-1}, atmosphere and ocean) of 2 Pg C yr^{-1} for anthropogenic CO2 is similar (in the same order of magnitude) to the overall uncertainty (±1.4 Pg C yr^{-1}) of estimation. The missing carbon sink could be the combined

result of uncertainty in flux estimates and the terrestrial biosphere uptake (Sabine et al. 2004). Until recent times, the coastal ocean has been largely ignored in global budgeting efforts, even though the related flows of carbon and nutrients are disproportionately high in comparison with its surface area (Smith and Hollibaugh, 1993, Wollast, 1998). Estuaries play a significant role in the global CO_2 cycle, as they could emit around 0.43 Pg C yr^{-1} roughly balancing the absorption of CO_2 by the ensemble of other coastal ecosystems of -0.32 Pg C yr^{-1} (Borges 2005). Although high pCO_2 in world rivers and estuaries is ubiquitous, factors controlling pCO_2 within estuaries may vary among systems according to environmental conditions as is the case of the Scheldt or the Amazon. Hence, simple extrapolation from these well-studied river and estuarine ecosystems to a global scale may result in inaccurate global estimates (Zhai et al, 2005). In this context, some investigators conclude the need for a better mapping of coastal surface CO_2, including riverine areas.

Diverse and intense mechanisms are responsible for such high levels of pCO_2 in estuaries; for instance, the residence time of the water in the estuary is the balance between the tidal effect and the river discharge, particularly in macrotidal estuaries, the increase in the residence time of the water in the estuary optimizes the conditions for organic matter degradation as well as carbonate dissolution processes

The CO_2 flux to the atmosphere is a function of the CO_2 partial pressure air-water gradient (ΔpCO_2) and the gas transfer velocity (k). Despite the availability of highly accurate and precise methods to determine ΔpCO_2, the largest source of uncertainty in the calculation of gas flux arises from the rate term k in both open and coastal environment processes (Borges et al. 2004b). The ability to accurately measure and predict atmospheric exchange is limited by a lack of understanding of the mechanisms controlling k. Rivers and estuaries are systems were wind and boundary friction act as source of turbulent energy. Laboratory experiments on transfer rates in rivers for

combined wind and bottom shear induced turbulence suggest that the processes within each regime are cumulative (Zappa et al. 2003).

Limited numbers of specific studies have been carried out on the gas transfer velocity in estuaries using methods such as dual tracer addition (Clark et al. 1995, Carini et al.1996), natural gas tracer (Clark et al. 1992) or floating dome technique (Marino and Howarth, 1993, Borges et al. 2004a). The former involves long term measurement of the gas transfer velocity over the entire estuary, while the floating dome is a short term measurement affected by system heterogeneity typical in estuaries. The floating dome technique yields higher values compared to the other methods (Raymond and Cole, 2001) which may yield higher flux values than those actually present. In any case, the selection of a particular value for *k* will affect the overall representation of the net ecosystem metabolism.

In addition to the high CO_2 ventilation of riverine DIC, the fluvial export of terrestrial alkalinity is also the predominant source of oceanic alkalinity and is a key regulator of the $CaCO_3$ saturation state in the ocean according to Raymond and Cole (2003). In this context, Huertas et al. 2006 develop a previous study about the pCO_2 in the surface water in the north-eastern shelf of the Gulf of Cadiz, and observed a phytoplankton bloom in spring and autumn, induced by the nutrients export of the Guadalquivir estuary. It was observed than in an annual data base, the continental shelf in front of the Guadalquivir behaves as a net sink for atmospheric CO_2.

BIOGEST and EUROTROPH projects are amongst European Union initiatives in the last decade which set out to further the understanding of trophic status in European estuaries and coastal waters, as well as the mechanism involved. Until now, no study of inorganic carbon dynamics has been performed in the Guadalquivir Estuary, is the Guadalquivir being one of the largest rivers of the Iberian Peninsula as well as the southernmost in Europe. In this study, pCO_2 and inorganic carbon distribution have been

measured for the first time in the Guadalquivir estuary. Moreover, biochemical processes involved in the pCO_2 variability in time and space have been studied in relation with organic matter degradation and carbonate dissolution processes. Last, it have been estimated the air-water CO_2 fluxes and the amount of riverine carbon ventilated along the estuary.

2. Material and methods

2.1. Study site

The 108 km long Guadalquivir estuary is located in the south-west of the Iberian Peninsula. The drainage basin of the Guadalquivir river covers an area approximately of 57.871 km^2, and the longitude of the river is about 560 km, crossing over the south of Spain from east to west and flushing out in the Atlantic Ocean. The geology of the drainage basin can be divided in a siliceous origin in the north side and a carbonated part to the south side. This composition contributes to the high concentration of suspended solids and dissolved carbonate characteristic of the Guadalquivir river water.

With respect to the mixing regime and according to the classification proposed by Beer (1983) the Guadalquivir estuary is a complete mixed or vertically homogeneous estuary (see fig.1). Although it is surrounded by inter-tidal salt marshes, the volume of water exchange between the river and these areas is minimal in comparison to the water volume of the estuary owing to dragging of the main channel of the river (6 m depth) to facilitate ship navigation with an estuary integrated cross section depth of 3m. The Guadalquivir Estuary is characterized by an irregular river discharge, this means low discharge most time of the year and extremely high during rainy February-March. The tidal velocity of around $1 m \cdot s^{-1}$ is 20 times the freshwater velocity meaning that the tide is the main factor influencing the hydrodynamics of the estuary. The Suspended Particulate

Matter (SPM) distribution along the estuary shows that the maximum turbidity zone is located around salinity 5 in the summer; nevertheless the position of this maximum is highly variable, being dependent on the river discharge and the tidal regime. The residence time of the water in the estuary, calculated from the most frequent freshwater flow (36 $m^3 \cdot s^{-1}$) was 18 days.

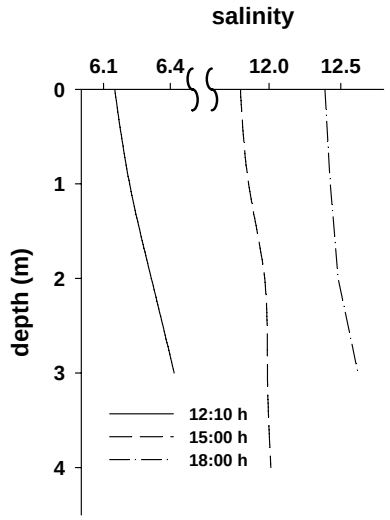

Figure 1. Salinity profiles at different tidal stage for the anchoring sampling on June-10-th 2002.

2.2. Sampling strategy

8 fixed sampling stations were selected along a 38 km stretch of the most marine part of the Guadalquivir estuary (Fig. 2, Table 1). The surveys were performed on board the R/V Mytilus in the summers of 2002 and 2003 as well as in a small vessel for the transects carried out in 2000 and 2001. In order to characterize the spatial pattern in the estuary five transects along the salinity gradients were performed. Furthermore, to study the effects of the tidal exchange on the estuarine carbon system, continuous monitoring of the selected parameters was performed at 3 anchor stations. This tidal exchange sampling was carried out for intervals of 13 to 24 hours and discrete water surface and

bottom samples were collected 1 hour intervals. Nevertheless, it would be desirable to have more information available for high runoff events (on February-March), which can increase considerable the river discharge on February-March.

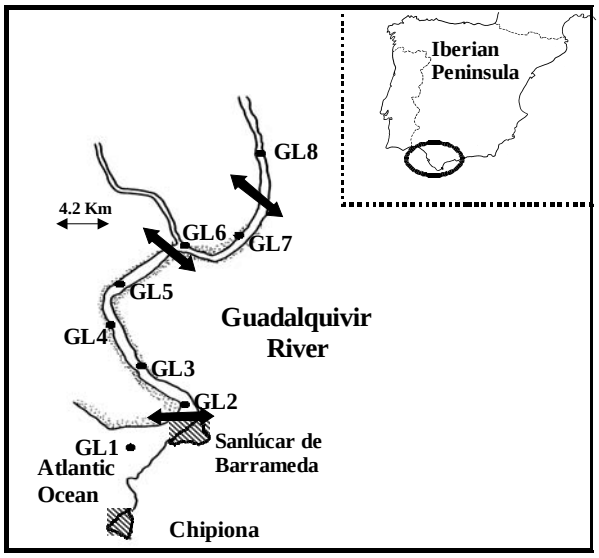

Figure 2. Map of the Guadalquivir estuary. There has been indicate the 8 fix sampling stations (•) as well as the locations for the tidal exchange sampling (⟷).

The underway ship's pump supplies water for the continuous measurement of salinity, temperature (SeaBird thermosalinometer) and CO_2 partial pressure, (sample frequency of 1 minute). The oxygen was fixed in a sealed flask and stored in darkness during 24 hours as is described by the Winkler method for later analysis by potentiometric titration (Metrohm 670 Titroprocessor). The samples for dissolved organic carbon (DOC) were fixed with phosphoric acid and measured with a TOC-5050-A analyzer (Shimatzu). Chlorophyll *a* (Chl*a*) was determined on a glass fiber filter by fluorescence after extraction in 90 % acetone (Turner Designs-10 fluorometer).

The Alkalinity and pH measurements of the filtered samples were carried out in the ship. The pH was measured with a glass combined electrode (Metrohm) calibrated in the NBS scale with pH 4 and 7 buffers. The Alkalinity analysis was performed by the potentiometric titration methods (Metrohm 716 DMS). The Alkalinity computation was made from the titration curve by means of the Gran Function and taking into account the correction for sulphate and fluoride interaction, using the constant proposed by Khoo (1977) and by Perez and Fraga (1987) respectively. For the dissociation of inorganic carbon the K1 and K2 acidity constants proposed for the NBS scale by Cai et al. (1998), specially adapted for estuaries as well as the K0 proposed by Weiss (1974) were selected. The method was validated with reference standards from A. Dickson (Scripps Institution of Oceanography, San Diego, USA) to a precision of ± 2 μmol kg^{-1}.

The equilibration technique was used to measure the continuous surface water pCO_2. The equilibration processes was a mixed of a laminar-flow and a bubble type connected to an infrared analyzer (Li-Cor 6262) according to the design of Koertzinger et al. (1996).

The wind speed data for the flux calculation were supplied from the meteorological station of the ship and daily river discharge data were provided by the Confederación Hidrográfica del Guadalquivir (see Table 1). The water current speed was measured by means of two Aanderaa (RCM7) Current Meters, one located at the water surface and the other near the bottom.

The CO_2 gas exchange across the air-water interface can be described as a function of the gas concentration gradient and a gas exchange coefficient (*k*) as stated below:

$$\text{Flux } CO_2 = k\,([CO_2]_{water} - [CO_2]_{air})$$

where the CO_2 gradient is the driving force and for the *k* calculation have been employed different wind speed parameterizations which are discussed in more detail in section 3.3.

The excess CO_2 is defined as the departure of free dissolved CO_2 from atmospheric concentration and is calculated as the in situ CO_2 concentration (µmol L^{-1}) minus a theoretical CO_2 concentration at equilibrium with the atmosphere at 370 µatm. The apparent oxygen utilization (AOU) is defined as departure of oxygen from an O_2 concentration in equilibrium with the atmosphere calculated from the Benson and Krause (1984) solubility equation.

3. - Results and Discussion

3.1. Longitudinal variation.

In table 1 the results for physicochemical variables obtained between 2000 to 2003 are shown. The first two transects correspond to winter and the next three to summer. The longitudinal distribution for Dissolved Inorganic Carbon (DIC) and Total Alkalinity (TAlk) along the estuary are presented in figure 3. TAlk and DIC decreased as salinity increased, in relation to freshwater and seawater mixing within the estuary. The DIC and TAlk concentrations at low salinities varied within a wide range: from 3.0 mmol kg^{-1} in June 2002 to 4.9 mmol kg^{-1} in December 2000 for DIC and from 3.1 to 4.8 mmol kg^{-1} for TAlk, on the same sample dates. The higher values on TAlk and DIC in the river endmember are observed in winter. This temporal pattern was not present in the seawater endmember where less variability was found (from 2.3 to 2.5 mmol kg^{-1} in DIC)

The high TAlk concentration in the Guadalquivir river water are due to the carbonated composition of the drainage basin. This cause that the Guadalquivir River means a significant source of TAlk to the Atlantic Ocean. In addition to that, the calcite and aragonite saturation solubility product and therefore the carbonate dissolution increase as temperature decrease (Mucci, 1983). This explains that the higher TAlk concentration in the river endmember occurs in winter when the average temperature is

Table 1: Range for physicochemical and chemical properties of surface water for each sampling. The longitudinal samplings are indicated as *Long* while the Outer, Middle and Inner Station are reflected in Figure 1 as the sites for tidal exchange sampling.

Sampling date		**Salinity**	**Temperature**	**Freshwater flow($m^3 \cdot s^{-1}$)**	**SPM ($mg\ L^{-1}$)**	**DIC ($mmol\ kg^{-1}$)**	**pH(NBS)**	**fCO_2 µatm**	**Total Alkalinity ($mmol \cdot kg^{-1}$)**
19 Dec 00	Long.	2.24-32.98	15.0	13.5	33.3 - 171.2	2.30-4.89	7.78-8.13	518 -3606	2.48-4.76
14 Nov 01	Long.	2.46-22.73	15.0	25.9	12.5 - 433.1	2.53-4.03	7.78-8.16	538 – 2640	2.70-4.01
8 Jun 02	Long.	9.79-31.67	21.0	35.1	--.	2.31-2.99	7.99 -8.13	627-1027	2.51-3.09
10 Jun 02	Long.	6.81-32.11	20.9	32.1	33.3 - 146.0	2.26-3.09	7.97-8.17	638-1029	2.44- 3.16
20 Jun 03	Long.	8.50-30.91	25.0	44.7	--	2.52-3.33	7.67-7.84	823 1617	2.58–3.34
7 Jun 02	Outer St.	19.64-36.29	21.2	43.9	65.8 - 543.7	2.25-2.75	7.93- 8.01	581 – 951	2.44–2.85
8 Jun 02	Middle St.	9.74-20.52	21.3	35.1	65.8 - 405.8	2.66-3.04	8.00-8.18	925 – 1065	2.81-3.13
10 Jun 02	Inner St.	2.48-13.61	21.8	32.1	121.0-846.6	2.90–3.18	8.00-8.20	922 - 1165	3.00-3.20

15 ºC. Cai, W. (2003) found similar values for TAlk and DIC in the near- zero salinity zone of the Missisipi River because of the high weathering rate of the drainage basin.

This is contrary to the positive slope reported in other estuaries for TAlk versus salinity, indicating a higher seawater concentration than in the river (e.g. Devol et al. 1987, Cai et al. 1998, Brasse et al. 2002).

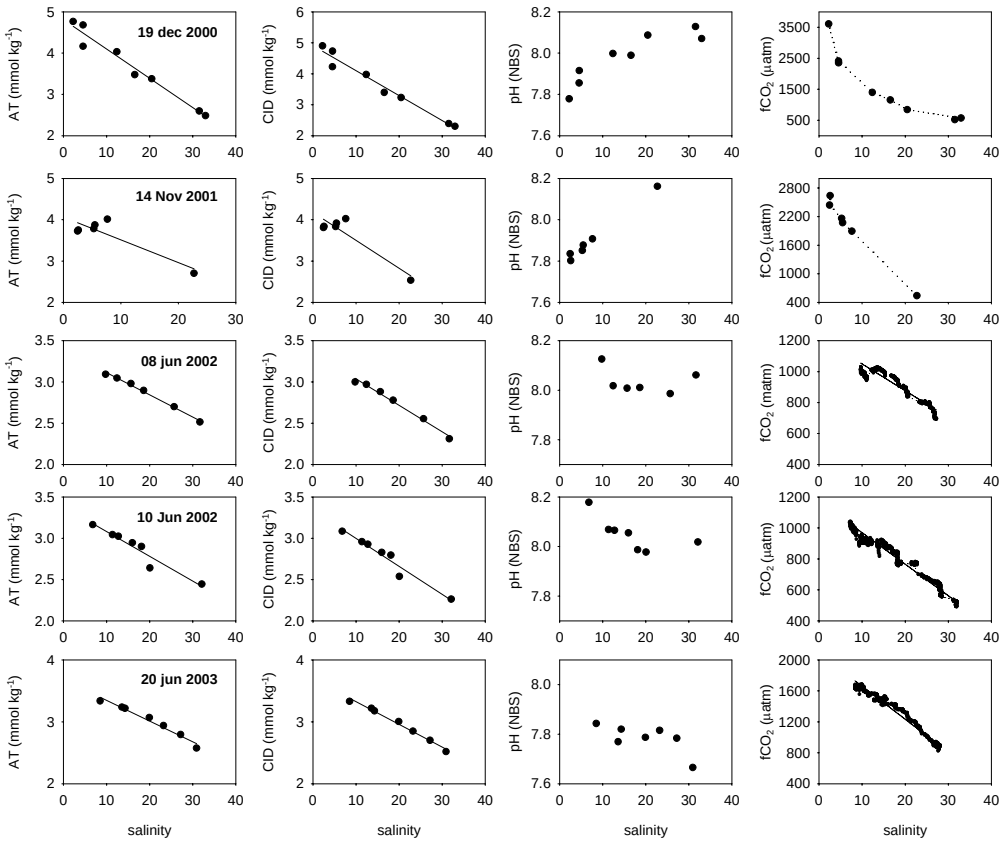

Figure 3. Longitudinal variation of Total Alkalinity (TAlk), Dissolved Inorganic Carbon (DIC), pH and CO_2 fugacity (fCO_2) along the salinity gradient in the Guadalquivir estuary. It should be noted that no samples were gathered for stations GL7 and GL8, for transects performed on November-14th, 2000 and June-8th, 2002.

DIC is greater in the upper part of the estuary than in the marine part; as is common in estuaries, being similar the values to those found in Loire (Abril et al. 2003) and Scheldt (Hellings et al. 2001), although the origin of the DIC estuarine values are different to the Guadalquivir River. These estuaries are characterized by high anthropogenic input of organic matter and nutrients responsible of intense remineralization processes mainly in the maximum turbidity zone.

The variation of pH (NBS) with salinity was not the same for all transects. While pH was more acid in November and December and increased with salinity (from 7.8 to 8.1/8.2), in June, upstream samples were more basic (8.0) than downstream. These seasonal variations in pH of the river endmember is thought to be due to the change in ratios of the river source, coupled to changed in biological activity (Howland et al., 2000). During winter, the river waters are derived of the runoff, which is relatively acidic, whereas in summer, the primary production activity is favored upstream and increase the pH (accompanied by a *Chl a* maximum at low salinity, see fig 6).

The values of water CO_2 fugacity (fCO_2) with respect to the atmosphere were largely in excess of equilibrium values, throughout the estuary (Table 1, figure 3). In the case of fCO_2, a linear relationship vs. salinity was found in most of the longitudinal sampling. The river water presented elevated fCO_2 values, related to the high levels of DIC found in the Guadalquivir River. The maximum value for fCO_2 of 3605 µatm was observed upstream in December 2000 with the minimum being recorded in June 2002 with a value of 1029 µatm. For the summer sampling the slight differences amongst the 2002 transects are due to varying river discharge and tidal coefficient. The Guadalquivir estuary follows common trends and presents a similar range of fCO_2 values when compared to other European estuaries such as the Elbe (Brasse et al. 2002), Rhine and Gironde (Frankignoulle et al. 1998) and Loire (Abril et al. 2003).

Assuming salinity is a satisfactory mixing indicator, then for any dissolved constituent subject only to physical mixing processes, the resultant plot will be linear, with a negative slope for components which are more concentrated in freshwater than in seawater (Liss, 1976). Table 2 represents the lineal regression equation for DIC versus salinity, where C_0 is the DIC concentration in freshwater, calculated from the equation at zero salinity. It can be deduced that the behaviour of DIC is conservative and that the main source of DIC to the estuary is from the freshwater, hence there is no apparent net reaction; DIC export from the river to the adjacent coastal areas is the product of the freshwater discharge and the freshwater DIC concentration. The DIC export obtained varied from 5.7 x 10^6 mol d^{-1} in December 2000 to 14,2 x 10^6 mol d^{-1} in June 2003. In the Guadalquivir estuary the high DIC export is due mainly to the high TAlk concentration in the river and not to internally addition as in the case of the Scheldt (Hellings et al., 2001) or the Loire (Abril et al., 2003) estuaries.

Table 2.-Parameters of the linear fittings of DIC versus salinity; the river DIC concentration (C_0), freshwater flow (Q) and the calculated DIC export defined as (C_0 • Q) have been included.

Date	Slope (mmol·kg^{-1} psu^{-1})	C_0 (mmol·kg^{-1})	r^2	Freshwater flow (m^3 s^{-1})	Export of DIC 10^6(mol d^{-1})
19-Dec-00	-0.081	4.91	0.97	13.51	5.72
14-Nov-01	-0.068	4.18	0.86	25.86	9.33
08-Jun-02	-0.032	3.36	0.99	35.12	10.17
10-Jun-02	-0.034	3.34	0.95	32.14	9.26
20-Jun-03	-0.037	3.70	0.99	44.69	14.23

3.2. Tidal variations

Semi-tidal cycles were performed in three different sites of the estuary in order to study the tidal influence on the inorganic carbon system. This sites where located to

cover the maximum salinity range associated to tidal variation. The Outer Estuary Station was the most marine site (near GL2, see fig.2) with the salinity ranging from 19.6 to 36.3 (table 1); the Middle Estuary Station (near GL6) varied between 9.7 and 20.5; and the more fluvial anchoring station referred to as the Inner Estuary Station (between GL7 and GL8) ranged from 2.5 to 13.6.

In this context some previous works have been done to study the tidal effect on the inorganic carbon cycle in estuaries (Raymond et al. 1997), marshes (Neubauer and Anderson, 2003) or mangroves (Biwas et al. 2004), as well as in laboratory simulations (Garcia-Luque et al., 2005).

Figure 4 shows tidal cycle effects and portrays the marine and freshwater mixing within the estuary. The friction phenomenon along the estuary combined with the river discharge mean that the tidal wave does not behave symmetrically. As a result, there is a slight gap between the salinity maximum and the high tide.

As is the case for the salinity gradient distribution, maximum salinities are linked to minimum TAlk, DIC, AOU and fCO_2. There were no significant differences found between the surface and bottom concentrations, which corroborates the theory that the Guadalquivir is vertically homogeneous (or completely mixed estuary). Minimum values of TAlk were found in the Outer Station (2.47 to 2.85 mmol kg^{-1}) and increased upstream due to an increase in the influence of fluvial water, while the tidal variability decreased. Variations for TAlk were 0.38 mmol kg^{-1} at the Outer Station, 0.26 mmol kg^{-1} in the Middle and 0.18 mmol kg^{-1} TAlk for the Inner Station. For DIC the variations were 0.46 mmol kg^{-1} in the Outer Station, 0.32 mmol kg^{-1} in the Middle Station and 0.26 mmol kg^{-1} in the Middle Station.

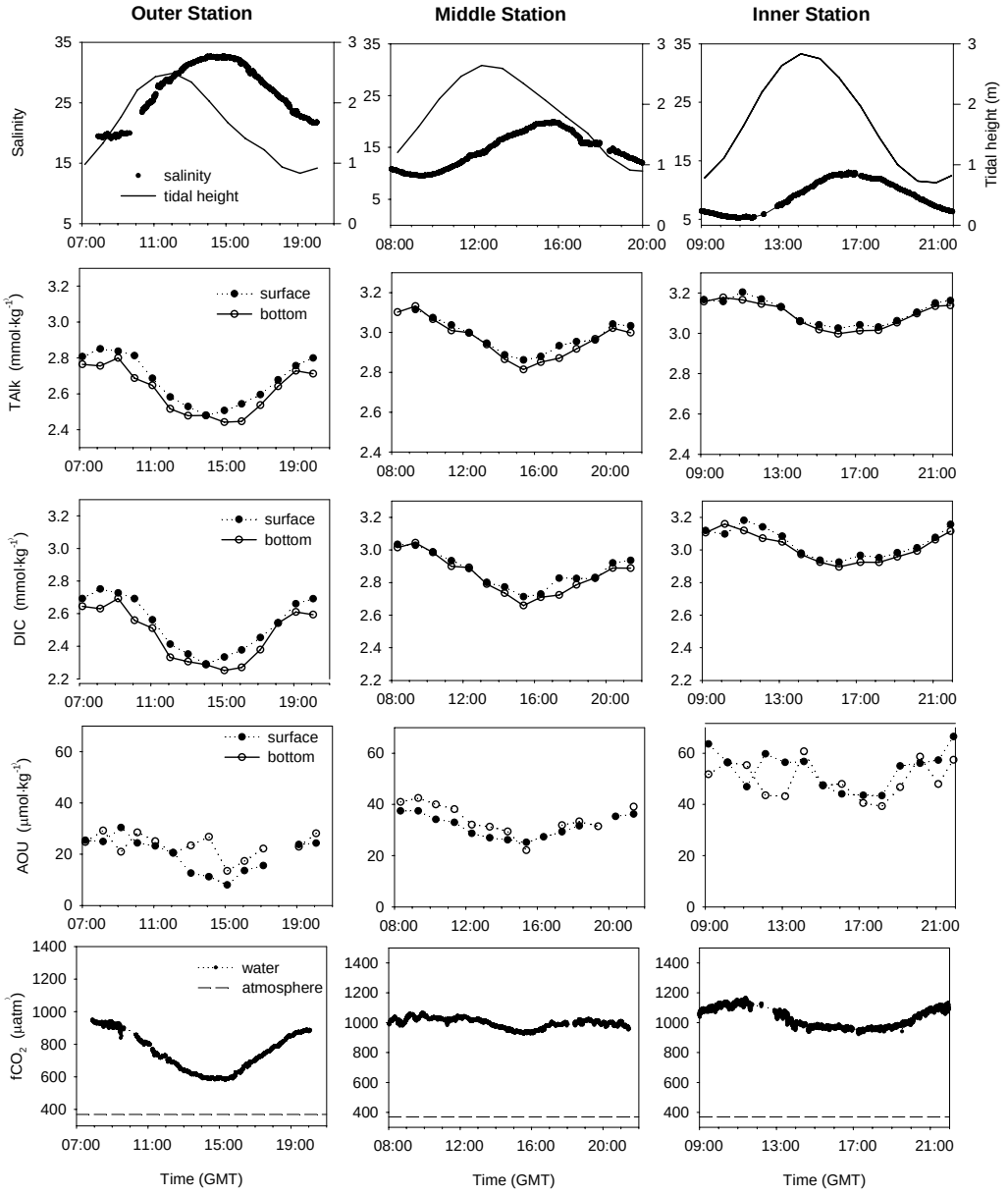

Figure 4. Tidal variation of tidal height, salinity, Total Alkalinity (TAlk), Dissolved Inorganic Carbon (DIC), Apparent Oxygen utilization (AOU) and CO_2 fugacity (fCO_2).

The fCO_2 of the surface water of the Outer Station presented a minimum at high tide of 580 μatm while reaching 950 μatm at low tide. At the Middle Station, high tide to low tide values varied from 925 to 1065 μatm with Inner Station values ranging from 922 to 1165 μatm. Anchor monitoring revealed that tidal variability is noticeably higher in the most marine station when compared with the more fluvial estuary and water advection is the key factor controlling the TAlk, DIC and AOU variability.

Diurnal changes accounted for an insignificant amount of the total change as indicated by the minimal difference in fCO_2, DIC and TAlk values between similar tidal phases. It can be deduced than the river discharge is more efficient than the tidal effect in the net transport of TAlk and DIC to offshore waters, and that the main effect, especially for macrotidal estuaries is the residence time of both water and suspended matter in the estuary (Wang and Cai, 2004).

Different biogeochemical processes may be associated with the surface water pCO_2 in the Guadalquivir estuary. The main processes involved are inorganic carbon respiration, carbonate dissolution and gas exchange with the atmosphere. Apart from highly reduced waters, it can be considered that oxygen depletion is closed to the fraction of excess CO_2 produced by heterotrophic processes (Abril et al. 2000). Previous work in estuaries applies the relationship between excess CO_2 and AOU to obtain a quantitative approach of the stoichiometry of the organic matter respiration processes (Ballester et al. 1999 and Zhai et al. 2005).

The excess CO_2 vs. AOU relationship was plotted (Figure 5) for the combined set of surface anchoring data. Excess CO_2 was calculated using the measurement taken from the equilibrator.

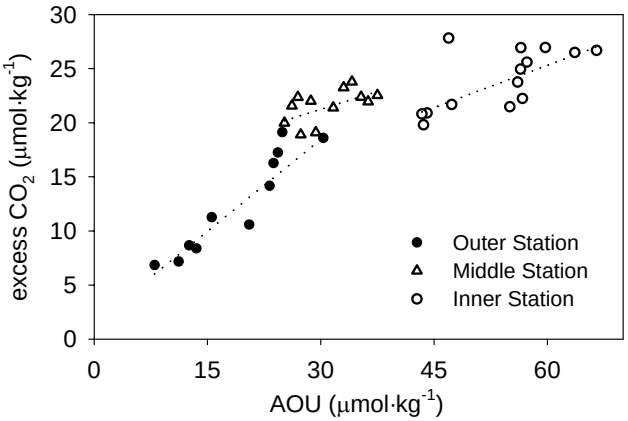

Figure 5. Excess CO2 versus Apparent Oxygen utilization (AOU). The equation for the regression lines are: Inner station (y = 0.24x+10.925, r^2 = 0.5), Middle Estation (y = 0.28x + 12.86, r^2 = 0.65), Outter Station (y = 0.62x + 0.81, r^2 = 0.89)

It can be observed that there is an increase in excess CO_2 with the AOU. Excess CO_2 varied from 6.85 to 27.81 μmol kg^{-1} while AOU values ranged between 8.01 and 66.49 μmol kg^{-1}, the higher values corresponding to the upper estuary. The values reach in the Guadalquivir estuary for excess CO_2 and AOU are relatively low compare to the amounts found in other estuaries as Piracacaba River, Brasil (Ballester et al. 1999) or the Perl River , China (Zhai et al. 2005) characterized by high organic matter inputs.

The slope of the plot excess CO_2 vs. AOU in the Outer Station is 0.62. Analogous values are found in Zhai et al. (2005) and references therein for the elemental composition of the organic matter in estuaries. However, the slope for the Inner and Middle Station decrease to 0.28 and 0.24 respectively suggesting the occurrence of other non-metabolic processes that removes CO_2 of the water column in this zone of the estuary.

Due to the high levels of HCO_3^- present in the estuary, it is possible to estimate the excess CO_2 in the free gas form (Ballester et al. 1999, Zhai et al. 2005) rather than the DIC

form (DeGrandpre 1997, Abril et al. 2003), under the assumption that the contribution of CO_2 dissolved from the organic matter respiration is negligible when taking into account the predominant effect of the bicarbonate buffer HCO_3^-.

The entire set of data points of the 3 anchoring sampling are display together versus salinity in order to portray the space-time variability in the concentration of Chl a, DOC and Suspended Particulate Matter (SPM) (fig. 6).The Dissolved Organic Carbon (DOC) concentration vs. salinity curve (figure 6) shows an increase in DOC toward the fluvial section, and a much more scattered pattern within the maximum turbidity zone. This may be due to internal or lateral contributions from the adjacent rice fields and salt marshes since the average Chlorophyll *a* concentration in the Guadalquivir of 6.7 $\mu g\ L^{-1}$ is not sufficient to sustain such levels of DOC through exudation. Abril et al. (2002) develop a cross comparison of organic carbon origin in estuaries arguing that two major variables control the intensity of the organic carbon mineralization: the lability /origin of the organic carbon, and the residence time of the particle in the estuary. The case of the Guadalquivir is comparable to that of the Sado and Ems estuaries whose DOC concentrations ranged from 1.9 to 9.6 $mg{\cdot}L^{-1}$ (Abril et al., 2002). The distribution of DOC may support in part the increase in the respiration processes toward the upper estuary, although it is not an intense process in the estuary.

Another possible mechanism responsible for buffering the increased pCO_2 values caused by the remineralization of organic carbon is carbonate mineral dissolution which can be represented by the following equation:

$$CO_2 + H_2O + CaCO_3 = Ca^{2+} + 2\ HCO_3^-$$

Calcite and aragonite solubility product (K_{sp}) (Mucci, 1983) for the Guadalquivir can be calculated as a function of the salinity and temperature as well as the saturation index. Despite the water column being oversaturated in calcite and aragonite, $CaCO_3$

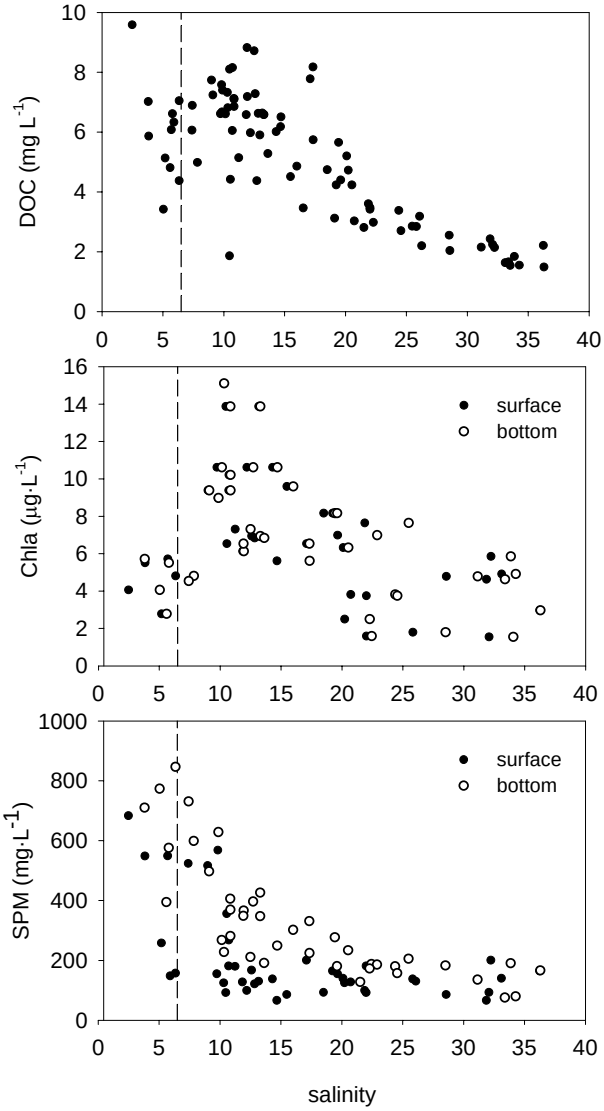

Figure 6. Dissolved Organic Carbon (DOC), Chlorophyll (Chl *a*) and Suspended Particulate Matter (SPM) vs. salinity for the three tidal exchange sampling data in 2002.

dissolution is able to take place. This dissolution is more significant in the bottom and in the maximum turbidity zone (dissolved suspended matter >400 mg L^{-1}), where the resuspension of the particulate material provides sufficient time and the increased in the

probability of reaction. Jhanke and Jhanke (2000) observed that although the bottom water was significantly supersaturated with respect to calcite and aragonite, $CaCO_3$ dissolution was found to occur in the pore water of the superficial sediment, as a result of acidification related to organic matter oxidation.

It was hypothesized that the mechanism involved in the departure from the expected CO_2 concentration in the water was due to carbonate dissolution. Additional information regarding the Ca^{2+} distribution along the estuary as well as sediment DIC and TAlk fluxes would assist in properly accounting for these processes. Detailed studies of this carbonate dissolution mechanism in the Loire (Abril et al. 2003), Gironde (Abril et al. 1999) and Seine (Roy et al. 1999) estuaries, have each taken into account the dissolution/precipitation processes in carrying out a carbon balance over the entire estuary.

3.3-Estuary- atmosphere CO_2 exchange

Fluxes for the Guadalquivir Estuary are calculated using various estuarine gas transfer parameterizations: a) O'Connor and Dobbins (1958) proposed a oxygen reareation rate as a function of the water current velocity and water column depth, b) Borges et al. (2004a), constructed an empirical relationship based on floating dome measurement in the Scheldt estuary that accounted for the wind stress effect and the current speed, using the relationship from O'Connor and Dobbins (1958), c) Carini et al. (1996) studied the gas transfer velocity in Parker River Estuary using SF_6 addition and d) Clark et al. (1995) derived an expression based on SF_6 tracer measurement in the Hudson River and ^{222}R mass balance in San Francisco Bay. After estimate the k using different algorithms, it has been converted to in situ temperature and density assuming a dependency of k proportional to $Sc^{-0.5}$. Sc was computed for in situ conditions using the Wanninkhof's relation (1992) and assuming that Sc varies linearly with salinity.

The estuary has been divided in three sections for the CO_2 flux calculation using the data from the anchoring sampling. The result for the CO_2 gas transfer velocities within the estuary as well as the wind speed and tidal current are shown in table 3. The daily wind velocity was highly random and variable oscillating between 5.0 m s^{-1} and 9.8 m s^{-1}. The maximum tidal current (from 60 cm s^{-1} to 99 cm s^{-1}) is explained since bathymetry and seawater/freshwater mixing values. Different parameterization can provide information on the spatial variability of *k* along the estuary because the relation is highly affected by the processes dominant at each station. The parameterization proposed by Borges et al. (2004b) gave the highest values throughout the estuary, followed by k_{Clark} for high wind speed or by k_{Carini} for lower wind speed. This is because the k_{Clark} relationship with wind speed is quadratic while for k_{Carini} the relationship is linear.

The maximum k values correspond to the Middle Station, where the wind speed computed that day was especially high. The expression of O'Connor and Dobbins (1958) produced the minimum k values since it considers water current alone. The values for $k_{O'Connor}$ are in the same range as those found by Zappa et al (2003) who described a daily variability in k from 2.2 to 12 cm h^{-1} for a low wind day in the Hudson estuary. The water current effect is estimated by applying the ratio $k_{O'Connor}$ / $k_{Borges,}$ representing around 30% of the gas transfer velocity along the estuary which is elevated yet comparable to other European macrotidal estuaries such as the Scheldt (Borges et al. 2004b). The maximum contribution of the water current corresponds to the Inner Station owing to the reduced cross-section creating higher friction, but in no case it is comparable to the wind speed effect.

Following Borges et al. (2004b) consideration that the water current and wind speed have an additive result on the gas transfer velocity, it have been selected a combination of a) the wind speed parameterization proposed by Carini et al. (1996) based on tracer addition technique which allows a best estimated for long term spatial and temporal scales and also because of the morphological similarities between the Park River and

Table 3. Daily average wind speed, maximum tidal current speed, air-water CO_2 concentration gradient and different parameterization for CO_2 gas transfer velocity in the three sections of the Guadalquivir estuary. Gas transfer velocity relationship: k_{Borges} (wind+water current), k_{Clark} (wind), k_{Carini} (wind) and $k_{O'Connor}$ (water current). The Water current contribution (%) was calculated as the ratio $k_{O'Connor}/ k_{O'Connor}+ k_{Carini}$

	Outer Station	**Middle Station**	**Inner Station**
Wind speed (m s^{-1})	7.9±2.0	9.8±3.2	5.0±1.9
Maximum tidal current speed (cm s^{-1})	84 ±9	60±6	99±14
ΔpCO_2 (µatm)	362.3±116.2	601.1±32.2	673±59
k_{Borges} (cm h^{-1})	27.2± 4.8	32.6± 8	22.1±3.5
k_{Clark} (cm h^{-1})	17.6±7.6	27.6±13.6	8.6±3.5
$k_{Carinni}$ (cm h^{-1})	15.8± 3.9	17.3±6.5	10.4±2.8
$k_{O'Connor}$ (cm h^{-1})	7.1±1.9	6.1±1.9	8.0±2.4
Water current contribution %	30±8	28±15	41±12

Guadalquivir River estuaries; b) and the water current expression from O'Connor and Dobbins (1958). The additive result will be $k = k_{O'Connor} + k_{Carini}$.

Following Borges et al. (2004b) consideration that the water current and wind speed have an additive result on the gas transfer velocity, it have been selected a combination of a) the wind speed parameterization proposed by Carini et al. (1996) based on tracer addition technique which allows a best estimated for long term spatial and temporal scales and also because of the morphological similarities between the Park River and Guadalquivir River estuaries; b) and the water current expression from O'Connor and Dobbins (1958). The additive result will be $k = k_{O'Connor} + k_{Carini}$.

It have been calculated an average gas transfer velocity to avoid the high spatial and temporal heterogeneities associated with wind speed measurement and tidal current velocity. The average wind speed for the sampling period was 7.35 m s^{-1} with an average

tidal velocity reported of 0.54 m s^{-1}, and an integrative depth for all the estuary of 3 m. The resultant gas exchange velocity (k) for the Guadalquivir Estuary is 22.5 cm h^{-1}.

CO_2 flux to the atmosphere in the distinct sections of the Guadalquivir estuary evaluated using k were: 68.9 mmol m^{-2} d^{-1} in the Outer Station, 114.3 mmol m^{-2} d^{-1} in the Middle Station and 128 mmol m^{-2} d^{-1} in the Inner Station. The air-water CO_2 flux data has been summarized in table 4. The daily flux to the atmosphere can be calculated multiplying the CO_2 flux value by the area in question, with the result that CO_2 emissions in the Outer Station were 1.8 10^6 mol C d^{-1}, 0.85 10^6 mol C d^{-1} in the Middle Station and 0.63 10^6 mol C d^{-1} in the Inner Station. It may be pointed out that the estuary has been divided according to the salinity range and not the area- width distribution. This may explain the apparently disproportionate range of emissions values in the different stations. To calculate the average daily flux over the entire estuary, CO_2 emission for the entire estuary (the sum of the emissions calculated for each area) was divided by the total area estimated in the Guadalquivir estuary. The average daily flux in the Guadalquivir reach the 85.2 mmol m^{-2} d^{-1} and the total CO_2 emission is 3.2 10^6 mol C d^{-1}.

Opposite distribution between flux and emission is the common pattern found in estuaries. Recent several compilations are found about CO_2 emission in European inner estuaries (Abril and Borges, 2004, Borges, 2005, Frankignoulle et al., 1998) but no data up to this time has been available for the Guadalquivir Estuary. The average daily flux in the Guadalquivir estuary is analogous to the data found in Borges (2005) for the Sado (Portugal), Gironde (France) and Rhine (Netherland). Huertas et al. (2006) estimated than CO_2 fluxes in the continental shelf in front of the Guadalquivir estuary oscillated between a CO_2 source of 0.8 mmol m^2 d^{-1} in summer and a net uptake in October of 2 mmol m^2 d^{-1}. This is worth noting the intensity of the fluxes in the inner estuary compared to the continental shelf.

Table 4. Area, average air-water pCO_2 gradient, air-water CO_2 flux and CO_2 emission at each estuarine station in summer time. An average gas transfer velocity for the entire estuary of k= 22.5 cm h^{-1} has been used.

	Outer Station	Middle Station	Inner Station
Area (km^2)	26.24	7.39	4.95
ΔpCO_2 (µatm)	362.3±116.2	601.1±32.2	673.0±59
Air-water CO_2 Flux (mmol m^2 d^{-1})	68.9	114.3	128
CO_2 emission (10^6 mol C d^{-1})	18.1	8.45	6.33

3.4.-Carbon balance in the Guadalquivir Estuary

It has been approach the summer inorganic carbon balance which includes the fluvial DIC input, the DIC output to the Atlantic Ocean and the air-water flux of CO_2. In this case, the conservative DIC distribution along the estuary implies than river input and DIC export are compensated. This does not mean that no processes affect to DIC when it cross the estuary, then the CO_2 flux to the atmosphere must be balanced by net CO_2 production processes in the water column or sediment. These processes are organic matter degradation and calcium carbonate dissolution, the former producing CO_2 and the latter consuming CO_2. Nevertheless, for the average CO_2 flux to the atmosphere and average DIC concentration (85 mmol m^{-2} d^{-1} and 3 mmol kg^{-1} respectively) the one day emission to the atmosphere means 0.9 % of the total water column DIC budget, this is not so much meaningful compared to the high longitudinal DIC gradient in the Guadalquivir estuary.

DIC exported includes flux to the atmosphere, which reached 3.2 10^6 mol C d^{-1} with export to the Atlantic Ocean of 9.7 10^6 mol C d^{-1}. It can be concluded than 25% of the DIC

exported from the Guadalquivir Estuary is emitted to the atmosphere, and 30% of the riverine DIC is ventilated. The percentage of riverine DIC ventilated to the atmosphere is highly variable from one estuary to another. Among European estuaries, the Douro and the Randers Fjord currently represent the higher and lower boundaries of reported air-sea flux, respectively (Borges et al., 2006). Abril et al. (2000) estimated than in the Scheldt the riverine origin of CO_2 emission is about 10% while in the Randers Fjord the contribution reached 50%.

4. Conclusions:

The results presented in this study provide a description of the inorganic carbon distribution along the Guadalquivir estuary. The fluvial water is rich in TAlk and the estuary acts as a net exporter of TAlk and DIC to the adjacent coastal water. The TAlk river concentration presents a seasonal variability with higher concentrations in winter than in summer. The average DIC export from the Guadalquivir is 9.7 10^6 mol C d^{-1}. Although the behaviour of the TAlk and inorganic carbon is mainly conservative along the estuary some biogeochemical processes can co-occur such as the aerobic respiration processes in organic matter which produce CO_2 in the water column and the carbonate dissolution process that cause a slight decrease in CO_2 concentration in water, even when it is originated by the superficial sediment. Moreover, CO_2 efflux has been estimated from the CO_2 air-water gradients and gas transfer coefficients that account for the tidal current and the wind speed effects. Comparison of the different parameterization available was carried out.

Neither, the organic matter respiration nor the carbonate dissolution reaction play the major role, as is the case for many European estuaries, where internal DIC production is significant such as in the Scheldt and Loire. In this study case, these afore-mentioned processes have been proposed to balance the CO_2 flux to the atmosphere.

The average CO_2 flux to the atmosphere was 85 mmol m^{-2} d^{-1} while the total CO_2 emission to the atmosphere was 3.2 10^6 mol C d^{-1}. Ventilation of riverine CO_2 can contribute to the emission of the CO_2 from inner estuaries although it seems highly variable. In the Guadalquivir 25% of the carbon exported is emitted to the atmosphere.

Acknowledgments:

This work was supported by the Spanish CICYT (Comisión Interministerial de Ciencias y Tecnología) of the Ministerio de Educación y Ciencia under contract CTM2005-01364/MAR. Thanks to the crew of the R.V. Mytillus for the collaboration during sampling task.

References:

Abril G. and Borges A.V., 2004. Carbon dioxide and metahne emissions from estuaries. In: Trembaly, A., Varfalvy, L., Roehm, C., Garneau, M. (eds). Greenhouse gases emissions from natural enviroments and hidroelectric reservoirs: fluxes and processes. Springer, Berlin, Heidelberg, New York: 187-212.

Abril, G., Etcheber, H., Delille, B., Frankignoulle, M. and Borges, A. V., 2003. Carbonate dissolution in the turbid and eutrophic Loire estuary. Mar. Ecol. Prog. Ser., 259:129–138.

Abril, G., Nogheira, E., Etcheber, H., Cabecadas, G., Lemaire, E., and Brogueira M. J., 2002. Behaviour of organic carbon in nine contrasting European estuaries. Estuar. Coast. Shelf Sci., 54:241–262.

Abril, G., Etcheber, H., Borges, A.V., and Frankignoulle, M., 2000. Excess atmospheric carbon dioxide transported by rivers into the Scheldt estuary. Earth Planet. Sci. Lett., 330: 761– 768.

Abril, G., Etcheber, H., Le Hir, P., Bassoullet, P., Boutier,B. and Frankignoulle,M., 1999. Oxic/anoxic oscillations and organic carbon mineralization in an estuarine maximum turbidity zone (The Gironde, France). Limnol. Oceanog., 44:1304–1315.

Ballester, M.V., Martinelli, L.A., Krusche, A.V., Victoria, R.L., Bernardes, M. and Carmago, P.B., 1999. Effects of increasing organic matter loading on the dissolved O_2, free dissolved CO_2 and respiration rates in the Piracicaba River basin, southeast Brazil. Water Res., 33:2119–2129.

Beer, T. 1983. Environmental Oceanography: An Introduction to the Behavior of Coastal Waters. Pergamon Press, Oxford. 226 pp.

Benson, B. B. and Krause, JR., 1984. The concentration and isotopic fractionation of oxygen dissolved in freshwater and seawater in equilibrium with atmosphere. Limnol. Oceanogr., 29: 620–632.

Biswas, H., Mukhopadhyay, S. K., De, T. K., Sen, S. and Jana, T. K., 2004. Biogenic controls on the air-water carbon dioxide exchange in the Sundarban mangrove environment, northeast coast of Bay of Bengal, India. Limnol. Oceanogr., 49:95–101.

Borges, A.V., Schiettecatte L.-S., Abril G., Delille B. and Gazeau F., 2006. Carbon dioxide in European coastal waters. Estuar. Coast. Shelf Sci., 70(3): 375-387.

Borges, A. V.,2005. Do We Have Enough Pieces of the Jigsaw to Integrate CO_2 Fluxes in the Coastal Ocean? Estuaries, 28 (1): 3–27.

Borges, A. V., Delille, B., Schiettecatte, L.-S., Gazeau, F., Abril, G. and Frankignoulle, M., 2004a. Gas transfer velocities of CO_2 in three European estuaries (Randers Fjord, Scheldt, and Thames). Limnol. Oceanogr., 49:1630–1641.

Borges, A. V., Vanderborght, J.-P., Schiettecatte, L.-S., Gazeau, F., Ferrón-Smith, S., Delille, B. and Frankignoulle, M., 2004b. Variability of the gas transfer velocity of CO_2 in a macrotidal estuary (the Scheldt). Estuaries, 27:593–603.

Brasse, S. Nellen, M. Seifert, M. and Michaelis, W., 2002 The carbon dioxide system in the Elbe estuary. Biogeochemistry**,** 59(1): 25 – 40.

Cai, W-J., 2003. Riverine inorganic carbon flux and rate of biological uptake in the Mississippi River plume. Geophys. Res. Lett., 30(2): 1029-1032.

Cai, W.-J. and Wang, Y., 1998. The chemistry, fluxes, and sources of carbon dioxide in the estuarine waters of the Satilla and Altamaha Rivers, Georgia. Limnol. Oceanogr., 43:657–668.

Carini, S., Weston, N., Hopkinson, C., Tucker, J., Giblin, A., and Vallino, J., 1996. Gas exchange rates in the Parker River estuary, Massachusetts. Biol. Bull., 191:333–334.

Clark, J.F., Schlosser, P., Simpson, H.J., Stute, M., Wanninkhof, R. and Ho, D.T., 1995. Relationship between gas transfer velocities and wind speeds in the tidal Hudson River determined by the dual tracer technique. In: B. Jhane and E. Monahan (Eds), Air-Water Gas Transfer. AEON Verlag & Studio, Hanau, Germany, pp.785-800.

Clark, .F., Simpson, H.J., Smethie, W.M. and Toles, C., 1992. Gas exchange in a contaminated estuary inferred from clorofluorocarbons. Geophys. Res. Lett., 19:1133-1136.

DeGrandpre, M.D., Hammar, T.R., Wallace D.W.R. and Wirick, C.D., 1997. Simultaneous mooring-based measurements of seawater CO_2 and O_2 off Cape Hatteras, North Carolina. Limnol. Oceanogr., 42: 21-28.

Devol, A.H., Quay, P.D., Richey, J.E. and Martinelli, L.A., 1987. The role of gas exchange in the inorganic carbon, oxygen, and ^{222}Rn budgets of the Amazon River. Limnol. Oceanogr., 32: 235-248.

Frankignoulle, M., Abril, G., Borges, A., Bourge, I., Canon, C., Delille, B. Liebert, E., and Theate, J.-M., 1998. Carbon dioxide emission from European estuaries. Science, 282:434–436.

García-Luque, E., Forja, J.M. and Gómez-Parra, A., 2005.Characterization of atmosphere–water exchange processes of CO_2 in estuaries using dynamic simulation. J. Marine Syst., 58: 98–106.

Hellings, L., Dehairs, F., Van Damme, S. and Baeyens, W., 2001. Dissolved inorganic carbon in a highly polluted estuary (the Scheldt). Limnol. Oceanogr., 46(6):1406-1414.

Howland, R.J.M., Tappin, A.D., Uncles, R.J., Plummer, D.H. and Bloomer, N.J. 2000. Distribution and seasonal variability of pH and alkalinity in the Tweed Estuary, UK. Sci. Total Environ., 251/252: 125-138.

Huertas, E., Navarro, G., Rodríguez-Galvez, S. and Lubián, L.M., 2006. Temporal patterns of carbon dioxide in relation to hydrological conditions and primary production in the northeastern shelf of the Gulf of Cadiz (SW Spain). Deep-Sea Res. PT II, 53:1344-1362.

Jahnke, R.A. and Jahnke, D.B., 2000. Rates of C, N, P and Si recycling and denitrification at the US Mid-Atlantic continental slope depocenter. Deep-Sea Res. PT I, 47:1405-1428.

Khoo, K. H., Ramette, R. W., Culberson, C. H. and Bates, R. G., 1977. Determination of hydrogen ion concentrations in seawater from 5 to 40°C: standard potentials at salinities from 20 to 45°/‰. Anal. Chem., 49(1):29-34.

Körtzinger, A., Thomas, H., Schneider, B., Gronau, N., Mintrop, L., Duinker, J.C., 1996. At-sea intercomparison of two newly designed underway pCO_2 systems - Encouraging results. Mar. Chem., 52:133-145.

Liss, P.S.,1976. Conservative and non-conservative behaviour of dissolved constituents during estuarine mixing. In: Burton, J.D. and Liss, P.S. (Eds.), Estuarine Chemistry. Academic Press, New York, pp 93-130

Marino, R. and Howarth, R. W., 1993. Atmospheric oxygen exchange in the Hudson River: Dome measurements and comparison with other natural waters. Estuaries, 16: 433-445.

Mucci, A., 1983. The solubility of calcite and aragonite in seawater at various salinities, temperatures and one atmosphere total pressure. Am. J. Sci., 283:780– 799.

Neubauer, S. C. and Anderson. I. C., 2003. Transport of dissolved inorganic carbon from a tidal freshwater marsh to the York River estuary. Limnol Oceanogr., 48:299–307.

O'Connor, D. J. and Dobbins, W. E., 1958. Mechanism of reaeration in natural streams. Trans. Am. Soc. Civ. Eng., 123:641- 684.

Perez, F.F. and Fraga, F., 1987. A precise and rapid analytical procedure for alkalinity determination. Mar Chem., 21:169-82.

Raymond, P.A. and Cole, J.J., 2003, Increase in the Export of Alkalinity from North America's Largest River. Science, 301:88-91.

Raymond, P. A. and Cole, J. J., 2001. Gas exchange in rivers and estuaries: Choosing a gas transfer velocity. Estuaries, 24:312– 317.

Raymond, P.A., Caraco, N.F. and Cole., J.J., 1997. Carbon dioxide concentrations and atmospheric fluxes in the Hudson River. Estuaries, 20:381-390.

Roy, S., Gaillardet, J. and Allègre, C.J., 1999. Geochemistry of dissolved and suspended loads of the Seine river, France: Antropogenic impact, carbonate and silicate weathering. Geochim. Cosmochim. Ac., 63(9):1277-1292.

Sabine, C. L., Feely, R.A., Gruber, N. Key, R. M., Lee, K., Bullister, J. L., Wanninkhof, R., Wong, C. S., Wallace, D. W. R., Tilbrook, B. Millero, F. J., Peng, T.-H., Kozyr, A., Ono, T. and Rios, A. F. 2004. The oceanic sink for anthropogenic CO2. Science, 305:367–371.

Smith, S. and Hollibaugh, J. T., 1993. Coastal metabolism and the oceanic carbon balance. Rev. Geophys., 31:75–89.

Wang Z. A. and Cai, W.-J., 2004. Carbon dioxide degassing and inorganic carbon export from a marsh-dominated estuary (the Duplin River): A marsh CO_2 pump. Limnol. Oceanogr., 49:341–354.

Wanninnkhof, R., 1992. Relationship between wind speed and gas exchange over the ocean. J. Geophys. Res., 97 (C5): 7373-7382.

Weiss, R.F., 1974. Carbon dioxide in water and seawater: the solubility of a non-ideal gas. Mar. Chem., 2:203–215.

Wollast, R., 1998. Evaluation and comparison of the global carbon cycle in the coastal zone and in the open ocean. In: K. H. Brink and A. R. Robinson (eds.), The Global Coastal Ocean, Volume 10. John Wiley & Sons, New York, pp. 213– 252

Zappa, C. J., Raymond, P. A., Terray, E. A. and Mcguillis, W. R., 2003. Variation in Surface turbulence and the gas transfer velocity over a tidal cycle in a macro-tidal estuary. Estuaries, 26: 1401–1415.

Zhai, W.Z., Dai, M. Cai, W-J. Wang, Y.,and Wang, Z., 2005. High partial pressure of CO_2 and its maintaining mechanism in a subtropical estuary: the Pearl River estuary, China. Mar. Chem., 93, 21-32.

Capitulo 3

Variabilidad del sistema del carbono inorgánico en zonas costeras someras

Las zonas costeras comprenden una gran diversidad de ecosistemas y tipos geomorfológico entre los que se incluyen la plataforma continental, bahías, manglares, humedales, arrecifes de coral, estuarios, etc. De hecho, esta heterogeneidad es uno de los principales problemas a la hora de abordar y modelizar el ciclo global del carbono en las zonas costeras. En el caso de los manglares y las marismas, estos ecosistemas se consideran de forma conjunta, ya que ocupan el mismo nicho ecológico y presentan grandes similitudes en el ciclo del carbono así como en el intercambio de CO_2 agua-atmósfera. La principal diferencia entre ellos estriba en la latitud donde se localizan, ya que los manglares ocupan la franja tropical y subtropical, mientras que las marismas son características de zonas templadas.

Las zonas de marismas actúan como fuentes significativas de CO_2 a la atmósfera (Gattuso et al., 1998; Borges, 2005). Las emisiones de CO_2 a la atmósfera en la zona estuárica de estos sistemas están principalmente alimentadas por un balance heterotrófico entre producción y respiración, tanto en la columna de agua como en el compartimiento bentónico, debido fundamentalmente a los elevados aportes de materia orgánica. Sin embargo, la producción primaria de estos sistemas es relativamente baja en

la columna de agua, aunque varía en función de su geomorfología, tiempo de residencia, turbidez y disponibilidad de nutrientes entre otros factores (Alongi, 1998; Gattuso et al., 1998).

La dinámica del carbono inorgánico en estos sistemas costeros está altamente influenciada por la intensa remineralización bentónica de la materia orgánica en estas zonas, favorecida por la acción de bombeo que llevan a cabo las mareas que impulsan el flujo del agua intersticial desde los sedimentos al agua sobrenadante. En las zonas de marismas, además de las altas tasas de intercambio de carbono agua-atmósfera y agua sedimento, la exportación de carbono inorgánico hacia aguas costeras adyacentes también es muy elevada, suponiendo más del doble de las emisiones de CO_2 a la atmósfera (Wang y Cai, 2004; Borges, 2005).

La evolución futura de las emisiones de gases con efecto invernadero en las zonas costeras está directa e indirectamente ligada a los cambios socio-económicos en estas zonas. Esta relación directa se ve reflejada en el creciente aporte al mar de precursores de oxido nitroso, metano, dimetil sulfuro y CO_2. Estos precursores son principalmente nutrientes, materia orgánica y sulfatos (Pacyna y Mano, 2006). En relación con el desarrollo socio-económico de la población mundial, las principales amenazas que este supone a los sistemas costeros proceden de la creciente demanda de actividades derivadas de la industria naval, urbanísticas, actividades de recreo y turísticas, acuicultura e industralización.

Alongi (2002) señaló la actividad acuícola como una de las principales amenazas para la conservación de los manglares. Dadas las similitudes entre los sistemas de marismas y de manglares, es de esperar que sufran las mismas perturbaciones. En este sentido, Alongi (2002) identificó y enumeró los principales problemas asociados a la acuicultura como: la obstrucción y aislamiento de los caños de marea, alteración de los flujos de marea naturales, aumento de las tasas de sedimentación y turbidez en la columna de

agua, descarga de efluentes "contaminados", reducción en la calidad del agua, introducción de exceso de nutrientes, alteración en las cadenas tróficas, etc. La capacidad de adaptación de estos ecosistemas dependerá en gran medida de la intensidad de la perturbación, así como de sus características hidrodinámicas.

La calidad de las agua en las naves de cultivo acuícola se mantiene mediante un intercambio con el exterior, que generalmente se realiza por bombeo o aprovechando la acción de las mareas. La necesidad de mantener altas densidades de cultivo para rentabilizar las inversiones realizadas puede afectar a la calidad ambiental de lo sistemas que actúan como receptores de estas aguas residuales de las piscifactorías.

Los vertidos que se generan en la acuicultura tienen una naturaleza compleja (Barg, 1992). El contaminante principal está constituido por la materia orgánica particulada, formado tanto por heces y seudoheces de los organismos cultivados como por restos de piensos no consumidos. Además, cuando el engorde se realiza en estanques de tierra, y como consecuencia del movimiento de los peces, suele existir una cantidad importante de sólidos inorgánicos que procedes de la resuspension de arenas y lodos. También se han señalado importantes algunos derivados metabólicos, fundamentalmente el amonio y el carbono inorgánico. Además, en los sistemas afectados por los vertidos de las granjas acuícolas, y limitado a la zonas mas próxima al punto de vertido, el metabolismo bentónico en estas zonas es hasta 10 veces mayor que en zonas costeras naturales. A pesar de que existe una estacionalidad de estos flujos bentónicos asociada al ciclo anual de temperatura en el sistema así como derivada de los ciclos de producción de las granjas, los flujos bentónicos mínimos que se detectan en invierno siguen siendo bastante superiores a los observados en zonas costeras naturales (Holmer y Cristensen, 1992).

Sin duda, además de los aportes de materia orgánica, uno de los impactos mas significativos en el medio es la eutrofización causada por la excesiva acumulación de

nutrientes. La alteración del equilibrio natural de los nutrientes en el medio puede llegar a inducir cambios importantes en la estructura y composición del fitoplancton, aunque su crecimiento en ambientes con altos aportes de nutrientes está limitado o controlado por el tiempo de residencia del agua en el sistema (Pitta, 1996)

Los sistemas de marismas de distintas zonas costeras del sur de la Península Ibérica se están dedicando cada vez con mayor intensidad a la actividad acuícola. En la Bahía de Cádiz, el modelo utilizado es el de piscicultura intensiva en estanques de tierra construidos en el espacio que ocupaban anteriormente las antiguas salinas. Estas se extendían sobre una superficie de unas 57000 Ha de terreno, en su mayoría en la región intermareal (aproximadamente sobre un 60%) y su transformación en piscifactorías es por el momento parcial. Además, vista la riqueza medioambiental que existe en la Bahía de Cádiz, se hace imprescindible detectar, y en cualquier caso controlar, las posibles alteraciones que desequilibren un sistema tan sensible como son los caños de marea y las marismas de la Bahía de Cádiz.

El presente estudio se ha centrado en uno de los caños más importantes y característicos de la zona, como es el Río San Pedro. Si se recorriese el caño en su totalidad, nos encontraríamos con los paisajes (playas, pinares, marismas inundables, marismas desecadas) y actividades (acuícolas, naval, investigadora recreativas, etc.) más característicos de la Bahía de Cádiz.

En este capítulo se aborda el estudio del caño de marea del Río San Pedro desde el punto de vista del sistema del carbono inorgánico. Así pues, se ha evaluado la variabilidad temporal del carbono inorgánico y pCO_2, junto con otras variables ambientales como son el oxigeno disuelto y la clorofila. Dicha variabilidad ha sido analizada a distintas escalas temporales desde la mareal, hasta la estacional. También se han estimado los flujos de CO_2 agua-atmósfera, así como la exportación de CID con las mareas hacia las aguas adyacentes de la Bahía de Cádiz.

El Río San Pedro antiguamente podía considerarse un afluente del Río Guadalete que fue cortado de modo artificial a mediados del siglo XX al realizarse la desecación de parte de las marismas situadas al norte de Puerto Real, por las que discurría. La desecación (5500 ha) puede ser hoy considerada como la acción de mas impacto llevada a cabo en la historia de esta zona, ya que supuso la perdida de la mitad de la superficie natural de la bahía interior y ocasionó el corte del Río San Pedro y la desecación de gran parte de su cauce, lo que condujo a un cambio importante en la hidrografía de la zona (Gutiérrez et al., 1991). Así pues es necesario remarcar que, actualmente el Río San Pedro es en realidad un caño de marea, con una longitud de unos 12 km. También en sus márgenes el Río San Pedro ha desarrollado una intensa actividad extractiva y recreativa, lo que le ha aislado considerablemente del antiguo sistema de marismas que lo rodeaba. Sin embargo, de todas estas actividades, la acuícola es la única que vierte sus efluentes sin tratamiento previo alguno, fundamentalmente la instalación localizada en la cabecera del caño.

La mayor parte experimental de este trabajo se desarrolló a lo largo del año 2004. Para los muestreos, se utilizaron las instalaciones destinadas al suministro de agua del centro de investigaciones piscícolas "Centro de Investigación y Cultivos Marinos, CICEM-El Toruño", situado a 7.5 km de la desembocadura y a 3.5 km del efluente de la granja. Esta infraestructura nos permitió la instalación del equipo de registro en continuo para la medida de la presión parcial del CO_2, la temperatura y la salinidad durante un total de 91 días, distribuidos estacionalmente en periodos de hasta un mes. De manera adicional a las medidas en continuo, se recogieron muestras discretas durante ciclos mareales, de entre 13 y 24 horas. A lo largo del 2004, se tomaron un total de 203 muestras para Alcalinidad total (AT) y pH, y 143 muestras para oxigeno disuelto (OD) y clorofila-a (tabla 3.1).

Tabla 3.1. Resumen de los muestreos llevados a cabo en el caño del Río San Pedro y Bahía de Cádiz, así como las fechas en la que se realizaron, variables medidas y numero de muestras (n). (RC: Registro en Continuo; pCO_2: presión parcial de CO_2; AT: alcalinidad total; OD: oxígeno disuelto; clorofila-a: Chl-a; SPS: sólidos en suspensión).

Localización estaciones	**Fecha**	**pCO_2**	**AT (n)**	**pH (n)**	**OD (n)**	**Chl-a (n)**	**SPS (n)**
Estación fija CICEM Río San Pedro	16 Feb 2004	RC	14	14	14	14	--
	19 Feb 2004	RC	25	25	13	13	--
	01 Mar 2004	RC	26	26	14	14	--
	27 Abr 2004	RC	25	25	13	13	--
	04 May 2004	RC	25	25	13	13	--
	19 May 2004	RC	26	26	13	13	--
	1 Jul 2004	RC	13	13	13	13	--
	12 Jul 2004	RC	13	13	13	13	--
	26 Jul 2004	RC	13	13	13	13	--
	07 Sept 2004	RC	13	13	13	13	--
	15 Sept 2004	RC	13	13	13	13	--
	13 Feb-8 Mar 2004	RC	--	--	--	--	--
	26 Abr - 26 May 2004	RC	--	--	--	--	--
	29 Jun-29 Jul	RC	--	--	--	--	--
	3 -21 Sept-2004	RC	--	--	--	--	--
12 estaciones longitudinales Río San Pedro	4 Jul 2003	--	12	12	--	--	12
	30 Oct 2003	--	12	12	--	--	12
Bahía de Cádiz	5 Jun 2003	RC	13	13	13	--	--
	7-8 Feb 2006	RC	26	26	26	26	--

Asimismo, con el fin de estudiar el gradiente espacial de concentraciones dentro del caño del Río San Pedro, se realizaron dos muestreos longitudinales en doce estaciones distribuidas desde la desembocadura hasta la cabecera del caño, en Julio y Octubre de 2003. En éstos se tomaron muestras discretas para TA, pH, y sólidos en suspensión. Además, para comparar las concentraciones características del caño y las de la aguas

adyacentes exteriores, se llevaron a cabo dos campañas a bordo del B. O. “Mytilus" en la Bahía de Cádiz en Junio del 2003 y Febrero del 2006 (ver tabla 4.1). En estas campañas se midió de manera continua salinidad, temperatura y la presión parcial de CO_2, y de manera discreta AT, pH y OD.

En el trabajo II describe la variabilidad temporal de la pCO_2 en el Río San Pedro, así como los principales factores de control en cada una de las escalas temporales de estudio. Para ello ha sido utilizada fundamentalmente la base de datos obtenida con el equipo de medida en continuo.

En el trabajo III se ha estudiado la variabilidad temporal del carbono inorgánico en el Río San Pedro, en tres escalas de tiempo distintas, desde la mareal hasta la estacional. Además, se ha evaluado el gradiente de concentraciones de CID desde el interior del caño hasta la Bahía de Cádiz. De forma adicional al CID, el estudio de las concentraciones de OD y Chl-a ayuda a esclarecer los principales mecanismos de control causantes de las variaciones encontradas.

Se ha observado un marcado gradiente espacial de las concentraciones de las distintas variables, correspondiendo los máximos valores de CID, pCO_2 y un pH más ácido la zona interna del caño, como consecuencia de los influencia del efluente de la granja acuícola y de los aportes terrestres.

A escala mareal, el patrón general observado en el caño corresponde a máximas concentraciones de pCO_2, CID en bajamar, mientras que las mínimas concentraciones se observan en pleamar. Asimismo, se observa que la salinidad es un buen trazador de la mezcla de agua y advección asociados a la marea. Utilizando la salinidad como trazador en la curva de dilución teórica, se advierte que el comportamiento del CID es prácticamente conservativo en la mayor parte de los muestreos. Sin embargo, la

variabilidad de los valores de la Chl-a y el oxígeno no parecen estar asociadas a la marea. Así pues, podemos decir que el Río San Pedro se aproxima a un sistema compuesto por dos masas de agua en sus extremos, de composición muy diferentes, y cuya mezcla está controlada por la acción de las mareas.

La amplitud de las variaciones mareales de la salinidad, CID, pCO_2 está modulada por el ciclo quincenal mareas muertas-vivas. Los valores en pleamar para CID y pCO_2 son menores en mareas vivas y mayores en mareas muertas, a consecuencia del distinto grado de dilución que experimentan las aguas del interior del caño con las aguas exteriores de la Bahía de Cádiz, ésta última con concentraciones menores de CID y valores mas homogéneos en el tiempo. A su vez, a lo largo del ciclo quincenal de mareas los valores de CID en bajamar son prácticamente constantes, sin embargo, la pCO_2 tanto en pleamar como en bajamar sufre un aumento con el tiempo de residencia, a consecuencia de un efecto sinérgico entre una menor dilución del efluente en mareas muertas, y el mayor tiempo para llevar a cabo los procesos de degradación de la materia orgánica. La chl-a también muestra un aumento en sus concentraciones con el tiempo de residencia, sobre todo en los meses de invierno.

Existe una estacionalidad significativa en los valores de pCO_2, CID, pH y consumo aparente de oxigeno (AOU). Dicha variabilidad estacional está relacionada directa e indirectamente con la temperatura del sistema. Por un lado, el aumento en la temperatura del agua esta ligado a un aumento de las tasas metabólicas que se corresponde con un aumento de la pCO_2 y el AOU y un descenso del pH en verano. Existe un segundo ciclo correspondiente al ciclo anual de producción de la granja acuícola, con un máximo de producción, y por tanto en la carga de materia orgánica y nutrientes, durante el verano.

En el trabajo II se han calculado los flujos de CO_2 agua-atmósfera. Estos flujos son una función del gradiente de concentraciones entre los dos compartimentos y de la

velocidad de transferencia. Así pues, la pCO_2 en el agua del Río San Pedro está saturada en CO_2 a lo largo de todo el año, llegando a ser diez veces mayores la pCO_2 en el agua que en la atmósfera. Esto determina que el Río San Pedro actúe como una fuente de CO_2 a la atmósfera a lo largo del todo el año con los máximos flujos resultantes en verano.

En el trabajo III se ha estimado el transporte de CID con las mareas. Debido a que las concentraciones de CID son siempre superiores en el interior del caño que en las aguas exteriores de la Bahía de Cádiz, se produce una exportación neta de CID, cuya magnitud es función del coeficiente de marea, siendo la máxima exportación durante las mareas vivas.

Bibliografía:

Alongi DM. 1988. Bacterial productivity and microbial biomass in tropical mangrove sediments. *Microb. Ecol.* 15:59– 79

Alongi, D. M., 2002. Present state and future of the world's mangrove forests. Environ. Conserv., 29:331–349.

Barg, U.C., 1992. Guideliness fro the Promotion of environmental managemenet of coastal aquaculture. FAO Fisheries Technical Paper, 328, 122 pp.

Borges, A. V., 2005. Do We Have Enough Pieces of the Jigsaw to Integrate CO_2 Fluxes in the Coastal Ocean? Estuaries, 28 (1): 3–27.

Gattuso, J.-P., Frankignoulle, M. and Wollast, R., 1998. Carbon and carbonate metabolism in coastal aquatic ecosystems. Annual Review Ecology Systematics, 29: 405-433.

Gutiérrez, J.M. Martín, A. Domínguez, S. y Moral, J. P.,1991. Introducción a la geología de la provincia de Cádiz, Servicio de publicaciones de la Universidad de Cádiz, Cádiz,

Holmer, M. y Kristensen, E., 1992. Impact of marine fish cage farming on metabolism and sulfate reduction of underlying sediments. Marine Ecology Progress Series 80:191-201.

Pacyna, J,M. y S. Mano, 2006. Trace gases in the European coastal zone. Estuarine, Coastal and Shelf Science 70:335-337.

Pitta, P. Apostolaki, E.T. Tsagaraki, T. Tsapakis, M. yKarakassis, I., 2006. Fish farming effects on chemical and microbial variables of the water column: a spatio-temporal study along the Mediterranean Sea. Hydrobiologia 563:99–108

Wang, C-F., Hsu, M-H. and Kuo, A. Y., 2004. Residence time of the Danshuei River estuary, Taiwan. Estuarine, Coastal and Shelf Science, 60:381-393.

Variability of the partial pressure of CO2 on a daily-to-seasonal time scale in a shallow coastal system affected by intensive aquaculture activities (Bay of Cadiz, SW Iberian Peninsula).

Mercedes de la Paz*, Abelardo Gómez-Parra and Jesús Forja.

Departamento de Química-Física, Facultad de Ciencias del Mar y Ambientales, Universidad de Cádiz, Campus Río San Pedro s/n, Puerto Real (Cádiz) 11510, Spain

Abstract

The present study describes the temporal variability of the water fCO_2 as well as the different driving forces controlling this variability, on time scales from daily to seasonal, in the Rio San Pedro, a tidal creek located in a salt marsh area in the Bay of Cadiz (SW Iberian Peninsula). This shallow tidal creek system is affected by effluents of organic matter and nutrients from the surrounding marine fish farms. Continuous pCO_2, salinity and temperature were recorded for four periods of approximately one month, between February and September in 2004. Major processes controlling the CO_2 variability are related to three different time scales. Daily variations in fCO_2 are controlled by the tidal mixing of the water from within the creek and the seawater that enters from the Bay of Cadiz. Significant cyclical variations of the fCO_2 have been observed with the maximum values occurring at low tide. On a fortnightly time-scale, the amplitude of the daily variability of fCO_2 is modulated by the variations in the residence time of the water within the creek, which are related to the spring-neap tide sequence. On a third time scale, high seasonal variability is observed for the temperature, salinity and fCO_2. Maximum and minimum values for fCO_2 were 380 μatm and 3760 μatm for February and July respectively. Data suggest that seasonal variability is related to the seasonal variability in discharges from the fish farm and to the increase with temperature of organic matter respiratory processes in the tidal creek. The fCO_2 values observed are in the same range as several highly polluted European estuaries or waters surrounding mangrove forests. From the air-water CO_2 flux computed, it can be concluded that the Rio San Pedro acts as a source of CO_2 to the atmosphere throughout the year, with the summer accounting for the higher average monthly flux.

Keywords: Carbon dioxide, salt marshes, seasonal variations, air-water exchange, aquaculture, Bay of Cadiz.

1. Introduction

Despite their relatively modest surface area, coastal zones play a significant role in the carbon biogeochemical cycle because they receive massive inputs of terrestrial organic matter and nutrients; they are among the most geochemically and biologically active areas of the biosphere; and they exchange large amounts of matter and energy with the open ocean (Gattuso et al., 1998). The waters of salt marshes and their surroundings are significant sources of CO_2 to the atmosphere. The air-water CO_2 fluxes in this system are fuelled by net heterotrophy in the aquatic and sediment compartment, while aquatic primary production is usually low in most salt marsh systems and creeks, varying with geomorphology, water residence time, turbidity and nutrients delivery (Alongi, 1998, Gattuso et al, 1998, Borges 2005).

The production of CO_2 in European coastal ecosystems, particularly estuaries, and the air-to-sea flux, has been studied in a few recent projects in the framework of EUROTROPH and the BIOGEST. Nevertheless, information on the production and air-water exchange in other coastal ecosystems like salt marshes are rather scarce.

Future changes to the sea-air emissions of trace gases in the coastal zone are both directly and indirectly related to changes in socio-economic and natural drivers of global change. The direct relationship between relevant socio-economic drivers and coastal trace gas emissions is illustrated by the increasing input of precursors of nitrous oxide, methane, DMS and CO_2 to the sea. These precursors include organic matter and nutrients.

Alongi (2002) pointed out the significant impact of urban development and aquaculture on mangroves. Given the similarities between the two systems, salt marshes can be expected to suffer similar disturbances. Global production of farmed fish and shellfish in coastal zones has more than doubled in the past 15 years (Naylor et al. 2000)

and as long as the human population continues to grow, present impacts will not diminish.

The Bay of Cadiz is becoming a focal point for intensive aquaculture in lagoons. The total area devoted to aquaculture in 1994 in the Bay of Cadiz was 29.2 10^6 m^2 including extensive, semi-intensive and intensive farming systems (Marquez et al., 1996). This development brings identified risks of negative environmental impact (Alongi, 2002). Attention has previously been focused on discharges of nutrients and organic matter, but thus far, only a limited number of studies are available on the CO_2 variability and water-sea exchanges in these systems.

The main objective of the present paper is to investigate the variability on various different time-scales of the partial pressure of CO_2 in the Rio San Pedro, a tidal creek running through the salt marsh area of the Bay of Cadiz; a secondary objective is to characterise the forces driving this variability, on scales from daily to seasonal periodicity. Daily air-water CO_2 fluxes have also been estimated

2. Material and methods

2.1. Study site

The Rio San Pedro is a tidal creek located in the Southwest of the Iberian Peninsula (Fig 1). Originally, it was a tributary of the Guadalete River, but it was artificially blocked 12 km from the river mouth during the 1960's. Tidal exchange is usually the primary driving force for interactions between the tidal creek and the Bay of Cadiz. The Rio San Pedro is subject to a semi-diurnal tidal regime with the height of the tidal column varying from 3.5m at spring tide to 0.5m at neap tide; the tidal creek has an average overall depth of between 3 and 5m. The water column is well mixed with no significant

differences between surface and bottom (Gonzalez-Gordillo et al., 2003). The main content of the Rio San Pedro is seawater except for occasional freshwater inputs from rainfall and land drainage inputs. The Bay of Cadiz is surrounded by a broad area of salt marshes subject to severe human pressure from increasing population density, as well as from the aquaculture and other industries discharging into the Bay and the salt marsh inlets. Although the landscape surrounding the Rio San Pedro was originally formed by an extensive area of salt marshes, progressive exploitation by the human population, such as salt marsh desiccation by blockage, fish farm construction, salt production factories, and other human activities, has significantly reduced the proportion of the area remaining as natural marsh. The actual channel of the Rio San Pedro is effectively isolated, laterally by mean of an embankment that separates the channel from the various industries that exploit the salt marsh environment, and the more inland reaches of the creek are restricted by a dam, which allows some water exchange between the upper salt marshes area and the tidal creek at times of very high water level. This human-made separation suggests that the influence of the salt marsh on the Rio San Pedro is only moderate. There is a fish farm located at the head of the creek. Tovar et al., (2000a) determined the loading of large quantities of dissolved nutrients, organic matter and suspended solids in the effluents of the marine fish farm, which is dedicated to the intensive culture of gilthead seabream (Sparus Aurata). It was estimated that 9105 kg of suspended solids, 843 kg of particulate organic matter, 36 kg of $N\text{-}NH^{+}_{4}$, 5 kg of $N\text{-}NO_2^{-}$, 7 kg of $N\text{-}NO_3^{-}$ and 3 kg of $P\text{-}PO_4^{3-}$ dissolved in saline water were discharged to the Rio San Pedro for each tonne of fish cultivated. The mean annual production of this fish farm is around 10^6 kg. This farm, with an extension of about 1,3 km^2, consists of a series of pools excavated in the sandy soil, with an average depth of 1m (Tovar et al, 2000a); the water volume of the farm is completely renewed once a day with the water of the Rio San Pedro.

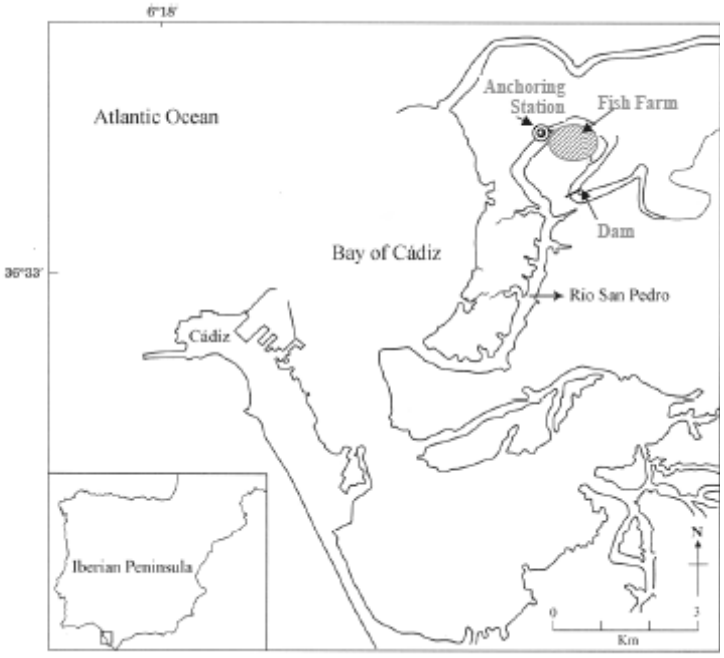

Figure 1: Map of the Bay of Cádiz and the Rio San Pedro. Locations of the sampling station and the fish farms are indicated.

2.2. Samplings and methods

Continuous monitoring of the CO_2 partial pressure, salinity and temperature was recorded at a frequency of 1 min intervals from the surface of water pumped from 1-2 m depth. The sampling times were distributed seasonally in four separate periods of approximately 1 month: 13th February to 8th March, 26th April to 26th May, 29th June to29th July, and 3rd September to 21st September. The sampling station was located 8 km distance from the mouth and 4 km from the head of the creek (fig 1, table 1)

Table 1: Range for physicochemical and meteorological data recorded for each sampling periods.

Sampling dates	Temperature (ºC)	Salinity	Cumulative precipitation (mm)	Wind speed (m s^{-1})	Evaporation (mm)
February (13 Feb-8 Mar)	11.5-18.3	19.8-35.2	768	1-9.7	89
May (26 Apr- 26 May)	16.5-24.0	31.0-35.7	674	1.9-12.2	173
July (29 Jun-29 Jul)	24.7-31.6	36.7-40.9	0	1-10.5	200
September (3 Sept-21 Sept)	22.2-27.3	35.6-39.7	0	0.5-7.7	125

Water salinity and temperature were measured, using a SeaBird thermosalinometer (Micro-SeaBird45), at the water intake of the pump and before its entry into the gas equilibrator. The equilibrator design is a combination of shower and bubble type similar to the system described by Koertzinger et al (1996). The CO_2 mole fraction (xCO_2) was detected by means of a non-dispersive infrared gas analyzer (Li-Cor 6262) which was calibrated daily using two standards of 523 ppm and 3000 ppm. Additional gas mixtures made and certified by Air Liquide (France) where used which have certified concentrations for CO_2 of 244.7 ppmv 998 ppmv. The temperature difference between the equilibrator and the water surface was around 0.7 ºC.

The water saturated CO_2 fugacity (fCO_2) in the equilibrator was calculated from the xCO_2 in dry air, atmospheric pressure and equilibrium water vapour, according to the protocol described in DOE (1994). The formulation proposed by Takahashi et al. (1993) was employed for the partial pressure corrections to *in situ* water temperature.

In addition to the fCO_2 in the water, the atmospheric CO_2 molar fraction was measured at a frequency of 30 minutes. Monthly averaged atmospheric fCO_2 data were calculated for the CO_2 flux estimation.

Meteorological data including the daily precipitation, wind speeds and air temperature data-base were provided by the Instituto Nacional de Meteorología from a station located about 15 km from our sampling station.

2.3. Hydrodynamic setting

The residence time of water within an aquatic system, or the length of time taken effectively to flush the system, is the strongest physical influence on water quality in the system. Residence time is often difficult to measure, so reliable estimates may be derived through the use of appropriate models (Sanford et al., 1992). In the case of the Rio San Pedro, this is a tidal creek where the only water input is by tidal exchange, not with the sea directly but with the Bay of Cadiz. The most predictable mechanism for flushing a small, well-mixed tidal system is the regular rise and fall of water of the astronomical tide, but a number of other factors also can affect the flushing, for instance winds, precipitation, and land drainage; however none of these are as predictable as the astronomical tides (Sanford et al., 1992).

Systems that are not well-mixed are likely to exhibit internal gradients of concentration, with areas remote from the open seawater mouth flushing more slowly than the rate predicted by tidal prism models. This is the case of the Rio San Pedro system, which present a marked salinity gradient between the two bay outlets and the inner creek parts.

The water renewal, expressed as the percentage of water volume that leaves the tidal creek each tidal cycle, has been selected as the variable for relating the physico-chemical parameters of the Rio San Pedro with the water transport; actually this variable is the inverse of the flushing time:

$$\%\text{water renewal} = \frac{P}{(P+V)}$$

where P is the tidal prism volume — the water volume between low tide and high tide — and V is the water volume at low tide. Information must be available on the geometry of the channel and tidal elevations. The dimensions of the channel have been approximated to a constant width of 110 m, a datum depth of 3m, and a length of 12 km. The heights at low and high tide have been obtained from the 2004 tide table provided by the Instituto Hidrográfico de la Marina.

The water budget can be complemented with the salt budget in order to perform a consistence test and to check the values obtained for V and P for each tidal cycle. Hence, a theoretical average salinity value can be calculated from the height at low and high tide and a constant salinity in both ends of the channel. The theoretical average salinity (S_T) can be formulated as:

$$S_T = (S_B\, P + S_c\, V\,)/\,(P+V)$$

Where S_B and S_C are the salinity in the Bay of Cadiz and in the inner part of the San Pedro creek respectively.

The measured and theoretical tidal average salinity values can be compared in figure 2. The similarity between real and estimated salinity proves that on a fortnightly scale the variability in salinity is associated with the spring-neap tidal cycle; it also provides a check on the reliability of the V and P volumes estimated.

The maximum difference between the real and estimated value is around 1%, this is considerably less than the range of salinity values between high and low tide.

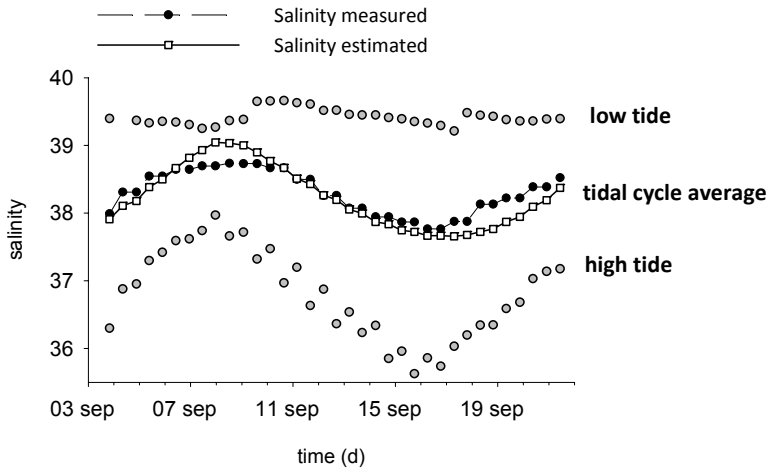

Figure 2: Salinity measured at high tide, low tide, and daily average salinity for September. The calculated salinity (●) and measured salinity (□) has been included from the salt budget and tidal prism model.

In the months of February and May this salt budget approximation cannot be carried out since the pluviosity shifts the salinity values of the endmembers and does not allow the values to be considered constant on a fortnightly scale

3. Results

Figure 3 presents the time series for temperature, salinity and CO_2 fugacity recorded, for the four periods sampled in 2004 in the Rio San Pedro. The ranges recorded for physicochemical properties and meteorological data are also available in table 1.

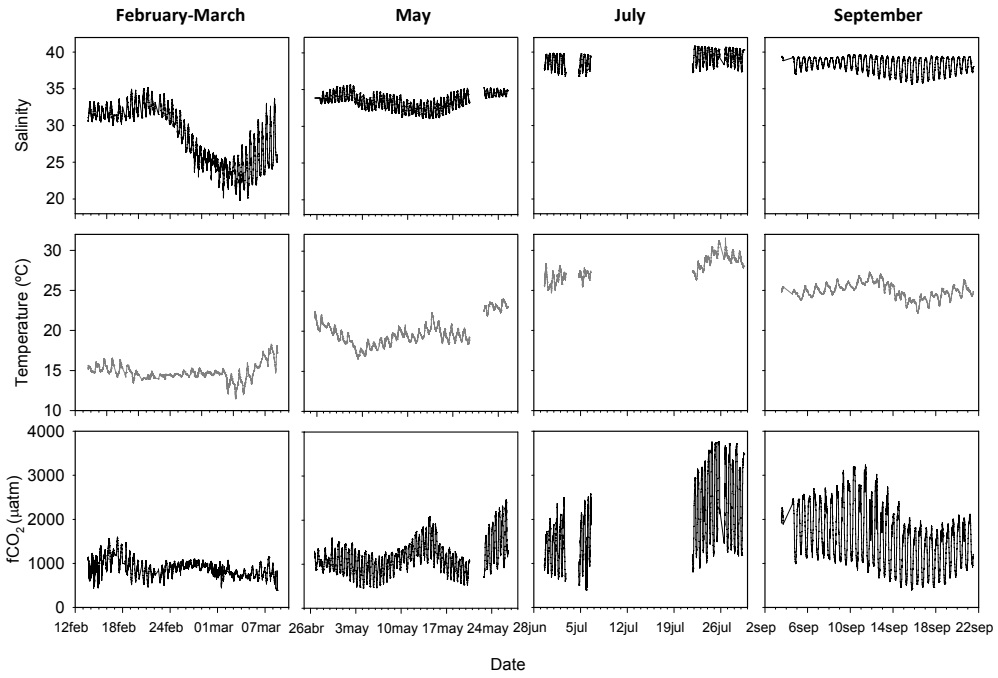

Figure 3: Variations of salinity, temperature and fCO_2 recorded for the sampling periods.

Temperature and salinity increase from February to July. The temperature of the system ranges between 12ºC on the first of March and 31ºC in July. The salinity value ranges between 20 in February and 41 recorded in July. The salinity in the tidal creek is strongly affected by the evaporation-precipitation ratio due to the shallowness of the system. Winter conditions are characterized by discrete precipitation, storms and diffuse land drainage inputs which make the water in the tidal creek fresher than the seawater of the Bay of Cádiz. The maximum salinity corresponds to a maximum in temperature and consequent evaporation in summer months.

The fCO_2 data reflect the high seasonal variability in the creek. Minimum fCO_2 values occurred in February, ranging between 383 and 1595 µatm, and the maximum in July, with a range between 389-3763 µatm. The amplitude of this oscillatory record increases

significantly from February to July, indicating the considerable CO_2 variability of each end of the tidal creek.

4. Discussion

The factors governing the fCO_2 variability must be discussed in relation to each different time scale: daily, spring-neap tidal cycle, and seasonal.

4.1. Daily variability.

In order to illustrate the daily variability the data recorded for salinity, temperature and fCO_2 in the Rio San Pedro have been plotted for one day in summer and winter as an example (fig 4). The tidal height is also given, displaying the semidiurnal signal typical of this area. Two patterns for salinity variability can be distinguished for winter and summer situations inside the tidal creek. The common tendency is that salinity tracks the tidal mixing with two maxima and two minima per day. Winter conditions are characterized by discrete precipitation, storms and lateral land drainage inputs making the water in the estuary fresher than the seawater of the Bay of Cadiz. The water of the Bay of Cadiz undergoes a smooth change in salinity compared to the tidal creek. Thus, the salinity shows a peak at high tide when the maximum water volume from outside has entered the creek. The summer situation is characterized by a total absence of freshwater inputs and the high temperature reached; as a result the creek water is more salty than the water from the Bay of Cádiz; thus high tide will be linked to a minimum in salinity. The daily temperature follows a day-night cycle and no temperature difference is observed between the two water masses (creek and bay). It presents high day-night variability (2-3 ºC) in summer as well as in winter, probably due to the shallowness of the estuary. Consequently, the salinity closely tracks the tidal mixing on a daily scale, even if there is a seasonal alternation in the sign of the slope of their relationship.

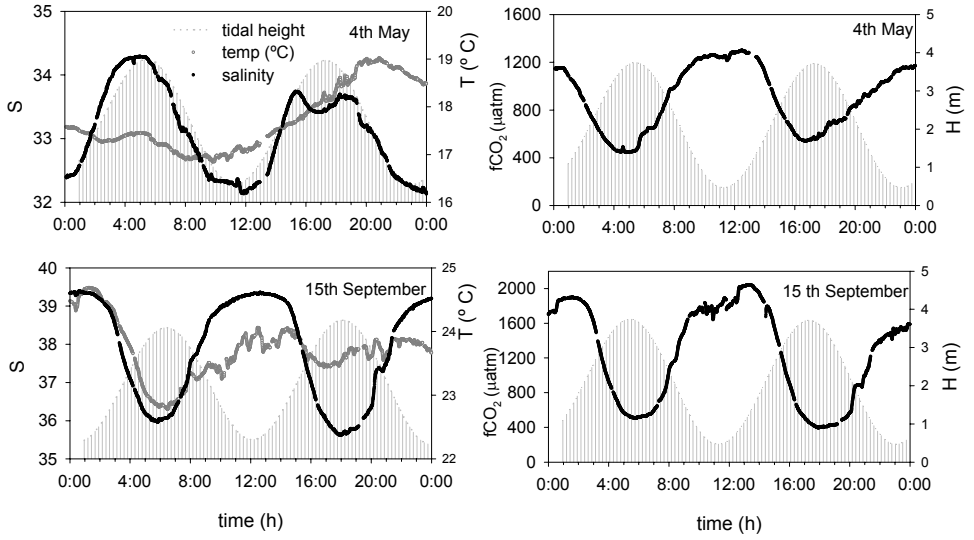

Figure 4: Daily variation of salinity (S), temperature (T), tidal height (H) and CO_2 fugacity (fCO_2) for May and September.

The CO_2 in the estuary is strongly influenced by the mixing of the two water masses of different CO_2 signature. In a daily time scale, the tidal cycle is the main mechanism responsible for CO_2 variations. Figure 4 presents the daily record for fCO_2 for winter and summer situations respectively. Maximum CO_2 values are linked to low tide, coinciding when the percentage of water from the inner creek is higher. Since the salinity changes it signature from winter to summer in the water of the creek, CO_2 peaks are linked to salinity minima in winter and to salinity maxima in summer.

The thermodynamics of temperature effects can be assessed according to Takahashi et al., (1993) using an average temperature for each sampling period. This method gives a correction of only 2% of the measured value, on average. Hence, it is suggested that the difference in the magnitude of fCO_2 between day and night is due to the different tidal height and not to effects of thermodynamics.

Despite the finding that, for the Rio San Pedro system, the mixing processes could explain most of the CO_2 variability reported in this study, the existence of other processes involved should be considered, such as production by respiration of organic matter in the water column, as well as in the benthic compartment (Wang and Cai, 2004).

4.2. Spring-neap tidal variability.

The variability over the time scale of spring and neap tides needs to be assessed by analysing the water renewal processes in the Rio San Pedro. Figure 5 displays the water renewal for each tidal cycle, the average daily salinity and the precipitation for the 4 samplings periods from February to September. The water renewal follows an oscillatory variation with fortnightly periods, and the amplitude depends on the tidal coefficient. It oscillates from 15 % to 50 % of water renewed from the Bay of Cádiz at neap and spring tides respectively. This corresponds to residence times for water in the tidal creek at the sampling station of 3.5 days to 1 day respectively. It is worth noting that a spatial gradient exist of the residence time (or water renewal) along the length of the channel, so the renewal will be much less in the innermost part of the channel.

The precipitation would directly affect the water volume of the creek. This can be observed in the salinity records of February and May, which show a continuous decrease in the average day salinity coinciding with the rainfall events (19-28 Feb) even though the decreased salinity lasts for 10 days afterwards, due to lags in the land drainage freshwater input. In May there is another rainfall event, which was more intense in quantity but only lasted 1 day, and resulted in a smaller decrease in average day salinity, which drops from 34.5 to 32.2. The water renewal (%) calculation does not include the water volume input from rain, hence for the rainy periods, the water renewal values will be underestimated.

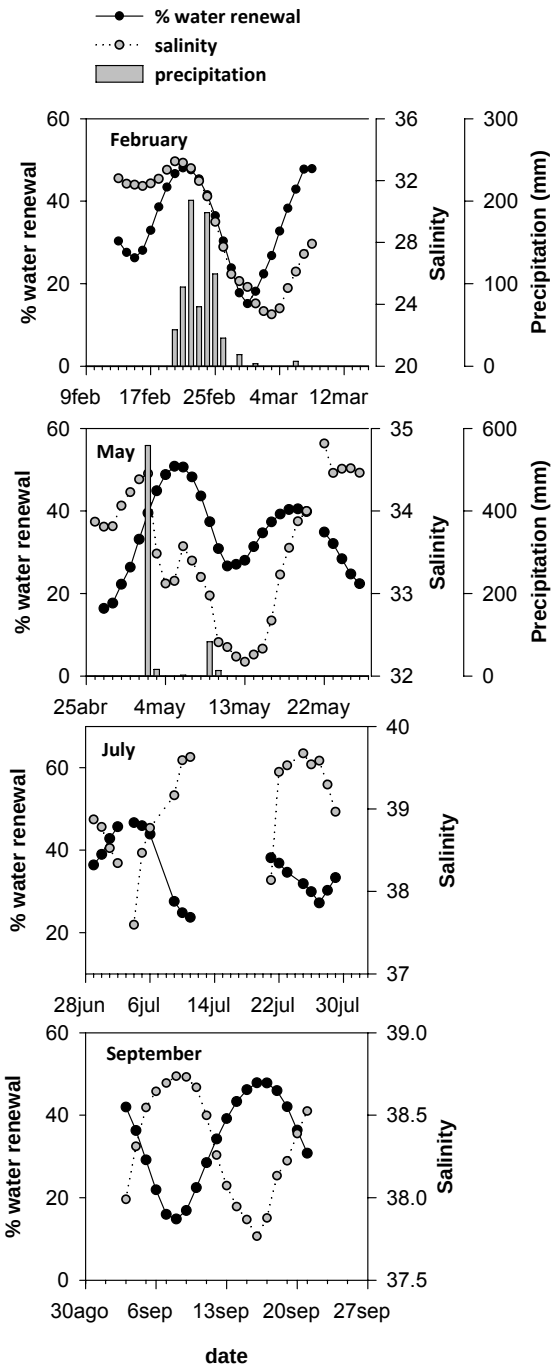

Figure 5: Variations in water renewal (%), salinity and precipitation for the sampling periods.

The complex geometry of the saltmarsh basin and the high surface/volume ratio in the zone of the fish farm causes a continuous and diffuse input of freshwater that is difficult to estimate. Apart from affecting the water and salt budgets, these lateral inputs also represent an important source of nutrients and organic matter. In the months of July and September, an inverse relationship can be observed between the average salinity and the % water renewal. These fortnightly spring-neap tide cycles can be significant in a long shallow channel and are a secondary mechanism of water mass movement along the tidal creek. This can have a major effect on the spatial distribution of dissolved compounds in salt marshes and mangrove systems (Dyer, 1997, Abril and Borges, 2004)

The salinity versus water renewal (%) (fig 6) shows that a direct relationship exists between high tide salinity and water renewal for dry months. In these periods, the salinity stays almost constant at low tide as a consequence of the low renewal of the water in the inner part of the creek. For rainy periods like February, salinity only loosely tracks the % water renewal due to land drainage inputs.

Figure 6 shows the fCO_2 high-tide and low-tide values for each tidal cycle versus % water renewal. In February and May the fCO_2-water renewal dependence is very loose due to the lateral inputs from land drainage caused by rainfall. The values are higher at low-tide than at high tide for all the samplings performed. Also, the maximum values correspond to lower water renewal rates (neap tide). The fCO_2 high-tide difference between spring and neap tides is 150 μatm in February, 180 μatm in May, 1300 μatm in July and 810 μatm in September; the value of these differences will depend on the seasonality of the two different parts of the water mass. In July and September there is a closer relationship between fCO_2 and water renewal due to the absence of land drainage inputs of rainwater. In dry months high tide fCO_2 variability seem to be linked to water advection, while low tide fCO_2 variability is linked to the consequences of the reduced renewal: less dilution from fish farm discharges and an increase in the organic matter

respiratory processes because of the longer residence time of the water in the inner part of the channel. It can be observed how, in the cycle from one high tide to next, the fCO_2 can increase or decrease by up to 25% (depending on whether it is from neap to spring or from spring to neap).

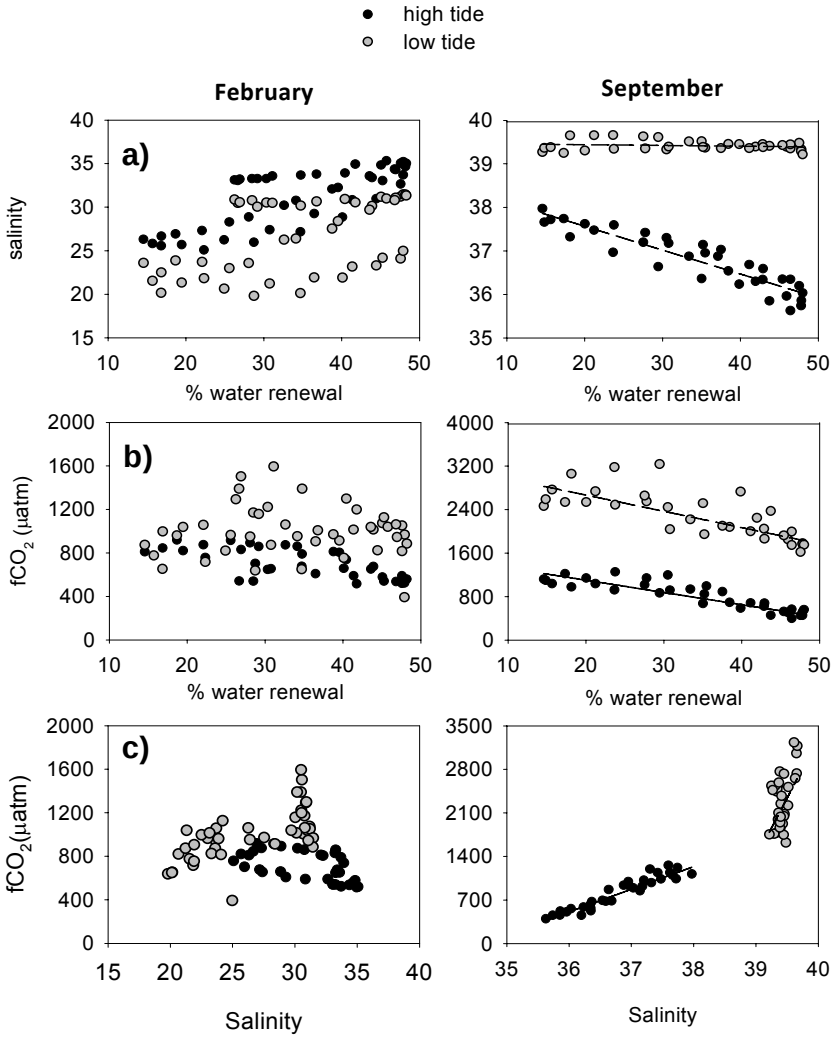

Figure 6: For February and September, as extreme cases. Relationships between: a) Salinity and water renewal (%) obtained for February and September; b) fCO_2 and water renewal (%); c) fCO_2 and salinity.

Furthermore, the fCO_2 at high tide and low tide versus salinity marks the difference in the water properties between the two ends of the tidal creek. Tovar et al., (2000a) studied the longitudinal distribution of various physico-chemical properties and found two zones. The first, with a length of about 8 km, extends from the mouth to the location of sampling station of this study, and the second zone from our station to the end of the creek (4 km length). Tovar et al. (2000a) found that the inner zone was strongly affected by the discharges from the fish farm, and that the outer part was more controlled by tidal renewal.

Therefore, the spring neap tidal variability on CO_2 seems to be controlled by the variability in the tidal water renewal in the creek, excepting for the rainy periods characterized by the allochtonous material inputs from diffuse land drainage.

4.3. Seasonal variability

As was shown in figure 4, the fCO_2 time series data reflect a high seasonal variability in the creek. In order to identify the factors driving this fCO_2 seasonality in the Rio San Pedro, the daily average values for salinity, temperature and fCO_2 have been calculated. Figure 7 shows the daily average fCO_2 for the overall annual database versus salinity and temperature. The minimum values for daily average fCO_2 occurred in February with 610 µatm and the maximum values are 2940 µatm measured in July.

A direct relationship exists between the fCO_2 and the water temperature, with a minimum in February and a maximum in July. The evolution of fCO_2 values is the result of several different interrelated processes that increase the fCO_2. Firstly, the discharges of effluent from the fish farm are highly seasonal. Tovar et al., (2000b) studied the seasonality in the outflow of the fish farm over a two year period. In this study, an increase in the fish production cycle was observed with the temperature, with a

maximum in summer and hence the maximum discharge of nutrients, dissolved organic carbon and particulate material to the tidal creek.

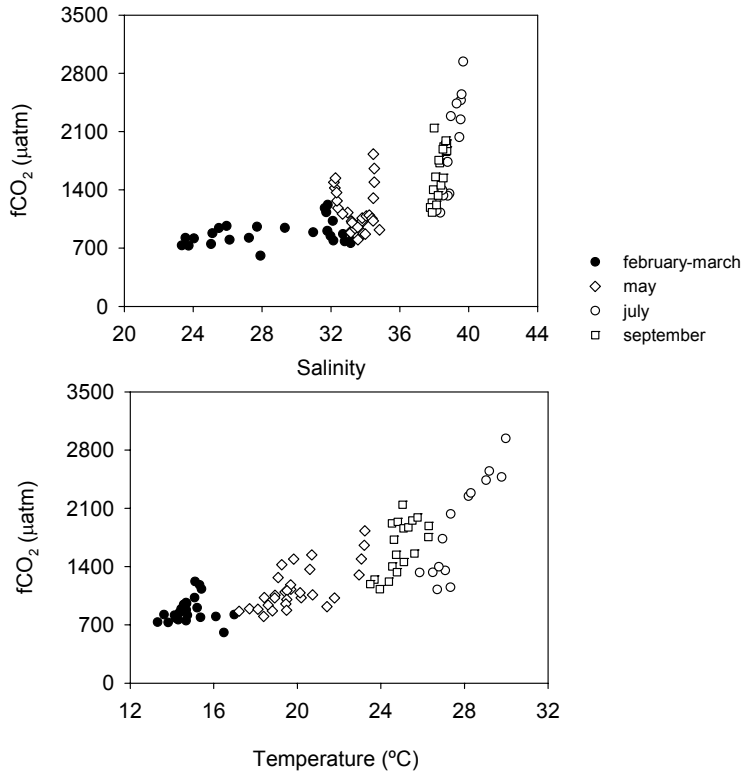

Figure 7: Relationship between fCO_2 and salinity and temperature. Data were obtained by averaging daily records for the entire data base available.

Secondly, the metabolic rates increase with the temperature in the water column of the tidal creek. This seasonal pattern, lower fCO_2 in winter and higher in summer months, has been described in several salt marsh systems like the Duplin River ((Wang and Cai, 2004) and the waters adjacent to salt marshes like the South Atlantic Bight (Cai et al., 2003). Wang and Cai (2004) suggested that temperature is probably a major factor

mediating the respiratory release of inorganic carbon from the marshes. This system dominated by salt marshes is characterised by high inputs of allochthonous dissolved inorganic carbon (DIC) and organic matter and by the importance of organic carbon respiratory processes. This seasonal pattern for CO_2 has been described for other biogases such as CH_4 and NO_2 in the Rio San Pedro by Ferrón et al (2006).

The seasonal dependence of the fCO_2 on the salinity is similar to its dependence on the temperature, although the relationship is strongly affected by the precipitation in the months of February and May (see fig 7).

In addition to the impact of temperature and fish farm effluent discharges on the high fCO_2 observed, the DIC dynamics in the water column of salt marsh systems is significantly affected by diagenetic degradation processes (Wang and Cai, 2004, Borges, 2005).

The fCO_2 range observed in the Rio San Pedro (380-3760 µatm) is high in comparison with open coastal water systems but is of the same order of magnitude as the mangrove system surrounding the Godavari estuary (Bouillon et al., 2003) and some highly polluted European estuaries for which information was compiled in several reviews of fCO_2 in coastal waters (Borges 2005, Borges et al 2006).

3.4. Air-water CO_2 exchange

The CO_2 flux to the atmosphere is a function of the CO_2 partial pressure air-water gradient (ΔpCO_2) and the gas transfer velocity (k). Despite the availability of highly accurate and precise methods for determining ΔpCO_2, the greatest source of uncertainty in the calculation of gas flux arises from the rate term k in both open and coastal environment processes (Borges et al. 2004b). Rivers and estuaries are systems where wind and boundary friction act as sources of turbulent energy. Therefore, two different parameterizations have been used in the computation of k: a) the relationship of k as a

function of wind speed, given by Carini (1996) and based on a SF_6 experiment in the Parker River, and b) the relationship from O'Connor and Dobbins (1958) for k as a function of the water current. The result obtained by Zappa et al. (2003) and Borges et al. (2004a) in estuaries emphasised the relevance of the water current contribution to water turbulence, especially under low wind conditions and it is concluded that the best k in estuaries is the site specific measurement. The CO_2 flux has been computed from the daily average data for water fCO_2, the wind speed and water current module, as well as the monthly averaged value for atmospheric fCO_2. The daily values for the sampling periods computed for the different gas transfer velocities, the air-water CO_2 gradient and the air-water CO_2 flux using the k proposed by Carini et al (1996) are shown in figure 8.

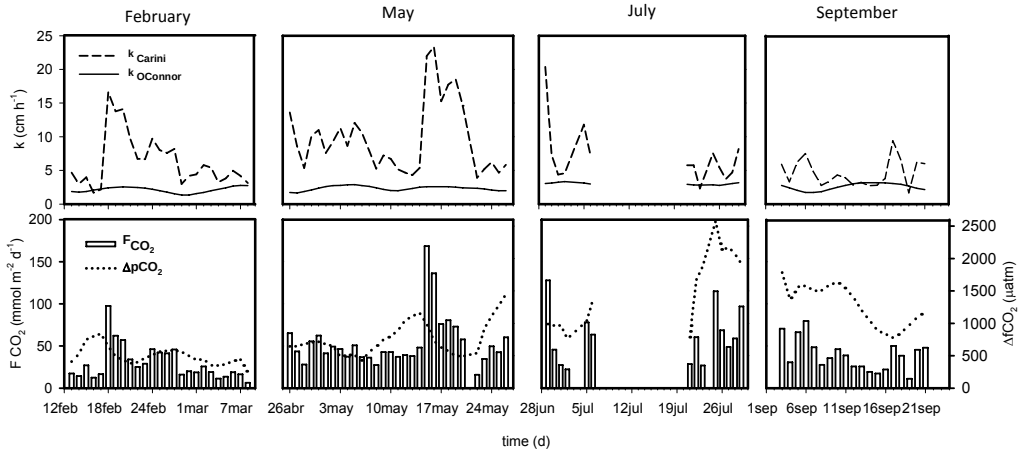

Figure 8: Annual variations in gas exchange velocity obtained with different parameterizations, air-water CO_2 gradient (ΔpCO_2) and air-water CO_2 flux.

The water current ranges between 5 and 20 cm s^{-1}, and the gas transfer velocities calculated using the formulation of O'Connor and Dobbins (1958) reach a maximum value of 3.3 cm h^{-1}(fig 8). On the other hand, the k calculated with the wind speed relationship of Carini (1996) has a maximum value of 23 cm h^{-1}. Because of the low values of water

current speed found in the Rio San Pedro, it has been considered that the water current contribution is not significant for the gas exchange in the Rio San Pedro compared to the wind speed; therefore the CO_2 flux has been calculated with the formulation of Carini (1996).

The CO_2 flux ranges from 6 to 168 mmol m^{-2} d^{-1}, the minimum occurring in February and the maximum in May (fig 8). Throughout the year the water of the tidal creeks acts as a source of CO_2 to the atmosphere. The CO_2 flux does not follow a clear seasonal pattern due to the temporal evolution of the wind speeds. Despite the ΔpCO_2 showing a marked seasonal pattern, the highest wind speeds are recorded in May and hence are accompanied by maximum CO_2 flux. The highest monthly average CO_2 fluxes are in July as a result of the combination of high wind speeds and ΔpCO_2. Monthly variability in the CO_2 flux is controlled by the wind speeds.

4. Conclusions

The results obtained in the present study describe the temporal variability of the water fCO_2 in the Rio San Pedro, as well as the different forces driving this variability on time scales from daily to seasonal. On a daily scale, tidal mixing is the main factor controlling the fCO_2 variations. Higher fCO_2 is always in phase with low tide waters, when the water of the inner tidal creek is measured. On a fortnightly time-scale, a spring-neap tidal cycle is observed for the fCO_2 on the water surface. Neap tides lead to higher residence time of the water within the tidal creek, decreasing the direct outflows of the fish farm nutrients and organic matter effluent to the more open waters of the Bay of Cadiz, and this causes an increase in the fCO_2, due to organic matter respiratory processes. On the longest time scale considered, high seasonal variability is observed for the temperature, salinity and fCO_2. Maximum and minimum values for fCO_2 were 380 μatm and 3760 μatm for February and July respectively. Data suggest that seasonal

variability is related to the seasonal variability of discharges from the fish farm and to the increase with temperature of organic matter respiratory processes in the tidal creek. The fCO_2 values observed are in the same range as several highly polluted European estuaries and waters surrounding mangrove forests. From the air-water CO_2 flux computed, it can be concluded that the Rio San Pedro acts as a source of CO_2 to the atmosphere throughout the entire the year, with the highest average monthly flux occurring in July.

Acknowledgments:

This work was supported by the Spanish CICYT (Comisión Interministerial de Ciencias y Tecnología) of the Ministerio de Educación y Ciencia under contract CTM2005-01364/MAR. Thanks are expressed to CYCEM "El Toruño" for providing the infrastructures, and to Dr. O. Alvarez for generous assistance with the processing of hydrodynamic data.

References:

Abril G. and Borges A.V., 2004. Carbon dioxide and methane emissions from estuaries. In: Trembaly, A., Varfalvy, L., Roehm, C., Garneau, M. (eds). Greenhouse gases emissions from natural environments and hydroelectric reservoirs: fluxes and processes. Springer, Berlin, Heidelberg, New York: 187-212.

Alongi, D. M., 1998. Coastal Ecosystem Processes. CRC Press, Boca Raton, Florida.

Alongi, D. M., 2002. Present state and future of the world's mangrove forests. Environ. Conserv., 29:331–349.

Borges, A. V., Delille, B. Schiettecatte, L.-S., Gazeau, F., Abril, G.and Frankignoulle, M. 2004a. Gas transfer velocities of CO_2 in three European estuaries (Randers Fjord, Scheldt, and Thames). Limnol. Oceanogr. 49:1630–1641.

Borges, A. V., Vanderborght, J.-P., Schiettecatte, L.-S., Gazeau, F., Ferrón-Smith, S., Delille, B., and Frankignoulle, M. 2004b. Variability of the gas transfer velocity of CO_2 in a macrotidal estuary (the Scheldt). Estuaries 27:593–603.

Borges, A. V.,2005. Do We Have Enough Pieces of the Jigsaw to Integrate CO_2 Fluxes in the Coastal Ocean? Estuaries,28 (1): 3–27.

Borges, A.V., Schiettecatte L.-S., Abril G., Delille B. and Gazeau F., 2006. Carbon dioxide in European coastal waters. Estuar. Coast. Shelf Sci., 70(3): 375-387.

Bouillon, S., M. Frankignoulle, F. Dehairs, B. Velimirov, A. Eiler, G. Abril, H. Etcheber, and A. V. Borges, 2003, Inorganic and organic carbon biogeochemistry in the Gautami Godavari estuary (Andhra Pradesh, India) during pre-monsoon: The local impact of extensive mangrove forests. Global Biogeochem. Cy., 17(4), 1114, doi:10.1029/2002GB002026.

Cai, W.-J., Z. H. A. Wang, and Y. C. Wang. 2003. The role of marsh-dominated heterotrophic continental margins in transport of CO_2 between the atmosphere, the land-sea interface and the ocean. *Geophys. Res. Lett., 30(16):1849-doi: 10.1029/2003GL017633.*

Carini, S., Weston, N., Hopkinson, C., Tucker, J., Giblin, A., and Vallino, J., 1996. Gas exchange rates in the Parker River estuary, Massachusetts. Biol. Bull., 191:333–334.

DOE, 1994. In: Dickson, A.G., Goyet, C. (Eds.), Handbook of Methods for the Analysis of the Various Parameters of the Carbon Dioxide System in Seawater, Ver.2, ORNL/CDIAC-74.

Dyer, 1997. Estuaries: a physical introduction, Wiley J. (Eds), 2nd Ed, London.

Ferron, S., Ortega, T., Gomez-Parra, A. and Forja, J.M., *In press*. Seasonal study of dissolved CH_4, CO_2, and NO_2 in a shallow tidal system of the Bay of Cadiz (SW Spain). J. Marine. Syst.

Gattuso, J.-P., Frankignoulle, M. and Wollast, R., 1998. Carbon and carbonate metabolism in coastal aquatic ecosystems. Annual Review Ecology Systematics, 29: 405-433.

González-Gordillo, J.I., Arias, A.M., Rodríguez, A., Drake, P., 2003. Recruitment patterns of decapod crustacean megalopae in a shallow inlet (SW Spain) related to life history strategies. Estuar. Coast. Shelf Sci. 56, 593–607.

Körtzinger, A., Thomas, H., Schneider, B., Gronau, N., Mintrop, L., Duinker, J.C., 1996. At-sea intercomparison of two newly designed underway pCO_2 systems - Encouraging results. Mar. Chem., 52:133-145.

Márquez, C., Narváez, A., Pérez, M. C. and Ruiz, J. (1996) In Estudios para la Ordenacion, Planificacion y Gestion Integradas en las Zonas Humedas de la Bahia de Cadiz, ed. J. M. Barragan, pp. 303-323. Oikos-tau, Barcelona.

Naylor, R.L., Goldburg, R.J., Primavera J.H., Kautsky, N., Beveridge, M.C.M., Clay, J., Folke C., Lubchenco, J., Mooney, H. and Troell, M. (2000). Effect of aquaculture on world fish supplies. Nature 405: 1017–1024.

O'Connor, D. J. and Dobbins, W. E., 1958. Mechanism of re-aeration in natural streams. Trans. Am. Soc. Civ. Eng., 123:641- 684.

Sanford, L. P., Boicourt, W. C. & Rives, S. R. 1992 Model for estimating tidal flushing of small embayments. *ASCE Journal of Waterway, Port, Coastal and Ocean Engineering* 118 (6), 635–655.

Takahashi, T., Olafsson, J., Goddard, J.G., Chipman, D.W. and Sutherland, S.C., 1993. Seasonal variation of CO_2 and nutrients in the high-latitude surface oceans: a comparative study. Global Biogeochem. Cy., 7 (4), 843–878.

Tovar, A., Moreno, C., Manuel-Vez, M.P. and García-Vargas, M., 2000a. Environmental impacts of intensive aquaculture in marine waters. Water Res. 34, 334–342.

Tovar, A., Moreno, C., Manuel-Vez, M.P. and García-Vargas, M., 2000b. Environmental implications of intensive marine aquaculture in earthen ponds. Mar. Pollut. Bull. 40, 981–988.

Wang, Z.A. and Cai,W.-J., 2004. Carbon dioxide degassing and inorganic carbon export from a marsh-dominated estuary (the Duplin River): a marsh CO_2 pump. Limnol. Oceanogr. 49 (2), 341–354.

Zappa, C. J., Raymond, P. A., Terray, E. A. and Mcguillis, W. R., 2003. Variation in surface turbulence and the gas transfer velocity over a tidal cycle in a macro-tidal estuary. Estuaries, 26: 1401–1415.

Tidal-to-seasonal variability in the parameters of the carbonate system in a shallow tidal creek, Rio San Pedro (SW Iberian Peninsula).

Mercedes de la Paz*, Abelardo Gómez-Parra and Jesús Forja.

Departamento de Química-Física, Facultad de Ciencias del Mar y Ambientales, Universidad de Cádiz, Campus Río San Pedro s/n, Puerto Real (Cádiz) 11510, Spain

Abstract:

The main objective of the present study is to assess the temporal variability of the carbonate system, and the mechanisms driving that variability, in the Rio San Pedro, a tidal creek located in the Bay of Cadiz (SW Iberian Peninsula). This shallow tidal creek is affected by effluents of organic matter and nutrients from surrounding marine fish farms. In 2004, eleven tidal samplings, seasonally distributed, were carried out for the measurement of Total Alkalinity (TA), pH, Dissolved Oxygen and Chlorophyll a (Chl-a) using a fixed station. In addition, several longitudinal samplings were carried out both in the tidal creek and in the adjacent waters of the Bay of Cadiz, in order to obtain a spatial distribution of the carbonate parameters. Tidal mixing is the main factor controlling the Dissolved Inorganic Carbon (DIC) variability, showing almost conservative behaviour on a tidal time scale. The amplitude of the daily oscillations of DIC, pH and chlorophyll show a high dependence on the spring-neap tide sequence, with the maximum amplitude associated with spring tides. Additionally, a marked seasonality has been found in the DIC, pH and oxygen concentrations. This seasonality seems to be related to the increase in metabolic rates with the temperature, the alternation of storm events and high evaporation rates, together with intense seasonal variability in the discharges from fish farms. In addition, the export of DIC from the Rio San Pedro to the adjacent coastal area has been evaluated, obtaining a net export of 1.05 10^{10} g C yr^{-1}. The export of remineralised organic material from the proximal zone to the adjacent continental shelf plays a considerable role in the productivity of this oceanic region.

Keyword: Inorganic carbon, tidal creeks, temporal variability, DIC export, Rio San Pedro, Bay of Cadiz.

1. Introduction

Coastal environments represent important pathways between land and the open ocean that significantly modify the flows of matter and energy between these two systems. They receive and exchange considerable amounts of dissolved and particulate matter, including nutrients, freshwater, energy and contaminants (Smith and Hollibaugh, 1993; Gattuso et al., 1998). Significant progress has been made in understanding seasonal and inter-annual processes affecting oxygen and carbon dynamics in temperate estuaries, but fewer studies have undertaken in tidal marshes system and surrounding waters. Furthermore, the impact of diurnal variations of carbon and oxygen parameters on seasonal and annual carbon budgets is not well understood (Yates et al., 2007).

During the last century, the coastal ocean has been exposed to large perturbations, mostly related to human activities on land. Prolonged and intensive used of inorganic fertilisers in agriculture, changes in land use pattern, and discharge of industrial and urban waste have all contributed to the eutrophication not only of river water but also of coastal ocean waters on a global scale. Over the past 50 years, the fluxes of natural and synthetic materials from the terrestrial environment to the coastal margin have increased by a factor of 1.5 to 2 because of human-induced perturbations (Maybeck and Ragu, 1995). However, it is expected that the natural control mechanisms in the coastal margin system will serve to reduce and perhaps eliminate the effect of the perturbation within a relatively short period, and that these mechanisms are efficient enough to prevent the accumulation of “pollutants” and their byproducts (Rabouille et al. 2001). Therefore the synthesis of data on input, burial, and oxidation of organic matter, and organic carbon metabolism is critical for developing coastal ocean carbon budgets (Smith and Hollibaught, 1993).

The Bay of Cadiz is becoming a focal point for intensive and extensive aquaculture in former salt marsh areas. The risk of negative environmental impact associated with this

development has been identified (Alongi, 2002). Previously, attention has been focused on discharges of nutrients and organic matter, but to date, only a limited number of studies are available concerning the inorganic carbon evolution in these systems.

Previous studies have been undertaken in pristine systems such as in the temperate regions of the south-eastern United States along the coast of Georgia, a coastal area also largely dominated by salt-marshes (Cai and Wang, 1998; Cai et al.,1999). High rates of respiration in the sediments of intertidal marshes, and transport of DIC from marshes to estuaries during the tidal cycle are thought to be the primary controls on carbon and oxygen dynamics that create a net heterotrophy of the system (Cai et al, 1999). However, few studies have been carried out in Europe on the complex salt-marshes-tidal creek system and the impacts of human activities on them, for the purposes of quantifying diurnal and seasonal variations in carbon and oxygen system parameters by means of direct measurements.

We report results from the *in situ* measurement of carbonate system parameters, from tidal to seasonal scales, in the Rio San Pedro tidal creek, a shallow system in the SW of the Iberian Peninsula that is highly affected by terrestrial and anthropogenic inputs.

2. Material and methods

2.1. Study site

The Rio San Pedro is a tidal creek located in the Southwest of the Iberian Peninsula (Fig 1). Originally, it was a tributary of the Guadalete River, but it was artificially blocked 12 km from the river mouth during the 1960's. Tidal exchange is usually the primary driving force for interactions between the tidal creek and the Bay of Cadiz. The Rio San Pedro is subject to a semi-diurnal tidal regime with the height of the tidal column varying

from 3.5m at spring tide to 0.5m at neap tide; the tidal creek has an average overall depth of between 3 and 5m. The water column is well mixed with no significant differences between surface and bottom (Gonzalez-Gordillo et al., 2003). The main content of the Rio San Pedro is seawater except for occasional freshwater inputs from rainfall and land drainage inputs. The Bay of Cadiz is surrounded by a broad area of salt marshes subject to severe human pressure from increasing population density, as well as from the aquaculture and other industries discharging into the Bay and the salt marsh inlets. Although the landscape surrounding the Rio San Pedro was originally formed by an extensive area of salt marshes, progressive exploitation by the human population, such as salt marsh desiccation by blockage, fish farm construction, salt production factories, and other human activities, has significantly reduced the proportion of the area remaining as natural marsh. The actual channel of the Rio San Pedro is effectively isolated, laterally by mean of an embankment that separates the channel from the various industries that exploit the salt marsh environment, and the more inland reaches of the creek are restricted by a dam, which allows some water exchange between the upper salt marshes area and the tidal creek at times of very high water level. This human-made separation suggests that the influence of the salt marsh on the Rio San Pedro is only moderate. There is a fish farm located at the head of the creek. Tovar et al., (2000a) determined the loading of large quantities of dissolved nutrients, organic matter and suspended solids in the effluents of the marine fish farm, which is dedicated to the intensive culture of gilthead seabream (Sparus Aurata). It was estimated that 9105 kg of suspended solids, 843 kg of particulate organic matter, 36 kg of $N\text{-}NH^{+}_{4}$, 5 kg of $N\text{-}NO_2^{-}$, 7 kg of $N\text{-}NO_3^{-}$ and 3 kg of $P\text{-}PO_4^{3-}$ dissolved in saline water were discharged to the Rio San Pedro for each tonne of fish cultivated. The mean annual production of this fish farm is around 10^6 kg. This farm, with an extension of about 1,3 km^2, consists of a series of pools excavated in the sandy soil, with an average depth of 1m (Tovar et al, 2000a); the water

volume of the farm is completely renewed once a day with the water of the Rio San Pedro.

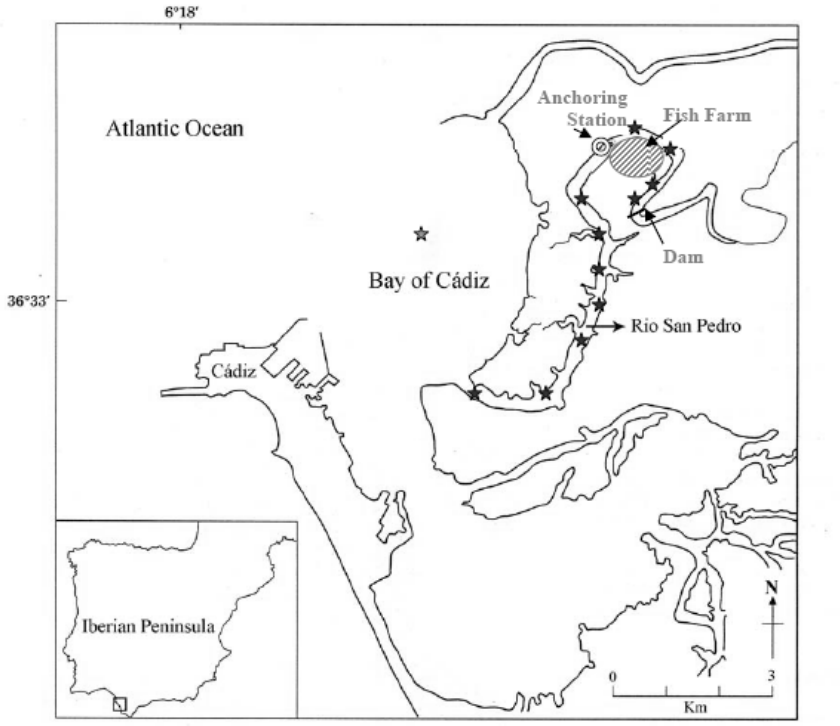

Figure 1. Location of the sampling stations along the Rio San Pedro. Longitudinal sampling station are indicated as black starts.

2.2. Samplings and methods

Several sampling strategies were carried out in order to characterise the temporal and spatial variability of the physicochemical properties in the Rio San Pedro and the adjacent Bay of Cadiz. To study the spatial gradient inside the tidal creek, two

longitudinal samplings were carried out at 12 stations, extending from the mouth of the creek to the upstream dam, on 4 June and 30 October 2003. Another 2 sampling campaigns were performed in the Bay of Cadiz, from on board the R/V Mytillus, to compare the characteristics of the salt marshes with those of more open coastal waters, in July 2003 and February 2006, as the two seasonal extremes. In addition, eleven tidal samplings were carried out at a fixed station located inside the tidal creek (see fig 1). Tidal samplings were seasonally distributed basically over four months covering a spring, neap and intermediate tide for each month (see table 1); those done in February/March and April/May lasted 24 hours for some of the variables (TA, DIC, salinity and temperature), whereas the July and September samplings lasted 12-14 hours. All the sampling locations are indicated in figure 1. Based on the seasonal temperature cycle, in this work seasons are defined as: winter (December-February), spring (March-May); summer (June-August) and autumn (September–November).

Subsurface water samples were taken in most of the samplings, continuously for temperature and salinity, and discretely for Total Alkalinity (TA), pH, Chlorophyll *a* (Chl-a) and Dissolved Oxygen (DO). Salinity and temperature were continuously recorded using a SeaBird thermosalinometer (SBD-45-MicroTSG) to which the water was supplied by an underway pump. The pH was measured using a glass-combined electrode (Methrom) calibrated in the Free pH Scale (Zeebe and Wolf-Gladrow, 2001). The alkalinity computation was made from the titration curve by means of the Gran Function and taking into account the correction for sulphate and fluoride interaction, using the constants proposed by Dickson (1990) and by Dickson and Riley (1979) respectively. For the dissociation of inorganic carbon, the K1 and K2 acidity constants proposed by Lueker et al. (2000) in the Total pH Scale were selected. The method was validated with reference standards obtained from A. Dickson (Scripps Institute of Oceanography, San Diego, USA) to an accuracy of ±2 μmol kg−1.

The oxygen was fixed in a sealed flask and stored in darkness for 24 h as described by the Winkler method, for later analysis by potentiometric titration (Metrohm 670 Titroprocessor). The Apparent Oxygen utilization (AOU) is defined as the deviation of oxygen from a DO concentration in equilibrium with the atmosphere calculated from the Benson and Krause (1984) solubility equation. Chlorophyll a (Chl-a) was determined in a glass fibre filter by fluorescence after extraction in 90% acetone (Turner Designs 10-AU). Suspended Particulate Matter (SPM) was determined in 500 mL of filtered water sampled following the methodology proposed by APHA (1992).

3. Results and Discussion

3.1. Spatial variability

Figure 2 represents the longitudinal gradient for SPM, DIC and pH in the Rio San Pedro tidal creek measured in June and October. There exists a pronounced spatial gradient for the three variables as a result of the impact of the aquaculture activities the outflow from which is located around 10 km upstream from the mouth of the creek. The SPM concentrations range from 10.8 mg L^{-1} at the mouth of the creek to 57.9 mg L^{-1} close to the wastewater discharge point. The DIC presents a maximum of 3240 ± 20 μmol kg^{-1} at the location of the wastewater discharge point and decreases almost linearly towards the mouth where the minimum concentration is 2560 ± 12 μmol kg^{-1}. The pH follows a similar longitudinal pattern, presenting a relatively acidic value (7.40±0.01) at the fish farm effluent discharge point and increasing towards the creek mouth to 7.83±0.03. Tovar et al. (2000a) studied the longitudinal distribution of various physico-chemical properties in the Rio San Pedro, and suggested that the low pH values in the fish farm effluent are due to the high ammonium concentration and to the acidic character of the faeces and fish food. Additionally, the large amounts of suspended solids present are

potentially one of the most serious environmental problems caused by aquaculture due to the decreased availability of light in the water and the inputs of organic particulate matter.

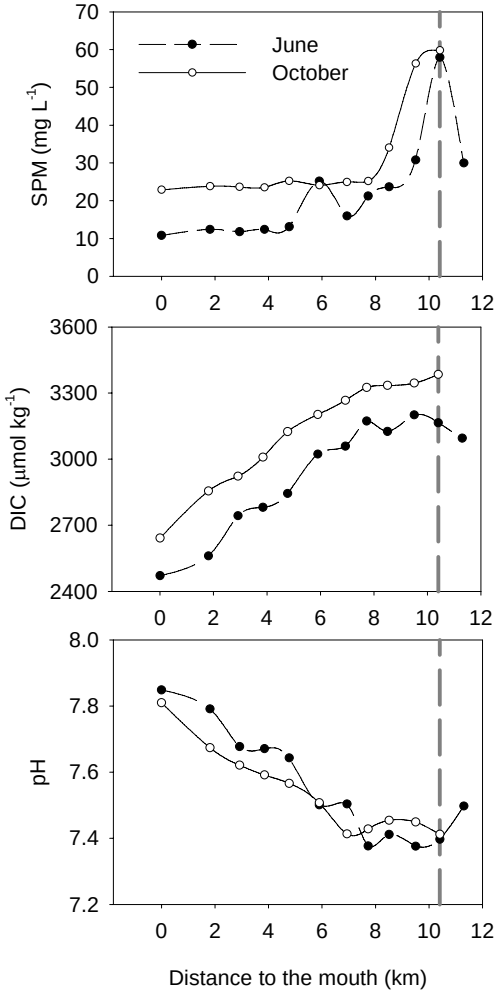

Figure 2. Longitudinal concentration gradients of suspended particulate matter (SPM), dissolved inorganic carbon (DIC) and pH along the Rio San Pedro. Locations of the sampling stations are described in figure 1.

The comparison of the physico-chemical parameters between the Bay of Cadiz and the Rio San Pedro helps in assessing the magnitudes of the various different processes taking place in the Rio San Pedro. Considerable differences in concentrations between the Rio San Pedro and the Bay of Cadiz were recorded. Two sets of data obtained in February and July in a sampled area in the Bay of Cadiz are presented as an example of the relative spatial heterogeneity in the values of the salinity and fCO_2 in the Bay compared to the values found in the Rio San Pedro (figure 3). In February the salinity is lower but increases with the distance from the coastline in February due to the rainwater and land drainage inputs, with an average value of 35.79±0.31, whereas in July the absence of significance freshwater inputs and increased evaporation rate gives a higher average salinity value of 36.67±0.24. Regarding the fCO_2 values, the average concentration ranges from 366 ±20 μatm in February to 455±39 μatm in July. It is notable that there is a change from CO_2 undersaturation to oversaturation from winter to summer due to the seasonal changes in temperature (14.6 - 24.2 ºC) as well as a change in the balance of primary production and respiration processes. In the Bay the fCO_2 variability in July is two times greater than in February but this is insignificant compared to the seasonal variability for fCO_2 found inside the Rio San Pedro tidal creek: the value recorded ranges from 380 in February to 3760 μatm in July.

The DIC concentration varies between 2125 ±28 μmol kg^{-1} in February and 2311 ± 20 μmol kg^{-1} in July. AOU ranges between 0.7 ± 20 μmol kg^{-1} in February and -15.5 ± 13 μmol kg^{-1} in July.

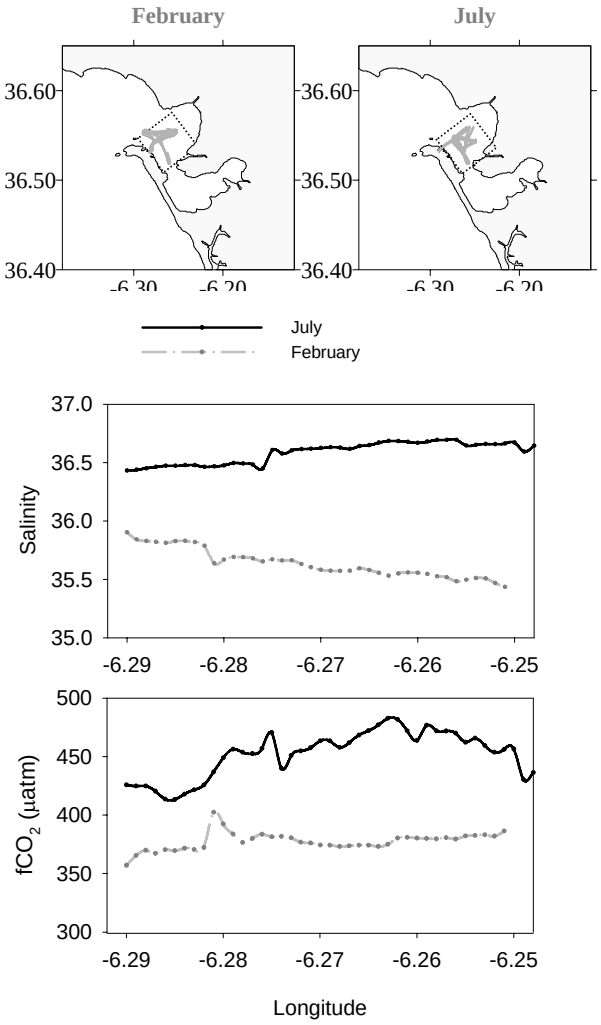

Figure 3. Spatial variability of salinity and CO_2 fugacity in the Bay of Cadiz, for February and July.

3.2 Temporal variability

Hydrochemical monitoring of tidal cycles seasonally distributed throughout the year allows the analysis of the effects of seasonal and daily fluctuations, as well as evaluation of the effects of the spring-neap tidal sequence.

3.2.1. Tidal (diurnal) variability

As an example, a set of tidal variations of temperature, salinity, DIC, TA, pH, Chl-a and AOU are depicted in figure 4; the range of concentrations and values measured for each tidal cycle are summarized in table 1. High temporal variability is found for all the variables during the tidal cycle. The common tendency is that salinity tracks the tidal mixing with two maxima and two minima per day. Winter conditions are characterized by discrete precipitation, storms and land drainage inputs making the water in the estuary fresher than the water of the Bay of Cadiz; thus the salinity shows a peak at high tide. The summer situation is characterized by total absence of freshwater inputs and the high temperatures and evaporation rates reached; as a result the creek water is saltier than the water of the Bay of Cadiz, and shows a salinity maximum at low tide. The daily temperature variability is related more to the solar insolation rather than to tidal mixing, as can be noted from the 24 hour samplings (February and May)

DIC and TA show maximum concentration at low tide and minimum at high tide throughout the year. The amplitude of the DIC and TA variability is highly dependent on the tidal coefficient, and proportional to salinity tidal amplitude. Tidal amplitude ranges from 286 to 278 μmol kg^{-1} and from 604 to 746 μmol kg^{-1} for TA and DIC values respectively. The differences in TA and DIC between day and night (February and March, Fig. 4), are proportional to salinity differences; this suggests that the influence of the daily biological cycle on TA and DIC is low. The minimum pH is generally observed at low

Table 1. Results from the tidal samplings in the Rio San Pedro for salinity, temperature. TA, DIC, pH, AOU, Chl-a and water renewal (%) values.

Date (2004)	**Salinity**	**Temperature** (ºC)	**TA** ($\mu mol\ kg^{-1}$)	**DIC** ($\mu mol\ kg^{-1}$)	**pH**	**AOU** $\mu mol\ kg^{-1}$	**Chl *a*** ($\mu g\ L^{-1}$)	**% water renewal**
16-Feb	30.1-33.5	14.8-16.5	2.86-3.15	2.79-3.08	7.54-7.73	3.2-32.6	0.8-4.5	28
19-Feb	30.6-35.3	13.5-15.0	2.54-3.14	2.40-3.16	7.53-7.84	9.1-49.4	1.4-2.1	43
01-Mar	20.2-25.7	12.5-15.2	2.81-3.12	2.76-3.04	7.57-7.78	-27.8-39.6	1.9-14.5	18
27Apr	33.1-34.8	18.9-21.6	2.57-2.87	2.48-2.77	7.51-7.87	-16.7-33.1	1.0-6.3	16
04-May	32.2-33.9	16.9-18.95	2.61-3.04	2.39-2.92	7.57-7.99	10.1-64.4	1.1-2.8	49
19May	32.7-35.1	18.4-20.3	2.75-3.31	2.55-3.18	7.61-8.16	10.7-33.0	1.2-2.5	41
01-Jul	36.9-39.8	26.1-28.1	2.56-3.08	2.33-2.96	7.48-7.84	20.5-120.5	3.1-9.1	43
12-Jul	38.4-40.4	25.6-27.3	2.83-3.17	2.71-3.11	7.31-7.59	26.6-63.5	1.1-5.7	24
26-Jul	38.4-40.6	29-31.4	2.80-3.13	2.69-3.09	7.31-7.80	32.4-67.5	1.5-7.8	30
07-Sept	37.8-39.2	24.5-26.1	2.83-3.15	2.74-3.11	7.37-7.58	17.8-49.8	1.6-6.5	16
15-Sept	35.7-39.3	23.4-24.1	2.55-3.13	2.33-3.07	7.42-7.89	-8.6-128.7	1.7-5.8	46

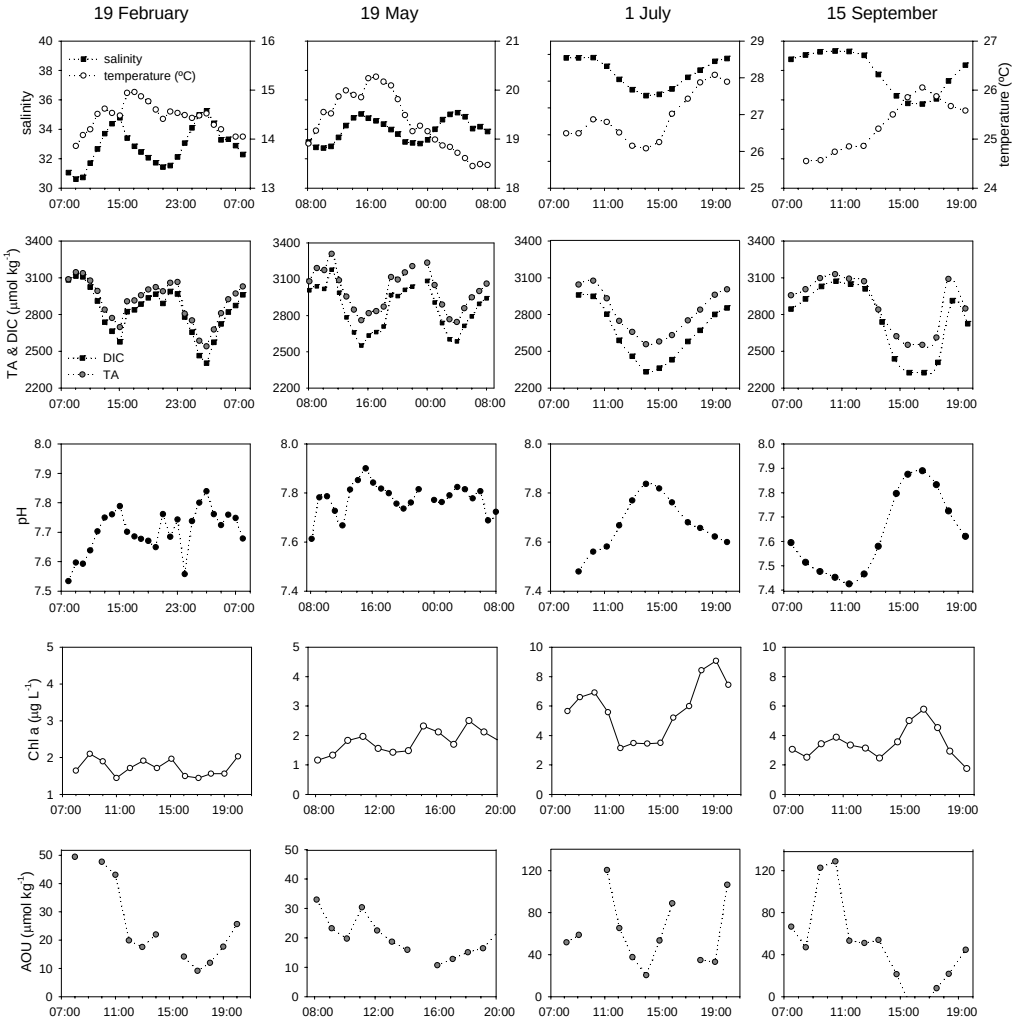

Figure 4. Tidal variability of salinity, total alkalinity (TA), dissolved inorganic carbon (DIC), pH, Chlorophyll -a (Chl-a) and apparent oxygen utilization (AOU) for four of the sampling dates. Most of the samplings are at spring tide, except one intermediate tidal coefficient on 19 May.

tide and maximum at high tide, although this pattern is more scattered for February and May. For most of the samplings, the AOU maximum is in the early morning and it decreases to a minimum in the hours of maximum solar irradiation and temperature (around 15.00 hours GMT); this finding is in good agreement with biological processes (balance production-respiration), unlike the behaviour of TA and DIC which seems to be linked to water level variations. The chlorophyll tidal pattern is very scattered for most of the tidal samplings, and no pattern associated with water level has been observed.

In order to study the conservative behaviour of the different physicochemical properties, the TA, DIC, Chl-a and AOU have been plotted versus salinity, to determine whether or not they follow a linear relationship. The results of the tidal sampling for spring and neap tides are shown in figure 5. The TA displays a conservative behaviour for most of the tidal sampling performed, and there is a good correlation versus salinity (the r^2 ranges between 0.81 and 0.98). Similarly, DIC presents a good linear fit versus salinity (with the r^2 ranging between 0.75 and 0.97). For both TA and DIC the slope of their fit versus salinity changes from negative in winter-spring to positive in summer-autumn due to the inversion in the salinity gradient in the tidal creek; however over the full year the maximum DIC and TA occur at low tide and hence in the innermost part of the creek. For the samplings carried out on 1 March and 4 May which are considerably affected by runoff, the r^2 drops to 0.4 and 0.2 for TA and DIC respectively, because of the inputs from land drainage. For the remaining dates, and especially for DIC and TA, the system could be described as two component endmembers whose mixing explains almost all the daily variability. In the case of the Chl-a and AOU, unlike inorganic carbon, for cases, no conservative pattern is observed.

Besides water mixing and advection, organic matter respiration in the water column (Cai and Wang, 1998) and benthic fluxes (Forja et al. 2004) are other mechanisms capable of influencing the tidal variability of inorganic carbon. Other authors emphasise the

relevance of lateral inputs of organic and inorganic carbon originating from the adjacent marshes via drainage and diffusion as the mechanisms that maintain the high respiratory rates usually found in salt marsh systems (Neubauer and Anderson, 2003; Wang and Cai, 2004). In the case studied here, however, the impact on the Rio San Pedro from the salt marshes has been largely reduced by human impact.

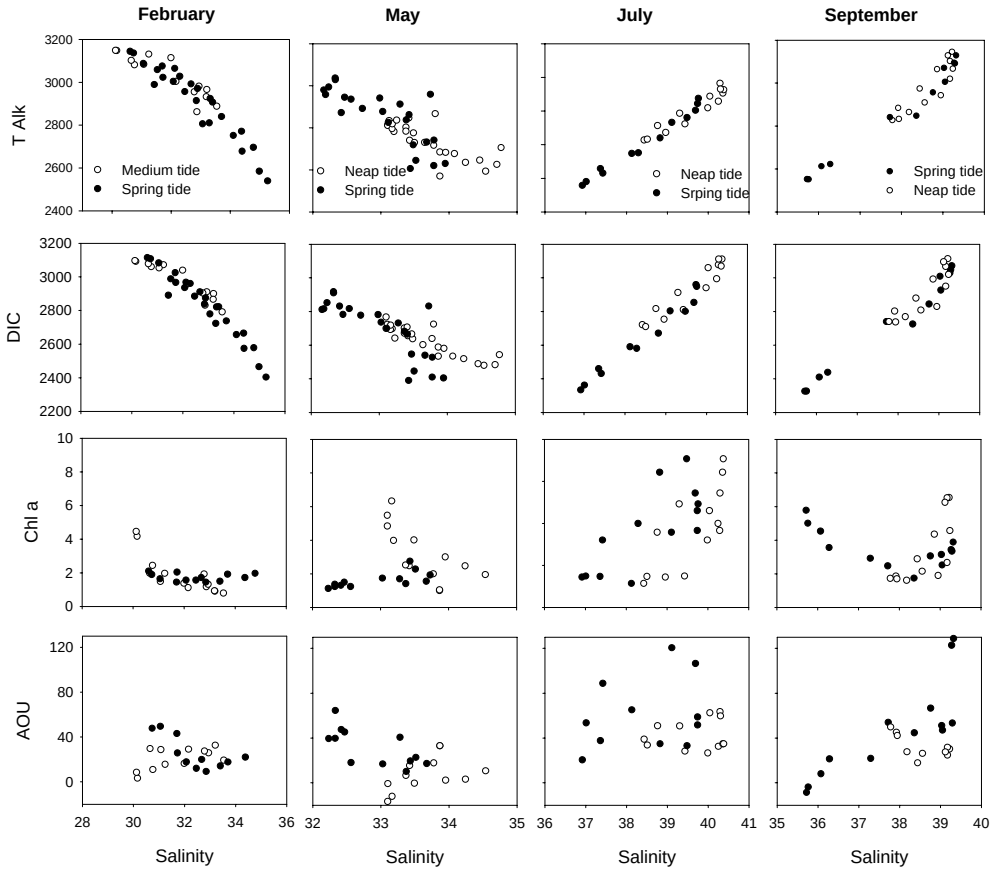

Figure 5. Total alkalinity (TA), dissolved inorganic carbon (DIC), Chlorophyll-a (Chl-a) and apparent oxygen utilization (AOU) versus salinity at spring and neap tides.

The Chl-a values exhibit high daily variability, but do not follow any reproducible tidal pattern nor theoretical dilution line. The reason for this could be that primary production activity is usually quite patchy in this system, due to the lateral inputs of nutrients from the salt marshes as well as the discharges of fish farm nutrients. It is possible that there is a spatial maximum Chl-a value, the location of which is a function of the balance between turbidity and nutrient availability, and that this maximum position is displaced with tidal movements in and out of the creek. This phenomenon has been previously described for other systems such as a Brazilian estuary (Pereira-Filho et al, 2001).

On a longer time scale, there is an evident spring-neap tidal cycle for most of the physicochemical properties as a function of the percentage of water renewal (see table 1). Water renewal has been calculated using the tidal prism method (Dyer, 1997) based on the tidal height chart provided by the Instituto Hidrografico de la Marina. In this context, DIC and TA show similar maximum low tide values for different water renewal percentages, while the minimum daily values, linked to high tide, decrease in line with the degree of dilution from the entry of water from the Bay of Cadiz. Similarly, the daily pH maximum increases with the water renewal. Chl-a presents higher values for neap tide than for spring tide. The explanation for this could be that an increase in the residence time of the water inside the creek favours the growth of the phytoplankton biomass when there are high concentrations of nutrients. In other estuaries the low residence time has been identified as the limiting factor for phytoplankton biomass growth, in spite of extremely high nutrient concentrations (Wang et al., 2004).

3.2.2. Seasonal variability

In order to assess the seasonal variability of the physicochemical properties and their controlling mechanism, the tidal average for DIC, salinity, pH, AOU and Chl-a have

been calculated for all the tidal samplings performed during 2004 (fig. 6). The seasonal pattern for salinity shows the precipitation-evaporation annual cycle, with minimum salinity observed in February, corresponding to a precipitation rate of 761 mm $month^{-1}$, followed by May, when a severe storm event occurred on 2 May (559 mm of precipitation), and a maximum salinity observed in July, when the precipitation was negligible. The annual precipitation in 2004 was 3802 mm, hence the period between February and May accounted for 56% of the annual precipitation. The annual maximum occurred in October (1055 mm $month^{-1}$), unfortunately not coinciding with our sampling period.

The seasonal amplitude in DIC variability is 186 μmol kg^{-1}, with the minimum observed in May and the maximum in February. The pH values range between 7.77 and 7.56 with the maximum reached in May and the minimum in July and September. Regarding the AOU and Chl-a values, a similar pattern is observed for both parameters, with minimum and maximum in February and July respectively. Different controlling mechanisms for DIC and pH, on the one hand, and AOU and Chl-a, on the other, explain the differences in the seasonal pattern.

Surprisingly, the maximum DIC values are observed in February, when fish farm activities are considerably reduced. Hence, this maximum is better explained by the land drainage inputs from the surrounded salt marshes and the soil washed out. This is accompanied by a relative decrease in pH due to the acidic character of the rain water drainage. Additionally, the carbonate dissolution processes, which would increase the DIC and TA concentration in the water column, are favoured at lower temperatures. This hypothesis holds well with the values of around 1 for the aragonite saturation index (calculated from Mucci, 1983) found in February. In summer and autumn, the degradation of organic matter together with intensified fish farm production would cause an increase in the TA and DIC concentration, in addition to a decrease in pH.

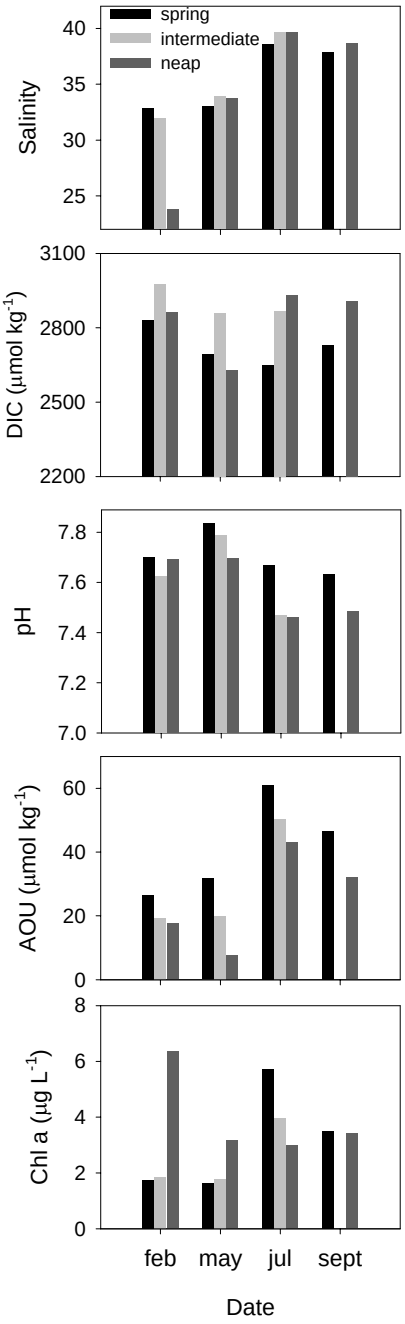

Figure 6. Seasonal evolution of salinity, dissolved inorganic carbon (DIC), Chlorophyll-a (Chl-a), apparent oxygen utilization (AOU) and pH.

The positive value of the AOU over the full year indicates that respiratory processes of the organic matter exceed those of photosynthesis. Its seasonal variability will be related to the seasonality in the organic matter concentration in the system, in addition to the temperature dependence of the metabolic rates, which explain the progressive increase in AOU values towards their maximum in summer. The seasonal evolution of Chl-a will be determined by the availability of nutrients. However, following the observation by Tovar et al. (2000a), the seasonal pattern of nutrients in the Rio San Pedro is different from the known seasonal pattern for coastal waters, which is a function of factors such as phytoplankton consumption, temperature and availability of light. In the area under study, the increase in the nutrient concentration generally took place in summer, and highest concentrations are found in the autumn. Then there is a decrease in winter, with the minimum nutrient concentrations being found in springs. This seasonal pattern follows the growth rate curve of the fish cultivated on the farm (Tovar et al, 2000b). Therefore, the Chl-a value will follow this trend, with some exceptions, such as that observed on 1 March, when a Chl-a peak occurred (up to 14$\mu g\ L^{-1}$), in response to high nutrient inputs, mainly nitrites and nitrates (nutrient data provided by the *Delegación de Medio Ambiente de la Junta de Andalucía*) and to the favourable conditions caused by the high residence time for that date (see figure 6, February neap tide).

Therefore, several interrelated processes are involved in the seasonality of the inorganic carbon system and related physico-chemical parameter such as AOU and Chl-a. Firstly, the high seasonality in the material inputs to the Rio San Pedro (mainly nutrients, organic matter and SPM) originating from the fish farm discharges. This is supported by the results founded by Tovar et al, (2000b), who studied the seasonality in the outflows from the fish farm over two year period. An increase was found in the fish production cycle with the temperature, with maxima in summer and autumn, and consequently the

maximum discharge of nutrients, dissolved organic carbon and particulate material to the tidal creek.

Secondly, metabolic rates increase with temperature in the water column as well as in the benthic compartment. In this context, the positive values of the AOU indicate that respiratory processes exceed production activities in the tidal creek (including water column and sediment). For a better understanding of the effect of the temperature on each parameter, the annual variability has been normalised to its average value. The annual normalization of each parameter has been calculated as:

$$C_{normalised} = (C_{annual\ mean} - C_{monthly\ mean})\ 100 / C_{annual\ mean}$$

where C refers to the concentration of DIC, salinity, AOU and Chl-a. Figure 7 illustrates the annual pattern of these four parameters with temperature. It can be observed that the oxygen consumed is highly dependent on temperature as a consequence of the increasing magnitude of the respiratory processes with the temperature. Likewise, Chl-a values also show a high seasonal temperature dependence.

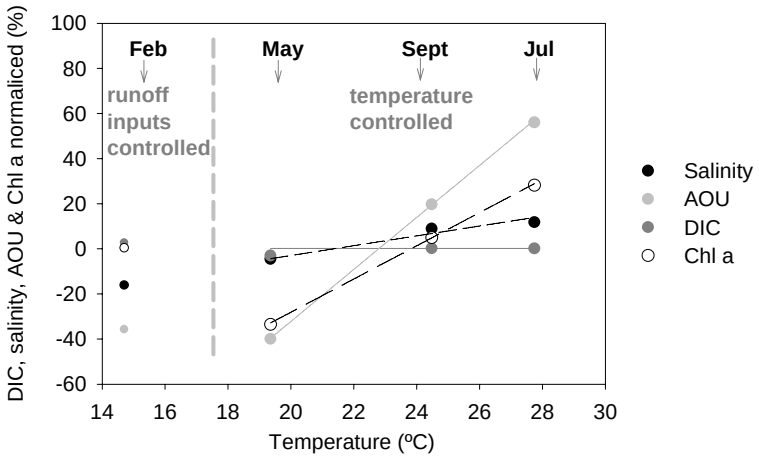

Figure 7. Seasonal dependence on temperature of salinity, dissolved inorganic carbon (DIC), Chlorophyll-a (Chl-a), apparent oxygen utilization (AOU).

This seasonal temperature dependence has been described for other salt marsh systems that have not been altered by human activities. For instance, in the Duplin river, the salt marsh respiration increases the release of organic and inorganic carbon in summer and autumn, and lower rates are found in winter and spring (Wang and Cai, 2004). Similar features are found for other tidal estuarine freshwater marshes (Neubauer and Anderson, 2003) and the waters adjacent to salt marshes like the U.S. South Atlantic Bight (Cai et al., 2003).

3.3. Inorganic carbon export to the adjacent coastal waters

The Rio San Pedro is a tidal creek where the only seawater input is by tidal exchange, and the only freshwater sources, mainly at the headwaters, are ultimately rainfall and inland drainage. The most predictable mechanism for flushing a small, well-mixed system is the regular rise and fall of water of the tide, but a number of other factors can also affect the flushing, for instance precipitation and land drainage inputs; none of these however have a significant value relative to the tidal prism, nor are they as predictable as the astronomical tides. In the present study, the classical tidal prism model has been used in order to asses the DIC export to adjacent coastal water. For this model, over each tidal cycle a volume of water (P) outside the tidal creek (i.e. in the Bay of Cadiz), with a DIC concentration of "DIC_B" enters the channel during the flood tide; it then mixes with the water of the creek with a volume V and a DIC concentration of "DIC_C" which dilutes after the mixing to a lower DIC concentration of DIC_T; later a volume equal to the tidal prism that entered (P) and with a final concentration of DIC_T, leaves the creek during the ebb. Then the mixing with ambient water outside the creek dilutes the tidal exported water to a concentration of DIC_B. The dilution processes in the Bay are highly favoured due to the disproportionately larger volume of the Bay of Cadiz in comparison to the Rio San Pedro, and to the circulation scheme of water in the Bay, where strong northward

currents have been described near the mouth of the creek (Parrado et al., 1996); such circumstances tend to prevent any return flow into the creek after a tidal cycle.

The equivalent tidal mass DIC flux out of the tidal creek can be calculated from a modified version of the formula proposed by Sandford et al. (1992):

$$F = Q\,(DIC_T - DIC_B)$$

where F is the DIC tidal flux and Q is the volume flow rate. The value of Q can be calculated as the ratio between the tidal prism volume (P) and the tidal period (T) (Q=P/T). The tidal prism volume is defined as the water volume between low tide and high tide, and V is the water volume at low tide. Information must be available on the geometry of the channel and tidal elevations. The dimensions of this channel have been approximated to a constant width of 110m, a datum depth of 3m, and a length of 12 km. The heights at low and high tide have been obtained from the 2004 tide table provided by the Instituto Hidrográfico de la Marina. The theoretical average DIC concentration, $C_{T,}$ can be calculated from the DIC concentrations at both ends of the channel, and formulated as:

$$C_T = (DIC_B\,P + DIC_C\,V) / (P+V)$$

To apply the tidal prism method it is necessary to make some assumptions: firstly, that the DIC in the creek presents a conservative behaviour: this assumption can reasonably be accepted observing the theoretical dilution line of DIC (figure 5) which shows that mixing is the key factor controlling DIC variability on a tidal scale. Secondly, since the DIC_B value has not been measured for every sampling, it has been assumed that the DIC concentration in the Bay is equal to the most diluted experimental DIC value measured at our sampling station, corresponding to high water concentration at spring tide. This assumption has been tested satisfactorily with the salinity and with the DIC for

various data available inside and outside the tidal creek in July 2003. DIC concentrations in the Bay of Cadiz were previously described on section 3.1.

The DIC_C value for the innermost end of the creek is the maximum DIC concentration reached for each month, which is highly reproducible for the samplings carried out in the same period of the year, besides the tidal coefficient, with some exceptions observed during high rainfall events, as is the case on 1March and 4th May. For these exception dates, C_T has been approximated to the average concentration measured over the tidal cycle at the tidal sampling station. The data for DIC concentrations have been multiplied by the water density in order to obtain the appropriate units (mol m^{-3}) for the DIC export calculation.

In order to check the consistency of the water budgets, the salinity data have been used to test the values obtained for V and P, as well as the applicability of the tidal prism model to the Rio San Pedro. The maximum difference between real and estimated values for salinity is around 1%, which is considerably less than the salinity range over a tidal cycle. Similarly, a comparison has been made between the average DIC concentration in a tidal cycle and the DIC_T resulting from the application of the tidal prism model. The average difference found between them is 3.5%, indicating that the tidal prism model, despite its simplicity, is a good approach for the DIC export calculation in the Rio San Pedro.

Table 2 shows the resulting DIC export calculated, together with other parameters required for the export calculations. It can be observed how the DIC export is a combination of the water flow (Q) and hence the tidal coefficient, as well as the DIC concentration gradient between the Rio San Pedro tidal creek and the Bay of Cadiz. The maximum DIC export, 43.7 10^5 mol C d^{-1}, is obtained on 1 July, coinciding with spring tide, and the minimum export, 9.9 10^5 mol C d^{-1}, on 27 April corresponding to neap tides and a higher DIC concentration in the Bay. To measure the relative effects of rain and water

drainage on the water flux rate, a longer salinity record available for the study site has been analysed. The freshwater inputs have been determined as the water volume needed to dilute the average salinity with respect to a non-rainy initial situation for each month. This calculation yields an additional flow to Q of 0.2 10^6 m^3 d^{-1} for 1 March (which is 11 times lower than the tidal flow for this date), and the net DIC export would increase from 9.9 10^5 to 10.8 10^5 mol C d^{-1}. Nevertheless, the additional freshwater volume for 4 May is negligible compared to the tidal prism since the rainfall event coincides with a spring tide. In any case, it is also likely that the volume contributed by rainfall inputs, as well as by water drainage, would be relatively negligible compared to the tidal prism volume, and would thus have little effect on the water fluxes. The main effect due to these washing-out inputs will be noted in the DIC concentration in the tidal creek, as can be appreciated in the theoretical dilution line in figure 5, especially on 1 March and 4 May, when some deviation of DIC values from the expected linear dilution line are observed.

Table 2. DIC export and the complementary parameters required for its calculation. Inorganic carbon in the Bay of Cadiz (DIC_B), tidal coefficient, inorganic carbon in the Rio San Pedro (DIC_T), tidal flow (Q), inorganic carbon export (DIC export).

Date	**Tidal coefficient**	**DIC_B (mol m^{-3})**	**DIC_T (mol m^{-3})**	**Q (10^6 m^3 d^{-1})**	**DIC export (10^5 mol C d^{-1})**
16-Feb	0.63	2467	2961	4.2	20.6
19-Feb	0.94	2467	2862	7.1	28.1
01-Mar	0.37	2467	2912	2.2	9.9
27Apr	0.32	2540	2783	2.3	5.6
04-May	1.05	2540	2746	8.8	18.1
19May	0.75	2540	2964	6.5	27.7
01-Jul	0.89	2391	2766	6.8	43.7
12-Jul	0.49	2391	2998	3.4	27.4
26-Jul	0.55	2391	2954	4.0	30.7
07-Sept	0.27	2383	3021	2.4	15.1
15-Sept	0.97	2383	2796	7.9	32.7

Seasonal variability of the DIC tidal export and the DIC concentrations in the innermost part of the creek follows the same pattern. It is worth noting that the highest variability can be observed on the fortnightly scale, following the spring-neap tidal cycle. This can be appreciated in figure 8, which shows that there is a relatively good linear correlation between DIC export and tidal coefficient (R^2 = 0.72, if the May result is not included), regardless of the season.

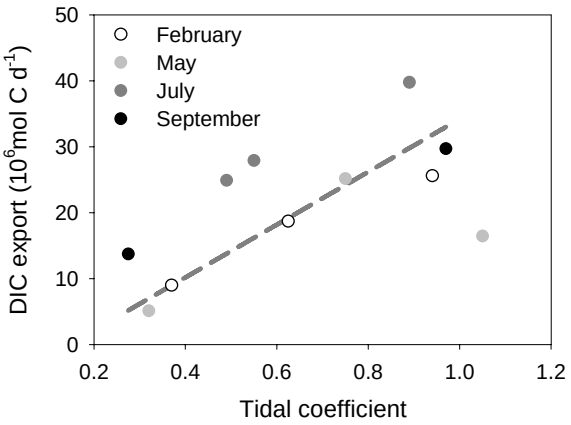

Figure 8. Relationship between export of inorganic carbon and tidal coefficient.

The net annual DIC export was estimated by averaging spring and neap tidal flux values for each season, which were then seasonally averaged, resulting in an annual DIC export of 8.72 10^8 mol C yr^{-1}, equivalent to 1.05 10^{10} g C yr^{-1}, with the maximum DIC export rates occurring in summer and autumn. The only previous study available on DIC tidal exchange in the area is the one conducted by Forja et al. (2003) in the Sancti Petri Channel in July 1999. Unlike the Rio San Pedro, this channel is connected at one end to the Atlantic Ocean and at the other end to the Bay of Cadiz. In turn, this channel is surrounded by intertidal marshes, and a complex network of secondary channels, in addition to several fish farms and an urban waste water discharge point. These authors found a net export of DIC to the Bay of Cadiz of 10^{11} g C yr^{-1}, which is one order of

magnitude higher than the resulting export from the Rio San Pedro. This higher export is explained by the higher net water flux and the greater area.

To gain a better understanding of the sources of this DIC exported, the DIC aereal export has been calculated. The DIC export (1.05 10^{10} g C yr^{-1}) was then divided by the sum of the entire water surface area of the Rio San Pedro (1.85 km^2) and the fish farm (1 km^2), obtaining an estimation of 3673 g C m^{-2} yr^{-1} for the DIC aereal export. This rate can be compared with other DIC sources. Due to the lack of information about the magnitude of the DIC export from the surrounding salt marshes to the tidal creek in our study area, we have analysed some data from the available literature corresponding to similar temperate ecosystems. Wang and Cai (2004) compiled some data available for the DIC export from salt marshes along the U.S. south-eastern Atlantic continental shelf, and reported values ranging between 156 g C m^{-2} yr^{-1} in the Duplin River (a marsh-dominated non-riverine tidal river) up to 194 g C m^{-2} yr^{-1} for tidal freshwater marshes in Virginia. The DIC aereal export from outside the Rio San Pedro is around 20 times higher than the DIC export from salt marshes described for other pristine systems, suggesting the existence of a significant source of DIC other than the surrounding salt marshes. Two principal sources of DIC to the Rio San Pedro water can be hypothesised: a) DIC inputs from the fish farm discharge, probably remineralised in the sediment, due to the farm's high ratio of surface to volume; b) organic matter respiration in the benthic and pelagic compartments inside the Rio San Pedro, principally of the organic material contained in the fish farm effluents. This evaluation of the possible DIC sources must be treated with caution because the extent of output from a particular marsh area is related to specific factors such as geographic location, morphology and hydrology rather than to a universal feature of marshes (Boto and Wellington, 1988). Nevertheless, the disproportionate differences between the DIC export from salt marshes and the DIC aereal export observed in the Rio San Pedro support the hypothesis about another non-natural (human induced) source and the impact of the fish farm. In turn, the Rio San Pedro is well-

isolated from the surrounding salt marshes, which suggests that the influence of the salt marsh on the Rio San Pedro is only moderate compared to similar systems, for instance the U.S. south-eastern Atlantic coast.

Recently, Garcia-Lafuente and Ruiz (2007), carried out a review of the different mechanisms involved in the seasonal productivity in the Gulf of Cadiz, the continental shelf near the Rio San Pedro. They highlight the role of the Rio San Pedro and nearby waters as continuous sources of nutrients from land to the sea by means of tidal pumping. This permanent input of nutrients to the continental shelf favours the high productivity observed in the region under the influence of the Bay of Cadiz, in the primary and secondary trophic levels.

4. Conclusion

The results obtained in this study describe the temporal and spatial variability of the carbonate system in the Rio San Pedro, a tidal creek located within the Bay of Cadiz (SW Spain). Together with the measurement of DIC, Chl-a and AOU values contribute to assessing the main biological processes involved in the high temporal variability. Very high concentration gradients have been found between the Rio San Pedro and the Bay of Cadiz, which emphasise the role of the inner part of the tidal creek and the fish farm located at the head of the creek as intense sources of inorganic carbon to the system. Different mechanisms driving these processes have been found on different time scales. On a tidal scale, salinity has been revealed as a good tracker of tidal mixing, suggesting that TA and DIC present a nearly conservative behaviour. On a fortnightly time scale, there is a notable increase of the Chl-a values at neap tides, explained by an increase in the growth of the phytoplankton biomass with the residence time of the water inside the creek. Over the full year, there are two main factors explaining the seasonality of the

inorganic carbon system and related parameters in Rio San Pedro tidal creek: the seasonality of the inputs (lateral inputs from marshes together with the production cycle of the fish farm effluents) and the seasonality of the metabolic rates. Furthermore, tidal creeks are extremely dynamic estuarine systems on a very short time scale as can be observed in the Rio San Pedro, where the magnitude of the seasonal amplitude of DIC is negligible compared with tidal and fortnightly time scales. The DIC tidal export from the Rio San Pedro to the Bay of Cadiz has also been calculated, and an annual average transport of 1.05 10^{10} g C yr^{-1} has been obtained, with tidal pumping being the key mechanism. The dynamic nature of this system makes it necessary to obtain and analyse data on a variety of time-scales in order to present an accurate and realistic picture of the carbonate system in this coastal area.

Acknowledgments:

This work was supported by the Spanish CICYT (Comisión Interministerial de Ciencia y Tecnología) of the Ministerio de Educación y Ciencia under contract CTM2005-01364/MAR. Thanks are expressed to CYCEM "El Toruño" for providing the infrastructures and to D. Gabriel, S. Ferron adn T. Ortega for her assistance with the field work.

References:

Alongi, D. M., 2002. Present state and future of the world's mangrove forests. Environ. Conserv., 29:331–349.

APHA, 1992. American Public Health Association. Standard methods for the examination of water and wastewater. Washington DC. 312 pp.

Benson, B. B., and Krause, JR. 1984. The concentration and isotopic fractionation of oxygen dissolved in freshwater and seawater in equilibrium with atmosphere. Limnol. Oceanogr. 29: 620–632.

Boto, K. G. and Wellington, J. T. 1988 Seasonal variations in concentrations and fluxes of dissolved organic and inorganic materials in a tropical, tidally-dominated, mangrove waterway. *Marine Ecology Progress Series* 50, 151-160.

Cai, W.-J. and Wang, Y. 1998. The chemistry, fluxes, and sources of carbon dioxide in the estuarine waters of the Satilla and Altamaha Rivers, Georgia.1998. Limnol. Oceanogr., 43:657–668.

Cai,W.-J., Pomeroy, L.R., Moran, M.A., Wang, Y., 1999. Oxygen and Carbon Dioxide Mass Balance for The Estuarine–Intertidal Marsh Complex of Five Rivers in the Southeastern U.S.

Cai, W.-J., Wang, Z. H. A. and Wang, Y. C. 2003. The role of marsh-dominated heterotrophic continental margins in transport of CO_2 between the atmosphere, the land-sea interface and the ocean. *Geophys. Res. Lett., 30(16):1849*

Dickson, A.G., 1990. Standard potential of the reaction: AgCl(s)+ ½ H_2(g)=Ag(s)+HCl(aq), and the standard acidity constant of the ion HSO^{4-} in synthetic seawater from 273.15–318.15 K. J. Chem. Thermodyn. 22, 113–127.

Dickson, A.G. and Riley, J.P., 1979. The estimation of acid dissociation constants in seawater media from potentiometric titrations with strong base. I. The ionic product of water — KW. Mar. Chem. 7, 89–99.

Dyer, Keith R., 1997. Estuaries : A physical introduction. London : John Wiley & Sons.

Forja, J.M., Ortega, T., DelValls, T.A., Gómez-Parra, A., 2004. Benthic fluxes of inorganic carbon in shallow coastal ecosystems of the Iberian Peninsula. Marine Chemistry, 85: 141:156.

Forja, J.M., Ortega, T., Ponce, R., de la Paz, M., Rubio, J.A., Gómez-Parra, A., 2003. Tidal transport of inorganic carbon and nutrients in a coastal shalt marsh (Bay of Cádiz, SW Spain). Ciencias Marinas 29(4): 469-481.

García Lafuente, J. and Ruiz, J., 2007. The Gulf of Cadiz pelagic ecosystem: an overview. Progress in Oceanography, 74 (2-3): 228-251.

Gattuso, J.-P., Frankignoulle, M. and Wollast, R., 1998. Carbon and carbonate metabolism in coastal aquatic ecosystems. Annual Review Ecology Systematics, 29: 405-433.

González-Gordillo, J.I., Arias, A.M., Rodríguez, A., Drake, P., 2003. Recruitment patterns of decapod crustacean megalopae in a shallow inlet (SW Spain) related to life history strategies. Estuar. Coast. Shelf Sci. 56, 593–607.

Lueker, T.J., Dickson, A.G. and. Keeling, C.D., 2000. Ocean pCO_2 calculated from dissolved inorganic carbon, alkalinity, and equations for K_1 and K_2 : validation based on laboratory measurements of CO_2 in gas and seawater at equilibrium. Mar. Chem., 90 (105-119)

Meybeck M. and Ragu A. (1995) *Water Quality of World River Basins*. UNEP GEMS Collaborating Centre for Fresh Water Quality Monitoring and Assessment, United Nations Environment Programme.

Mucci, A., 1983. The solubility of calcite and aragonite in seawater at various salinities, temperatures and one atmosphere total pressure. Am. J. Sci., 283: 780-799.

Neubauer, S. C. and Anderson. I. C., 2003. Transport of dissolved inorganic carbon from a tidal freshwater marsh to the York River estuary. Limnol Oceanogr 48:299–307.

ParradoJ.M., Gutierrez MasJ.M. and Achab,M. (1996) Determinación de direcciones de corrientes mediante el análisis de 'formas de fondo' en la Bahía de Cádiz. *Geogaceta,* 20, 378-381.

Pereira-Filho, J.C. A. F. Schettini, L. Rorig and E. Siegle, 2001. Intratidal Variation and Net Transport of Dissolved Inorganic Nutrients, POC and Chlorophyll *a* in the Camboriú River Estuary, Brazil. Estuarine, Coastal and Shelf Science*,* 53, 249–257.

Rabouille, C., Mackenzie, F.T. and Ver, L.M., 2001. Influence of the human perturbation of carbon, nitrogen, and oxygen biochemical cycles in the global coastal ocean. Geoquimica et Cosmoquimica Acta, Vol 65 (21), 3615-3641.

Sanford, L. P., Boicourt, W. C. & Rives, S. R. 1992 Model for estimating tidal flushing of small embayments. *ASCE Journal of Waterway, Port, Coastal and Ocean Engineering* 118 (6), 635–655.

Smith, S.V. and Hollibaugh, J.T., 1993. Coastal metabolism and the oceanic organic carbon balance. Rev. Geophys. 31, 75–89.

Tovar, A., Moreno, C., Manuel-Vez, M.P. and García-Vargas, M., 2000a. Environmental impacts of intensive aquaculture in marine waters. Water Res. 34, 334–342.

Tovar, A., Moreno, C., Manuel-Vez, M.P. and García-Vargas, M., 2000b. Environmental implications of intensive marine aquaculture in earthen ponds. Mar. Pollut. Bull. 40, 981–988.

Wang, Z.A. and Cai, W.-J., 2004. Carbon dioxide degassing and inorganic carbon export from a marsh-dominated estuary (the Duplin River): a marsh CO2 pump. Limnol. Oceanogr. 49 (2), 341–354.

Wang, C-F., Hsu, M-H. and Kuo, A. Y. , 2004. Residence time of the Danshuei River estuary, Taiwan. Estuarine, Coastal and Shelf Science, 60:381-393.

Yates, K.K., Dufore, C., Smiley, N., Jackson, C. and Halley, R.B., 2007. Diurnal variation of oxygen and carbonate system parameters in Tampa Bay and Florida Bay. Mar. Chem. 104 (110-124)

Zeebe, R. E., and Wolf-Gladrow, D. A., 2001. CO_2 in Seawater: Equilibrium, Kinetics, Isotopes, 346 pp., Elsevier Sci., New York.

Capitulo 4

Dinámica del carbono inorgánico en el Estrecho de Gibraltar

La línea de costa a nivel mundial tiene una longitud de 350.000 km, que multiplicada por 70 km de anchura nos da idea de la magnitud de la extensión de la plataforma continental a nivel global (Gattuso et al., 1998). Como ya se mencionó en la introducción de esta Tesis, para el estudio del ciclo del carbono en las zonas costeras algunos autores realizan una subdivisión de las zonas costeras entre "distal" y "próxima" (Rabouille, 2001). La zona costera distal se refiere fundamentalmente a la plataforma continental, y supone el 93 % de la superficie total de los sistemas costeros a nivel global.

Debido a las diferencias significativas de las propiedades físicas, químicas y biológicas entre la región nerítica y la oceánica, existe un marcado gradiente de propiedades en los márgenes continentales que genera importantes flujos en estas zonas. Sin embargo, el flujo neto de nutrientes y carbono orgánico e inorgánico en estos sistemas es complicado de establecer y presenta un alto grado de incertidumbre (Mantoura et al, 1991, en Gattuso 1998).

La plataforma continental se caracteriza por estar dividida en un compartimento superficial o capa de mezcla, dominada por la producción primaria, y otro compartimento más profundo, dominado por los procesos respiración y de remineralización de la materia orgánica, de forma que el CID producido en aguas profundas es exportado posteriormente a zonas más oceánicas. Este desacoplamiento vertical entre producción y respiración hace que sean zonas con un intenso potencial de captación de CO_2 atmosférico. Sin embargo, sobre esta tendencia general existen variaciones en la magnitud y sentido de los flujos de CO_2 agua-atmósfera en función de la latitud. En latitudes altas y templadas, la plataforma continental actúa como sumidero de CO_2 atmosférico, mientras que en la franja tropical y subtropical se comportan como fuentes significativas de CO_2 a la atmósfera (Borges, 2005). Aunque en líneas generales en la plataforma continental existe un transporte neto de carbono hacia el océano, su papel como fuente o sumidero de CO_2 puede variar en función del grado de estratificación de la columna de agua. En las plataformas continentales estratificadas estacionalmente, el carbono fijado por el fitoplancton en forma de materia orgánica puede transportarse a través de la picnoclina y posteriormente ser remineralizado en aguas profundas. Sin embargo, en las plataformas continentales que presentan una mezcla completa permanente, este desacoplamiento entre procesos de respiración y producción de la materia orgánica no ocurre, y por tanto, además de una menor eficiencia en el transporte de CID hacia el océano abierto, existe una mayor ventilación de este CO_2 a la atmósfera (Borges, 2005).

Asimismo, en la plataforma continental aparecen zonas de *afloramientos costeros,* donde existe una importación de carbono y nutrientes desde el océano. En estas zonas, debido a la entrada de aguas profundas ricas en carbono inorgánico, la pCO_2 se encuentra por encima del valor en equilibrio con la atmósfera. No obstante, no sólo se ven enriquecidas en CID, sino que también se produce una entrada de nutrientes en la superficie que provoca una fertilización del agua superficial, y por tanto una retirada de

CO_2 del medio. El balance entre estos dos procesos antagónicos determinará el sentido y magnitud de los flujos de CO_2 en estas zonas (Borges y Frankignoulle, 2002).

En este capítulo se aborda el estudio del Estrecho de Gibraltar, que constituye una frontera entre el continente africano y el europeo, y a su vez, es el único punto de conexión del Mar Mediterráneo con el océano. Este sistema, debido a su situación geográfica y a sus condiciones hidrodinámicas, se encuentra menos influenciado que otras plataformas por procesos en sus márgenes laterales y por aportes continentales.

El flujo de salida de agua mediterránea hacia el Atlántico tiene indirectamente un papel importante en la circulación del océano Atlántico Norte (Reid, 1979), y por tanto, en la circulación termohalina global (Wu y Haines, 1996). A su vez, debido a que el Mar Mediterráneo es uno de los pocos lugares de la Tierra en los que se produce la formación de aguas profundas además de los polos (Reid, 1979), la cuenca mediterránea supone un laboratorio perfecto para el estudio de la captación de CO_2 atmosférico, que posteriormente será inyectado en aguas profundas a través del Estrecho de Gibraltar para formar parte de la circulación termohalina global (Bethoux et al., 2005).

El Estrecho de Gibraltar supone la única conexión entre dos mares con características muy diferentes. Una de las principales diferencias radica en la amplitud de la carrera de marea, que es prácticamente inexistente en el Mediterráneo, mientras que en la fachada Atlántica del Golfo de Cádiz puede alcanzar los dos metros. Esta transición entre un régimen mareal medio a uno inexistente genera una gran cantidad de energía potencial que se puede emplear en la modificación de los flujos medios.

La circulación promedio de las masas de agua en el Estrecho de Gibraltar se describe usualmente como una circulación bicapa, de tipo estuarina inversa, con una entrada neta

de agua atlántica en superficie y una salida profunda de agua mediterránea (Army y Farmer, 1988).

Sobre este flujo medio, una de las mayores fuentes de variabilidad está inducida por la interacción de los flujos con la topografía del canal del Estrecho. La sección más somera de todo el canal se encuentra sobre un bajo denominado umbral de Camarinal, que se sitúa en la mitad occidental del Estrecho, y que supone un cambio drástico en la batimetría pasando en muy poca distancia de 900 a 300 m de profundidad. Esta interacción de los flujos de agua con esta elevación submarina, es capaz de causar fenómenos ondulatorios en la interfase entre la masa de agua atlántica y mediterránea como bores (Boyce, 1975; Armi y Farmer, 1985) u ondas internas (Bruno et al, 2001). Estas ondulaciones son capaces de romper dicha interfase produciendo la mezcla vertical entre el agua atlántica y la mediterránea (Bray et al., 1995). A su vez, la intrusión de agua profunda en la superficie, provoca una inyección de nutrientes y carbono inorgánico, que tiene una gran implicación en los ciclos biogeoquímicos del contiguo del Mar de Alborán (Gómez et al., 2000).

Las fluctuaciones típicas en los flujos medios a escala estacional y subinercial (inducida por la meteorología) son de 0.1 Sv y 0.5 Sv (Candela, 1990; Garcia-Lafuente et al., 2002), siendo estas mucho menores que la escala mareal. Las variaciones con las mareas pueden a alcanzar los 4 Sv en mareas vivas, esto es 4 veces mayor que el flujo medio en el Estrecho (García-Lafuente y Vargas, 2003). Este fenómeno hace especialmente complicado el estudio estacional y temporal de los distintos procesos biogeoquímicos en el Estrecho de Gibraltar.

Debido a tan especiales circunstancias, el Estrecho de Gibraltar ha sido objeto de numerosos estudios en el campo de la oceanografía física (e.g. Armi y Farmer, 1985, Bray et al., 1995, Bruno et al. 2001), sin embargo, existe un menor numero de estudios desde

el punto de vista de la oceanografía biológica y química. En este contexto, la principal fuente de datos biológicos y físico-químicos recogidos en esta zona fueron las campañas realizadas en el marco del proyecto europeo CANIGO (Canary Island Azores-Gibraltar Observations). Dentro de la contribuciones científicas sobre el carbono inorgánico que se produjeron en este proyecto cabe destacar las realizadas por Dafner et al., (2001) y Santana-Casiano et al. (2002) en las que se estudiaba la distribución espacial y el transporte de carbono entre la cuenca atlántica y mediterránea. Otros trabajos relevantes sobre carbono inorgánico realizados en la marco de otros proyectos son los de Copin-Montegut (1993) en la sección este del Estrecho y Mar de Alborán, y el de Ait-Ameur y Goyet (2006) en el sector atlántico del Estrecho.

En este capítulo se ha distribuido en dos trabajos distintos el estudio de la dinámica del carbono inorgánico en el Estrecho de Gibraltar. El trabajo IV, se aborda la distribución espacial y vertical del CID en la columna de agua, así como la variación temporal de dicha distribución con las mareas. A su vez, se ha estimado el transporte de carbono inorgánico entre el Atlántico y el Mediterráneo. En el trabajo V se han estudiado las variaciones estacionales de la pCO_2 en las aguas superficiales del Estrecho, y se ha evaluado el intercambio de CO_2 agua-atmósfera a lo largo del año.

Los datos que se presentan en el trabajo IV se generaron durante una campaña realizada entre el 7 y el 19 de Noviembre del 2003 a bordo del BIO “Mytilus” junto con los grupos de investigación pertenecientes al área de Física Aplicada y de Ecología de la Universidad de Cádiz. Se llevaron a cabo dos mallas para la descripción espacial de las concentraciones de CID, pH y oxígeno disuelto en la columna de agua, junto con 4 muestreos para evaluar la variabilidad con las mareas. Respecto a estos muestreos con la mareas, 2 de ellos se realizaron sobre el Umbral de Camarinal, y otros dos en la región este del Estrecho, a la altura del Peñón de Gibraltar (tabla 4.1)

Se ha observado la existencia de un aumento de CID y del consumo aparente de oxigeno con la profundidad debido a la particular composición de la masa de agua mediterránea, caracterizada por haber sufrido intensos procesos de remineralización en su tránsito por la cuenca mediterránea. Por otra parte, las variaciones en la distribución vertical de carbono inorgánico y oxígeno dependen en gran medida tanto de la posición de la interfase entre la capa atlántica y la mediterránea, como de la intensidad de los procesos de mezcla. Las mayores concentraciones en carbono inorgánico en la capa mediterránea es el factor responsable del flujo neto de CID hacia el Atlántico, aunque la estimación del transporte está sometida a cierto grado de incertidumbre que responde fundamentalmente a la definición de la interfase y a la estimación usada para el flujo de agua en el Estrecho.

En el trabajo V, se presentan los resultados obtenidos en cuatro campañas realizadas entre Septiembre del 2005 y Mayo del 2006 (tabla 4.1). En cada campaña se ha realizado un trasecto norte-sur a la altura del Umbral de Camarinal, y un transecto Este-Oeste a lo largo del canal central del Estrecho. Además de la medida en continuo de salinidad, temperatura y pCO_2, se tomaron muestras discretas de 7 estaciones para la medida de OD, AT y pH en el agua superficial. La distribución espacial de pCO_2 a lo largo del Estrecho muestra poca variabilidad en comparación con la escala estacional. Se ha evaluado cual es el principal factor que controla estas variaciones estacionales de pCO_2, siendo las variaciones termodinámicas inducidas por cambios de la temperatura el principal factor que explica la amplitud estacional de estos valores. En el Estrecho de Gibraltar, la pCO_2 se encuentra por debajo de su valor de equilibrio con la atmósfera la mayor parte del año, exceptuando Septiembre, y por tanto a escala anual, el sistema actúa como un sumidero de CO_2 atmosférico.

Tabla 4.1 Resumen de las campañas realizadas en el Estrecho de Gibraltar y de las variables medidas (AT: Alcalinidad Total; OD: oxigeno disuelto; pCO_2: presión parcial de CO_2 ; RC: registro continuo).

Fecha	Descripción muestreo	AT (n)	pH (n)	OD (n)	pCO_2 (n)
11 Nov 2003	Distribución vertical 7 estaciones	41	41	41	--
17 Nov 2003	Distribución vertical 7 estaciones	41	41	41	--
13 Nov 2003	Estación fija observación con mareas Umbral Camarinal	35	35	35	--
19Nov 2003	Estación fija observación con mareas Umbral Camarinal	34	34	34	--
7 Nov 2003	Estación fija observación con mareas Sección Este	24	24	24	--
14 Nov 2003	Estación fija observación con mareas Sección Este	25	25	25	--
7-8 Sept 2005	Distribución espacial agua superficial 7 estaciones	7	7	7	RC
12-13 Dic 2005	Distribución espacial agua superficial 7 estaciones	7	7	7	RC
20-21 Mar 2006	Distribución espacial agua superficial 7 estaciones	7	7	7	RC
22-23 May 2006	Distribución espacial agua superficial 7 estaciones	7	7	7	RC

Bibliografía

Aït-Ameur, N. and Goyet, C., 2006. Distribution and transport of natural and anthropogenic CO_2 in the Gulf of Cadiz. Deep-Sea Research II, 53: 1329-1343.

Armi, L., y D.,Farmer, 1985. The internal hydraulics of the Strait of Gibraltar and associated sill and narrows. Oceanologica Acta 8 (1): 37– 46.

Armi, L., Farmer, D., 1988. The flow of Mediterranean Water through the Strait of Gibraltar. Progress in Oceanography 21, 41–82.

Bethoux, J.P., El Boukhary, M.S., Ruiz-Pino, D. Morin, P. Copin-Montégut, C, 2005. Nutrient, Oxygen and Carbon Ratios, CO_2 Sequestration and Anthropogenic Forcing in the Mediterranean Sea. In: The Handbooks of Environmental Chemistry, Part K. Springer-Verlag Berlin Heidelberg, pp: 67-86.

Borges, A. V. y M. Frankignoulle. 2002c. Aspects of dissolved inorganic carbon dynamics in the upwelling system off the Galician coast. *Journal of Marine Systems* 32:181–98.

Borges, A. V., 2005. Do We Have Enough Pieces of the Jigsaw to Integrate CO_2 Fluxes in the Coastal Ocean? Estuaries, 28 (1): 3–27.

Boyce, F.M., 1975. Internal waves in the Strait of Gibraltar. Deep-Sea Research 22, 597–610.

Bray, N.A., Ochoa, J., Kinder, T.N., 1995. The role of the interface in exchange through the Strait of Gibraltar. Journal of Geophysical Research 100 (C6), 10755–10776.

Bruno, M., J.J., Alonso, A., Cózar, J., Vidal, A., Ruiz-Cañavate, F., Echevarría, J., Ruiz, 2002. The boiling-water phenomena at Camarinal Sill, the strait of Gibraltar. Deep-Sea Research II 49: 4097–4113.

Candela, J., 1990. The barotrophic tide in the Strait of Gibraltar. The Physical Oceanography of Sea Straits. K.A. Publisher, pp. 457–475.

Copin-Montégut, C., 1993. Alkalinity and carbon budget in the Mediterranean Sea. Global Biogeochemical Cycles 7 (4), 915–925.

Dafner, E.V., González-Dávila, M., Santana-Casiano, J.M., Sempere, R., 2001a. Total organic and inorganic carbon exchange through the Strait of Gibraltar in September 1997. Deep-Sea Research II 48, 1217–1235.

García-Lafuente, J., Delgado, J., Vargas, J.M., Vargas, M., Plaza, F., Sarhan, T., 2002. Low frequency variability of the exchanged flows 646 through the Strait of Gibraltar during CANIGO. Deep-Sea Research II 49 (19), 4051–4067.

García-Lafuente, J. y Vargas Domínguez, J.M., 2003. Recent observations of the exchanged flows through the Strait of Gibraltar and their 642 fluctuations at different time scales. Recent Research Development in Geophysics 5, 73–84.

Gattuso, J.-P., M., Frankignoulle, y R., Wollast, , 1998. Carbon and carbonate metabolism in coastal aquatic ecosystems. Annual Review Ecology Systematics, 29: 405-433.

Gómez, F., González, N., Echevarria, F., García, C.M., 2000. Distribution and fluxes of dissolved nutrients in the Strait of Gibraltar and its relationships to microphytoplankton biomass. Estuarine Coastal Shelf Science 51, 439–449.

Mantoura RFC, Martin J-M, Wollast R, eds. 1991. *Ocean Margin Processes in Global Change*. 469 pp. Chichester, UK: Wiley & Sons

Reid, J.L., 1979. On the contribution of the Mediterranean Sea outflow to the Norwegian-Greenland Sea. Deep-Sea Research 26, 1199–1223.

Santana-Casiano, J.M., González-Dávila, M., Laglera, L.M., 2002. The carbon dioxide system in the Strait of Gibraltar. Deep-Sea Research II 49, 4145–4161.

Wu, P. y Haines, K., 1996. Modeling the dispersal of Levantine Intermediate Water and its role in Mediterranean deep water formation. Journal of Geophysical Research, 101 (C3): 6591–6608.

Inorganic carbon dynamic and the influence of tidal mixing processes on the Strait of Gibraltar

Mercedes de la Paz [a*], Bibiana Debelius [a], Diego Macías [b], Agueda Vázquez [c], Abelardo Gómez-Parra [a], Jesus. M. Forja [a]

[a] *Departamento de Química-Física, Facultad de Ciencias del Mar y Ambientales, Universidad de Cádiz, Campus Río San Pedro s/n, Puerto Real (Cádiz) 11510, Spain*

[b] *Departamento de Biología, Facultad de Ciencias del Mar y Ambientales, Universidad de Cádiz, Campus Río San Pedro s/n, Puerto Real (Cádiz) 11510, Spain*

[c] *Departamento de Física Aplicada, Facultad de Ciencias del Mar y Ambientales, Universidad de Cádiz, Campus Río San Pedro s/n, Puerto Real (Cádiz) 11510, Spain*

Abstract

This study presents the distribution of the dissolved inorganic carbon (DIC) along the Strait of Gibraltar, its temporal variability, as well as the inorganic carbon exchange between the Atlantic Ocean and Mediterranean Sea. During November 2003, water column samples were collected on 9 stations to measure Total Alkalinity (TA), pH, and dissolved oxygen (DO) for the spatial characterization of the carbonate system. At the same time, anchored samplings were carried out, above the Camarinal Sill and in the Eastern Section of the Strait, in order to assess the tidal mixing effects for oxygen and DIC distribution on the water column. Three distinct water masses can be discerned in this area: the Surface Atlantic Water (SAW), the Mediterranean Water (MW), and the less abundant North Atlantic Central Water (NACW). The observations show an increase in the DIC and a decrease in oxygen concentration with depth, related to the different physico-chemical features of each water mass. The results show the high time-dependence of the vertical distribution of DIC with the interface oscillation, affected by the intense mixing processes taking place in the Strait. Intense mixing episodes over the Camarinal Sill are responsible for an increase in the DIC concentrations in the upper layer of the Eastern Section of the Strait. Higher DIC concentrations in the Mediterranean than in the Atlantic waters are responsible for the net DIC transport to the Atlantic Ocean. Nevertheless, the net exchange is highly sensitive to the interface definition, as well as to the estimate of water volume transport used.

Keywords: inorganic carbon, AOU, tidal mixing, carbon exchange, Strait of Gibraltar

1. Introduction

The Strait of Gibraltar is the only connection of the Mediterranean Sea with Atlantic Ocean. The Mediterranean outflow plays an important indirect role in the North Atlantic circulation (Reid, 1979) and, consequently in the thermohaline "conveyor belt" at global scales and on time scales of global climate change (Wu and Haines, 1996). The Mediterranean Sea provides an interesting case study for the processes that take part in the atmospheric sequestration of CO_2 through the outflow of deep waters across the Strait of Gibraltar, which transfers carbon from the sea surface to the intermediate waters of the Atlantic, where it is isolated from the atmosphere for several centuries (Bethoux et al., 2005); in part, this interest rests on the fact that the Mediterranean Sea is one of the few places in the world where deep convection and water mass formation takes place, and thus it constitutes a strong marine sequestration of CO_2. Recently, Alvarez et al. (2005) put into context the relevance of the Mediterranean Water in the global CO_2 cycle, estimating than 0.06 GtC yr^{-1} are drawn down from the surface to intermediate waters and 0.03 GtC yr^{-1} are exported to the North Atlantic mainly by horizontal circulation; these quantities are stated merely for information, since the anthropogenic carbon increase in the ocean is about 1.85 GtC yr^{-1}.

Studying the biogeochemical properties of the Mediterranean and Atlantic water masses constitutes a good way to track the water exchange through the Strait of Gibraltar. In this context, several biogeochemical research studies have been carried out previously in the area, for example, on the nutrients pattern and its associated biological effects (Minas et al., 1991; Gomez et al., 2001;Echevarría et al., 2002; Macias et al., 2006) but relatively few studies have been made of the carbonate system. The European funded CANIGO project, with the observation published by Dafner et al. (2001a) and Santana-Casiano et al. (2002) are the most specific studies conducted on the Gibraltar Strait. Other studies carried out on the region but not specifically designed to study the

Strait include those by Ait-Ameur and Goyet, (2006), which was centred on the Gulf of Cadiz and the Western entrance of the Strait, and by by Copin-Montegut (1993) on the Alboran Sea.

The changes in the biogeochemical parameters of waters interacting through the Strait are largely controlled by hydrodynamic phenomena. In the Strait of Gibraltar, a variety of physical processes are superimposed on the average Mediterranean-Atlantic flows, with large fluctuations at different time scales, and even greater variability is observed on the tidal scale (Garcia-Lafuente et al., 2000). This is mainly due to the interaction of the average flow with the shallow topography at the Camarinal Sill (300 m depth), which produces large fluctuations at the interface between the upper Atlantic layer and the deeper Mediterranean layer, favouring the formation of internal hydraulic jumps, especially at spring tides (Armi and Farmer, 1986), or the arrested internal waves (Bruno et al., 2002) which are more likely at weak neap tides. Such undulatory processes enhance interfacial mixing and can inject deep, nutrient-rich water into the upper layer of Atlantic water. The upwelling inorganic nutrients are advected towards the Mediterranean Sea in the upper layer, and enhance the primary production in the Alboran Sea to the east of the Strait (Macias et al., 2007).

The present study aims to contribute to existing knowledge of the carbonate system in the Strait of Gibraltar, and in particular to evaluate the short-term temporal variability experienced on the tidal scale in the different sections over the length of the Strait. The main elements that must be taken into account in calculating the carbon exchange between the Atlantic Ocean and the Mediterranean Sea at the Strait have then been analysed.

2. Material and methods

Between 7 and 19 November 2003, 9 stations were sampled for hydrology and water chemistry parameters (dissolved oxygen, TA and pH) in the Strait of Gibraltar, from on

board the R/V *Mytillus*. Three stations were located at the western entrance to the Strait (St. D1 to D3), one over the Camarinal Sill (St. D4), three at the Tarifa Narrows (St. D5 to D7) and two fixed stations at the eastern entrance (A1 and A2). Seawater samples were collected at different depths of the water column using a CTD Rossete sampler with conventional Niskin bottles; a total of 230 discrete samples were taken. At each station (see figure 1), 5 to 6 depths were sampled, from the surface to 225-250 m. Additionally, four tidal samplings (3 to 12 hours observation at each station) were performed at selected fixed stations over the Camarinal Sill (S1 and S2) and in the Eastern Section (A1 and A2). For each profile, CTDs were sampled at several depths down to 250-300 m every 15-30 minutes, and discrete samples for biogeochemical parameters were taken every 1 to 2 hours.

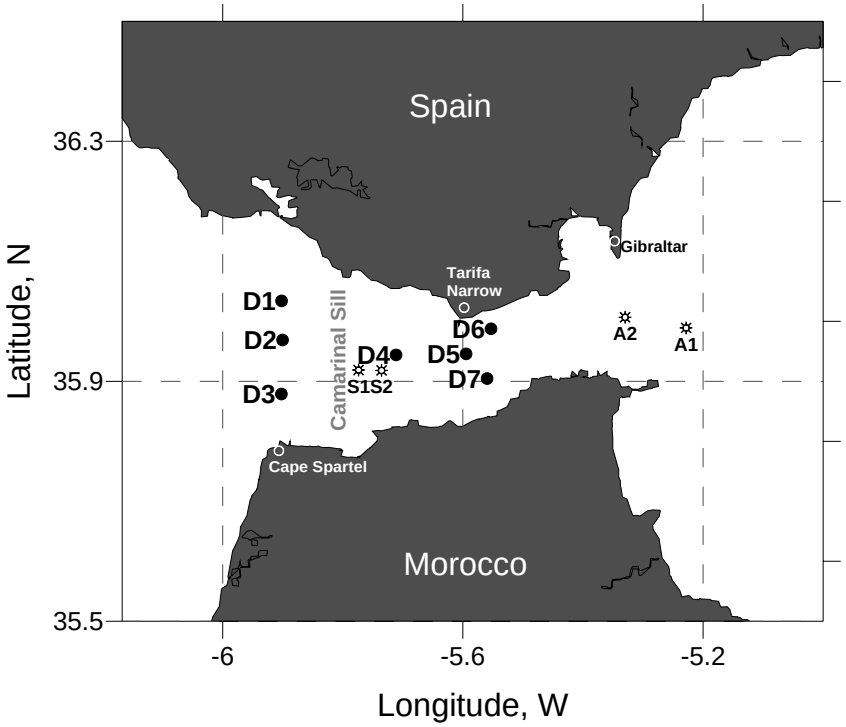

Figure 1. Map of the Strait of Gibraltar showing the locations of the sampling stations. The tidal fixed station are indicated as (¤).

The pH was measured with a glass combined electrode (Methrom) calibrated on the Free pH Scale (Zeebe and Wolf-Gladrow, 2001). The alkalinity computation was performed from the titration curve by means of the Gran Function and taking into account the correction for sulphate and fluoride interaction, using the constants proposed by Dickson (1990) and by Dickson and Riley (1979) respectively. For the dissociation of dissolved inorganic carbon (DIC), the K_1 and K_2 acidity constants proposed by Lueker et al. (2000) in the Total pH Scale were selected. The method was validated with reference standards obtained from A. Dickson (Scripps Institution of Oceanography, San Diego, USA) to an accuracy of ±2 µmol kg^{-1}.

The oxygen was fixed in a sealed flask and stored in darkness for 24 h, as described by the Winkler method, for later analysis by potentiometric titration (Metrohm 670 Titroprocessor). The Apparent Oxygen utilization (AOU) is defined as the deviation of oxygen from an O_2 concentration in equilibrium with the atmosphere calculated from the Benson and Krause (1984) solubility equation. All the measurements for TA and oxygen were made on board within a maximum of 24 hours after sampling. The estimation of the tidal current velocity has been made using the method of Alonso del Rosario et al. (2003).

3. Results and discussion

3.1. Spatial distribution

3.1.1. Hydrology

The normal regime in the Strait of Gibraltar consists of two superimposed flows; a shallow Atlantic inflow and a deeper Mediterranean outflow. The interface between these flows is characterised by a high salinity gradient and is subject to high spatial-temporal variability over the length of the Strait. Three different water masses participate in the circulation scheme (Gascard and Richez, 1985): the Mediterranean Outflow Water (MW) is cold and saline (temperature and salinity ranges respectively

between 13.0-13.5ºC and 38.2-38.5), the Surface Atlantic Water (SAW) is warm and fresh (temperature and salinity ranges respectively between 19.0-20.0ºC and 36.4-36.2) and the North Atlantic Central Water (NACW, temperature and salinity ranges respectively between 13.5-14ºC and 35.6-36) is colder and fresher than SAW; the volume of the less abundant NACW is highly variable in time (as a function of the tidal phase) and along the Strait (Bray et al., 1995; Macias et al., 2006). The temperature/salinity diagram for the CTD profile obtained in this study at stations from D1 to D7 (figure 2) allows the relative abundance of the different water masses to be discerned. Additionally, in each T/S diagram, the three types of water mass have been plotted following the characteristics proposed by Gacard and Richez (1985). A key feature that identifies the penetration of NACW through the Strait of Gibraltar is the appearance of a salinity minimum which separates surface Atlantic water from the underlying mixture of Atlantic-Mediterranean waters. The NACW signal is more significant in the southern (D3, D7) than in the northern (D1, D6) stations, and in the western (D1-D3) than in the eastern (D6-D7) stations. This is consistent with the previous characterization of water masses in the Strait of Gibraltar carried out by Bray et al, (1995), which shows a dramatic decrease in the NACW fraction eastward, and with the report of Gascard and Richez (1985), who observed that the injection of NACW into the Mediterranean Sea is highly influenced by the tides and the internal waves. The colour gradient in figure 2 reveals information about the east-west differences in the depth level of the different water masses. The T/S diagrams show how the NACW signal tends to appear preferentially to the south of the Strait, where the Atlantic-Mediterranean interface is deeper (Garcia-Lafuente et al., 2000); the entry of the NACW over the Sill becomes easier in the south because of the geostrophic transport (Bray et al., 1995), whereas in the centre or north, it can only cross the Sill under maximum tidal forcing conditions, when the Atlantic layer is thicker and the interface occurs at a greater depth.

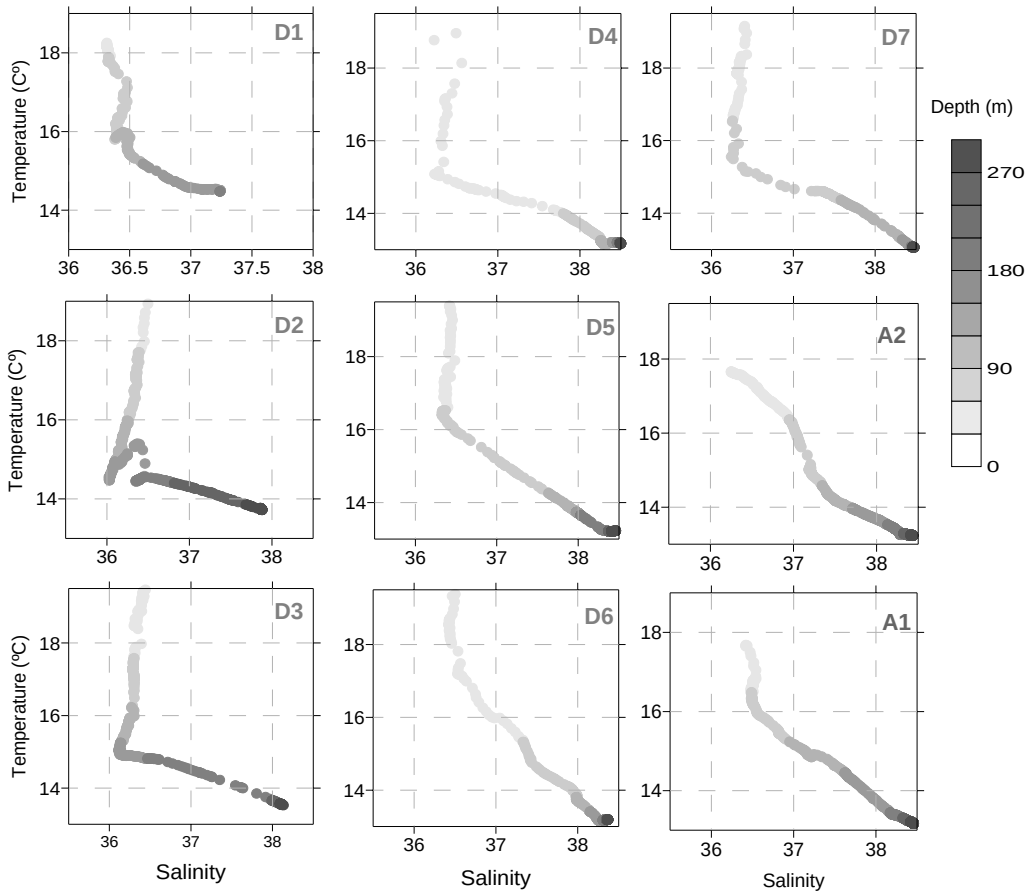

Figure 2. Temperature/salinity diagrams for the different stations. Colour code indicates depth.

3.1.2. Vertical and spatial patterns of TA, DIC and AOU

Due to the high tidal variability that characterises the Strait of Gibraltar, the spatial distribution picture must be made up taking into consideration the tidal stage at the sampling time for each station. In spite of this tidal variability, the main features of the

DIC, pH_T (25) and AOU are evident in figure 3. The Atlantic inflow water is characterised by lower TA and DIC content than the Mediterranean outflow water; in turn, the shape of the profile will depend on the interface thickness. Hence, the DIC and AOU values present a gradual increase down to the lower part of the interface and more homogeneous values for the deeper layer, following the salinity profile. In turn, the pH_T (25) values present a gradual decrease down to the interface and nearly constant values for the lower Mediterranean layer. Maximum DIC concentrations in the upper layer are found in the D1 station (for both the samplings), where the relative shallowness (~150 m depth) of this coastal station makes this area more fertile, enhancing the primary production and causing lower AOU and higher pH_T (25) values. Previous observations at this coastal station (Gomez et al., 2000; Macias, 2006) show an increase in nutrient and chlorophyll concentration, and link this station to its specific hydrodynamic processes, characterised by the absence of MW. The largest oscillation of the interface are found at D4, the station located above the main Sill (figure 3, table 1), where the interface layer can extend to the bottom or the surface in function of the tidal oscillation. This leads to colder and saltier water in the Atlantic layer (temperature 16.1 ºC and salinity 36.34) and to higher DIC (2125.0 μmol kg^{-1}). These high mixing rates found over the Sill cause the upwelling of the deep Mediterranean waters which are advected towards the eastern part of the Strait; this advection, together with the Spanish coastal upwelling, leads to the high productivity characterising the Alboran Sea (Gomez et al., 2000; Minas et al., 1991).

Another specific feature is observed at the south-eastern station D7, where appear deep (250 m depth) minimum values are found for DIC (2147 μmol kg^{-1}) and AOU (52.16 μmol kg^{-1}) and a maximum value for pH (7.8) is found. This holds with previous observations in the Strait performed by Minas et al. (1991) and Santana-Casiano et al. (2002) for oxygen and DIC respectively. These authors link these minimum values to the presence of the Western Mediterranean Deep Water (WMDW) that rises along the African slope and the phenomenon is known as the banking of WMDW.

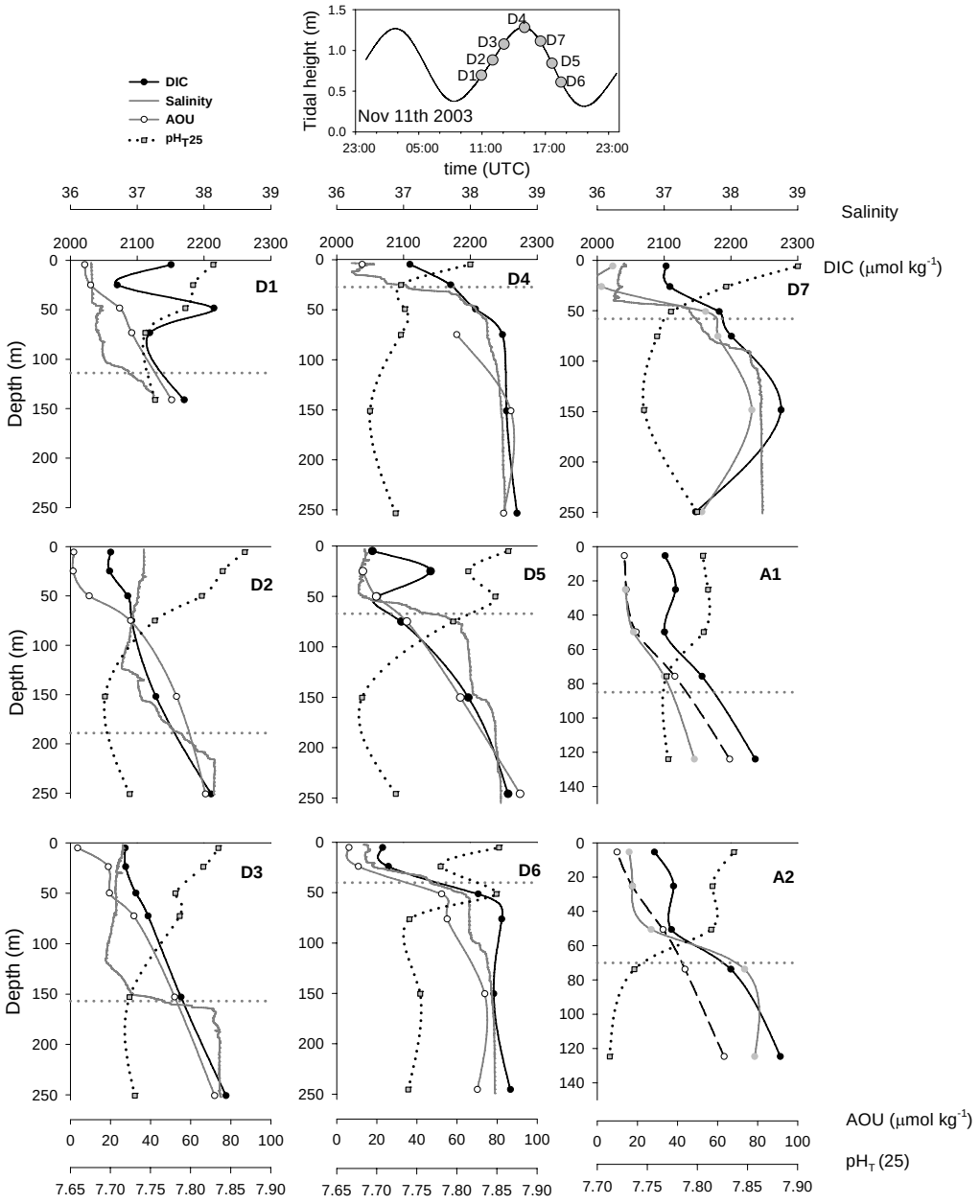

Figure 3. Vertical distribution of salinity, DIC, AOU, and pH_T (25) along the Strait of Gibraltar. Stations D1 to D3 were situated over the Spartell Sill, D4 is located over the Camarinal Sill, D5 to D7 at Tarifa Narrow, and A1 and A2 are located at either side of the Gates of Hercules (See figure 1). The horizontal dotted lines indicate the interface location.

Table 1. Chemical characteristics of the different water layers observed in the Strait of Gibraltar. [a] The code 1 or 2 after the station D1 to D7 reefers to the sampling date: "1" for the sampling carried out the 11th Nov 2003 and "2" for the sampling date 17th Nov 2003. The station A1 was sampled the 7th Nov 2003, and the station A2 on the 14 Nov 2003; [b]: HW = high water; HW+2= two hours after HW; LW= Low Water. [c] The upper and lower limits of the interface layer has been defined between the salinity 36.5 and 38, following Dafner et al. (2001b).

			Atlantic Layer					**Interface layer** [c]					**Mediterranean Layer**				
Station[a]	time[b]	Interface Depth (m)	Salinity	Temp	DIC μmol kg^{-1}	AOU μmol kg^{-1}	pH_T25	Salinity	Temp	DIC μmol kg^{-1}	AOU μmol kg^{-1}	pH_T25	Salinity	Temp	DIC μmol kg^{-1}	AOU μmol kg^{-1}	pH_T25
D1_1	HW-4	98-141	36.39	16.92	2135.9	22.18	7.78	36.90	14.80	2153.9	44.19	7.75	--	--	--	--	--
D1_2	LW-2	86.5-141	36.35	17.07	2134.9	13.41	7.79	37.08	14.64	2136.5	30.71	7.78	--	--	--	--	--
D2_1	HW-3	156-251	36.29	16.43	2086.1	19.98	7.79	37.40	16.43	2171.0	60.50	7.71	--	--	--	--	--
D2_2	LW-1	144-203	36.29	16.83	2098.3	22.14	7.79	37.53	14.12	2187.8	46.14	7.73	38.16	13.47	2227.5	63.36	7.74
D3_1	HW-2	145-165	36.28	16.60	2116.6	29.62	7.78	37.13	14.37	2168.4	56.50	7.72	38.09	13.57	2203.4	67.10	7.73
D3_2	LW	182-227	36.28	16.77	2119.9	25.65	7.79	37.40	14.21	2199.0	60.74	7.74	38.25	13.44	2233.4	73.84	7.73
D4_1	HW	16-45	36.34	16.07	2125.0	19.56	7.79	37.34	14.27	2176.3	30.04	7.74	38.4	13.2	2253.7	76.54	7.71
D4_2	LW+1	107-151	36.33	16.73	2116.1	22.22	7.79	37.45	14.37	2170.5	50.64	7.73	38.3	13.26	2229.6	71.10	7.72
D5_1	HW+3	52-120	36.38	17.30	2084.6	16.39	7.84	37.69	14.16	2109.6	37.43	7.78	38.3	13.33	2214.7	71.68	7.70
D5_2	LW+3	92-151	36.37	17.69	2095.8	15.56	7.83	37.58	14.24	2179.8	46.00	7.77	38.23	15.28	2269.8	62.14	7.73
D6_1	HW+4	20-91	36.45	18.82	2073.0	8.49	7.81	37.63	14.59	2193.5	43.29	7.78	38.3	13.22	2246.9	66.27	7.74
D6_2	LW+5	101-127	36.37	17.52	2136.9	33.31	7.79	37.28	14.58	2225.5	58.98	7.76	38.42	13.19	2249.7	66.31	7.74
D7_1	HW+2	42-87	36.32	17.43	2117.4	10.99	7.85	37.50	14.38	2191.1	55.81	7.77	38.4	13.11	2223.6	66.67	7.77
D7_2	LW+4	44-138	36.30	17.06	2063.5	16.59	7.85	37.59	14.33	2135.0	49.33	7.77	38.24	13.25	2236.9	80.10	7.76
A1	HW	44-126	36.49	16.65	2106.4	16.06	7.807	37.24	14.92	2174.1	35.88	7.77	38.35	13.28	2236.6	48.43	7.77
A2	HW-2	12-128	36.34	17.55	2089.2	16.10	7.834	37.32	14.95	2189.3	57.69	7.76	38.29	13.33	2274.0	78.53	7.71
Average			**36.35**	**17.09**	**2106.2**	**19.27**	**7.81**	**37.40**	**14.44**	**2172.5**	**47.74**	**7.75**	**38.29**	**13.46**	**2238.4**	**68.62**	**7.74**

water is characterised by lower content of DIC and lower AOU than the upper Mediterranean Levantine Intermediate Water (LIW).

In order to study the role of the tide on the variability of the physico-chemical spatial distribution, two descriptive samplings were performed on 11th and 17th of November, each at a different tidal amplitude and tidal phase, and both samplings were performed down to a depth of 250 m (figure 3 corresponds to 11th November, except for the eastern A1 and A2 Stations). For the prime sampling, the maximum current velocities were around 1.9 m s^{-1}, higher than the 1.4 m s^{-1} that recorded in the second grid. As well as the differences in tidal amplitude, the stations were sampled at different times in the tidal cycle (table 1), i.e. the first grid was performed coinciding mainly with the outflowing and the second grid during the inflowing tide. Under these conditions, maximum interfacial mixing occurs during the sampling for the first grid. In addition to the descriptive sampling at these seven stations, the spatial description of the carbonate system obtained includes two profiles performed on the eastern side of the Strait (see fig 1) as part of the tidal sampling strategy (see section 3.2). Table 1 shows the integrative average values for each of the three layers of water interacting in the Strait of Gibraltar. The horizontal distribution of the chemical parameters over the length of the Strait depends on the location of the interface layer. Although the actual thickness and characterization of properties of the interface must be defined in accordance with the halocline location and not with specific salinity values (Bray et al., 1995), the salinity values of 36.5 and 38 can be used to locate the upper and lower limits of the interface, adopting the same criterion as in previous studies such as those by Bryden et al. (1994) and Dafner et al. (2001a). Hence the Atlantic layer and the interface are much deeper on the western side of the Strait (St D1-D3) than on the eastern side (St D5-D7, A1-A2). In turn, in both the eastern and western parts of the Strait, the interface is shallower in the north (St D1, D6) than in the south, so the interface is deeper, colder, thicker and fresher

on the western side of the Strait, as has been described in other studies (Gascard and Richez, 1985, Bray et al., 1995). The integrative DIC value found for the Atlantic layer ranged from 2036.0 μmol kg^{-1} at D7 to the maximum of 2135.9 μmol kg^{-1} at D1. The general distribution in the Atlantic layer on the western side shows higher DIC and AOU values, and lower pH_T (25), salinity and temperature values in the south compared with the north (except for the station D1 influenced by the coast). This can be explained by the greater presence of the NACW in the south, with higher DIC and AOU values than the SAW. To the east of the Sill, the northern part is warmer and saltier, but different patterns are found for DIC and AOU values, for the different sampling dates. Thus, as mentioned already, the first grid sampling corresponded to a higher tidal coefficient, which causes the interface to be relatively shallow. This in turn results in the NACW being displaced to the south as it enters the Mediterranean and explains the higher AOU and DIC values found at station D7. Additionally, in the north, the nutrients and DIC are more bio-available as the interface rises, together with the enrichment of nutrients caused by vertical mixing, enhancing the primary productivity and causing a lower AOU in this zone, compared with the second grid. For the sampling performed on 17th November (2nd grid), the pattern persists on the western side of the Sill, but a different situation is found in the east. The fortnightly tidal cycle results in a deeper interface just after the neap tide (Bryden et al., 1994). Such a circumstance favours the entry of the NACW to the north and central parts and explains the greater presence of the NACW on the eastern side, compared with the first grid. Moreover, because the upper layer on the eastern side is less fertile at neap tides, higher AOU values are found in this zone in the second grid. This is in agreement with the observation of Macias et al. (2006), who found that, in the eastern part, intense vertical mixing episodes at spring tides were more effective in enhancing primary production than the presence of the nutrient-enriched NACW. The differences between the first and second grids can be mainly explained as follows: in the first grid, the intense vertical mixing is favoured by the higher tidal amplitude and the

coincidence with the outflow; however, in the second grid, such mixing phenomena are less probable because of the lower tidal amplitude, and the samples were collected during the water inflow.

These biochemical gradients are in accordance with the abundance of water masses over the length of the Strait observed by Bray et al. (1995), who described increases, from the westernmost to the easternmost sections, of 12% of the SAW and 5-10% of the MW in the upper layer, accompanied by a decrease of 20% of the NACW. Moreover, in the lower layer, the MW decreases from 95% to 83%, from east to west.

In summary, the average DIC and AOU values found in this study for the SAW are 2106.2 ± 22.8 μmol kg^{-1} for DIC, and 19.3 ±6.5 μmol kg^{-1} for AOU; in the interface layer the values found are 2172.6 ±28.2 μmol kg^{-1} for DIC and 47.7 ±10.3 μmol kg^{-1} for AOU; and for the MW, 2238.4 ±20.2 μmol kg^{-1} and 68.6 ±8.3 μmol kg^{-1} respectively. These values are in accordance with previous literature on the carbonate system (Santana-Casiano et al., 2002, Dafner et al., 2001a) and for oxygen (Minas et al., 1991; Dafner et al., 2001b) available in the Strait of Gibraltar and in the Gulf of Cadiz (Gonzalez-Davila et al., 2003; Ait-Ameur and Goyet, 2006). It should be noted that the lower values for DIC in the MW compared to previous studies are due to sampling to a maximum depth of 250 m, where the Mediterranean waters may be disturbed by the phenomenon of interface oscillations. In comparison with the relative homogeneous vertical concentration of DIC observed in the Mediterranean layer, previous studies performed in the Strait show a slight increase down to a depth of 300 m (Dafner et al., 2001a; Santana-Casiano et al., 2002).

3.2. Tidal variability of DIC and AOU

In order to obtain a better understanding of factors controlling the temporal variability of the inorganic carbon and oxygen, two fixed stations were sampled twice:

one located at the main Sill (above Station D4) and the other at the easternmost section of the Strait (A1 and A2, see figure 1). The tidal cycle in the Strait is essentially semi-diurnal but the diurnal component is quite detectable (Gascard and Richez, 1985). The T/S diagram in figure 4 shows the composition of the water masses for each sampling. As noted previously, there is usually a relatively larger volume of the NACW at the Sill than in the eastern section. The tidal oscillation of the interface has a significant effect on the vertical distribution of DIC and AOU. Normally, the current flows eastward in the upper layer and westward in the lower layer, although they are considerably affected by the tidal cycle: at the Sill, especially at spring tide, the current flows from east to west, in the upper layer 5 to 6 hours before high water (HW), and then flows in reverse, back to the east, 1-2 hours before HW (Gascard and Richez, 1985). At the beginning of the high tide, the arrested internal waves generated as a consequence of the interaction of the tidal flow with the bottom elevation at the Sill are liberated and began to propagate towards the east (Bruno et al., 2002). These internal waves are expected to take 8-9 hours to arrive to the easternmost station A1 and A2, passing through this point at around HW-4. These phenomena are discernable in figure 4. At HW the interface is at its shallowest depth over the Sill, where there is a noticeable increase in salinity from 25 to 150 m of depth, accompanied by higher DIC and AOU values. This upwelling of deeper and colder waters reaches the shallowest depth in the sampling performed on 13th November since the tidal coefficient is higher than for the sampling of 19th November; this also results in a shallower interface. At Low Water at the Sill (LW=HW±6), the interface is at its deepest position, allowing the NACW to pass through the Sill at a depth of 75-150 m, identified by a minimum salinity value (<36.2). This presence of the NACW, identified by the minimum salinity (S<36.2), is associated with an increase in AOU and DIC, to 40-45 μmol kg^{-1} and up to 2080-2100 μmol kg^{-1} respectively, at intermediate depths. The maximum velocity of current estimated is around 1.8 m s^{-1} on 13th November and 1.5 m s^{-1} on 19th November. The greater intensity of mixing leads to a higher vertical fluctuation of the isolines for

salinity, DIC and AOU on 13th than on 19th November. The maximum interface thickness can be found at the Sill between HW-3 to HW+2 when the internal waves are expected to be arrested; this situation can be appreciated in the salinity, DIC and AOU values, especially on 13th November. The lower intensity of mixing at the Sill on 19th November is reflected in the weaker oscillation of the DIC and AOU isolines, and therefore lower DIC and AOU concentrations for the first 100 m of depth, due to less injection of deep water into the upper layer.

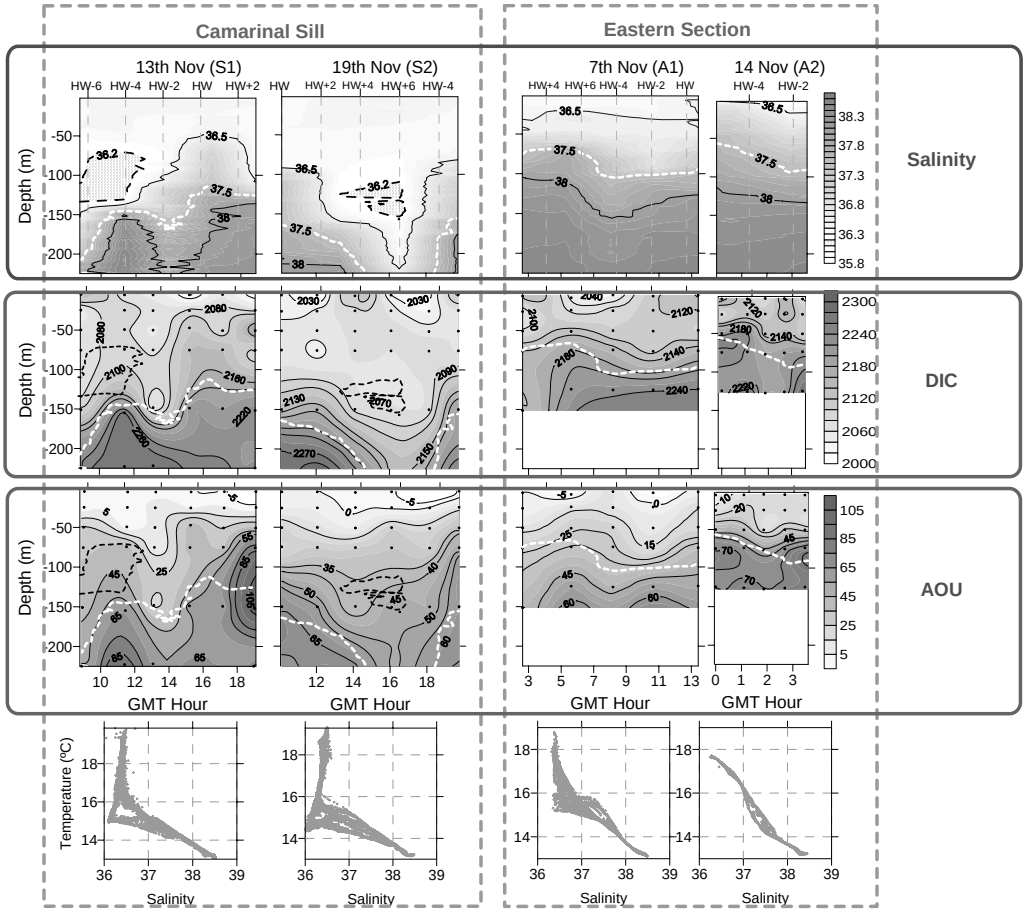

Figure 4. Temporal evolution for salinity, DIC and AOU for the samplings performed at the Sill (13 and 19 Nov 2003) and eastern section (7 and 14 Nov 2003) and T/S diagrams. The white dashed line indicates the interface location. The black dashed line marks the presence of the NACW.

At the eastern entrance of the Strait, the interface is shallower at LW and begins to descending around HW-4 as a consequence of the passing of the internal wave liberated in the previous tidal cycle and the arrival of the undulatory disturbances, which lead to the undulations in the DIC and AOU isolines. The shallowness of the interface at LW explains the relatively high values for DIC (2130 μmol kg^{-1}) and AOU (23.7 μmol kg^{-1}) at 50 m. There is a significant difference in the AOU values between the first and the second samplings at the eastern station, and higher values are found for the entire water column for 7^{th} compared with 14^{th} November. Two different causes are plausible: the second sampling was performed during the night, without the irradiance needed for the primary producers, whereas the first sampling takes place during the day; secondly, the first sampling is performed during the spring tide but the second during the medium to low tide. As previously mentioned, at spring tide the maximum vertical mixing rates at the Sill, as well as the enrichments in nutrients in the upper layer, are recorded (Macias et al., 2007). As a result, the advected nutrients from the Sill reach a more bio-available area, enhancing the primary productivity and causing a lower AOU in this zone. This coincides with the result obtained at the same station by Macias et al., (2006), who found maximum chlorophyll values related to the occurrence of the maximum mixing rates at the Sill. This chlorophyll maximum could be related to the inputs of coastal water by suction action at the Sill during the outflowing of the Atlantic flow, and not to internal growth in the Strait. Several investigations (Gomez et al., 2001; Macias et al., 2006) have been performed at the eastern entrance of the Strait in order to gain a better understanding of the tidal variability on nutrients, their sources and the implication for the phytoplankton community. The main factors controlling the carbon and oxygen variability are the vertical oscillation of the interface as well as the intensity of the tidal mixing processes.

3.4. Relationship DIC and AOU versus salinity

Having assessed the tidal influence on the DIC and AOU values, in the previous section (3.3), the mixing diagrams of DIC, AOU and pH_T (25) versus salinity (figure 5) will be used in order to remove discrepancies due to tidal oscillations. For this analysis the entire data base available on the Strait of Gibraltar from the samplings performed during November, with a total of 183 samples, has been used. With the objective of obtaining a better characterization of the Atlantic and Mediterranean water mixing, the NACW samples (S<36.2) have been disregarded. Figure 5 shows a good linear correlation between DIC and salinity (S), a relationship which can be formulated precisely as DIC = 86.96 S – 1079 (r^2=0.82). This high degree of correlation applies to the entire water column sampled, but the Atlantic layer displays a higher variability for a narrower salinity range than the Interface and Mediterranean layers, due to the greater intensity of biological processes, as well as to the air-water exchange and coastal inputs. The DIC-S relationship obtained is similar to that in previous inorganic carbon studies performed in the Strait of Gibraltar during the CANIGO expeditions in September 1997 (Dafner et al., 2001a, Santana-Casiano et al., 2002) except for some slight differences in the fitting parameters; these differences can be explained because the previous formulation effectively disregarded the Atlantic layer by only taking into account salinities higher than 37. In order to study the sources of variability in the DIC values of surface water, Santana-Casiano et al. (2002) proposed a different formulation only for surface waters; this formulation gives values very close to those obtained in this study for the Atlantic Layer.

As with DIC, the relationship of AOU vs. salinity shows a high linear correlation, which can be formulated as: AOU = 33.62S–1213.1 (r^2=0.82). This linear relationship is noteworthy since, even if the oxygen is subject to biological and gas exchange processes, these are much lower in magnitude and much slower for the endmembers than the Atlantic-Mediterranean water mixing due to the short residence time of the water

masses in the Strait of Gibraltar. This same explanation was put forward by Minas et al. (1991) for the oxygen-salinity relationship.

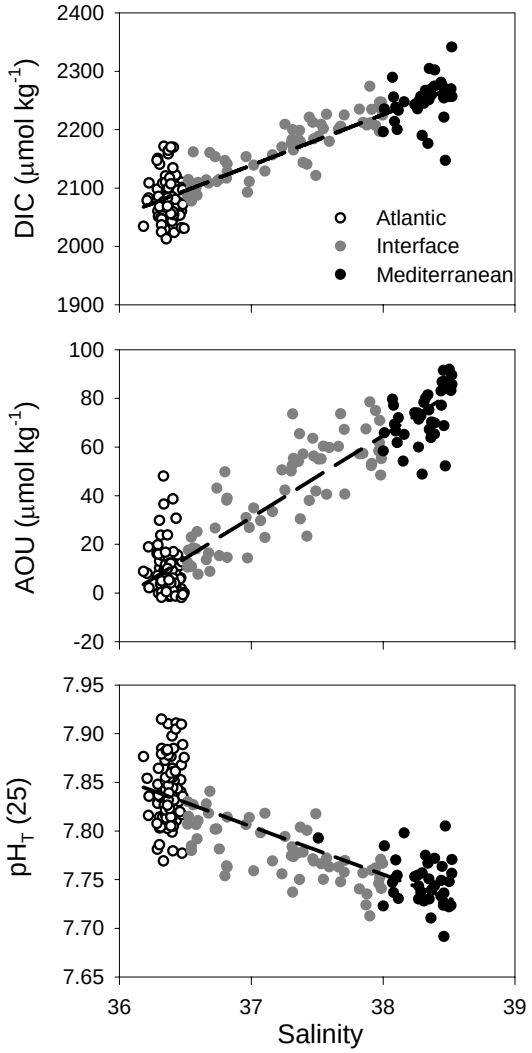

Figure 5. Theoretical dilution line for DIC, AOU and $pH_T(25)$. The linear regression line (black dashed line) has been drawn.

The decrease of $pH_T(25)$ with salinity is related to the more acidic nature of the Mediterranean compared to Atlantic waters, and this parameter shows a less conservative behaviour than DIC and AOU especially in the upper Atlantic layer (linear fit $pH_T(25) = -0.049S+9.63$; $r^2=0.65$). This departure from linearity for surface waters suggests that biological activity has a greater effect on pH.

To assess the stoichiometric relationship between DIC and oxygen, the surplus DIC has been calculated, following DeGrandpre et al. (1997). The surplus DIC is defined as the difference between the observed DIC, and the DIC calculated from TA and the monthly average atmospheric CO_2 value for November; this last value corresponds to data measured at the Tenerife Atmospheric Observatory (Spain), taken from the World Data Centre for Greenhouse Gases (WDCGC / WMO) air sampling network (available at http://gaw.kishou.go.jp/wdcgg.html). The departure of the observed DIC from the DIC in equilibrium with the atmosphere enables the remineralization ratios with respect to oxygen to be assessed, and can be seen as the carbon analogy to the AOU. Although the relationship between AOU and surplus DIC (see figure 6) is very scattered ($r^2=0.34$), the plotted slope of 1.2 tracks the molar ratios for the western Mediterranean basin proposed by Bethoux et al. (2005), and is equal to $C:\Delta O_2=192:237$. Therefore, although it may be considered from the DIC and AOU mixing lines that most of the variability of these biochemical parameters is explained by the strong mixing processes taking place in the Strait of Gibraltar, the value of the slope plotted for AOU vs. surplus DIC suggests that the main difference in DIC and AOU content between the Atlantic and Mediterranean Waters can be explained by the mineralization processes occurring during their cycle around the Mediterranean Sea.

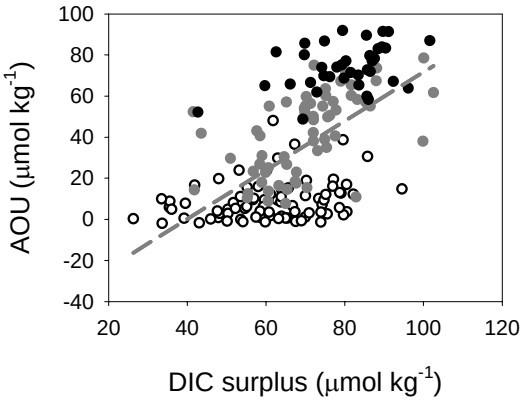

Figure 6. AOU versus surplus DIC in the Strait of Gibraltar.

3.5. Inorganic carbon exchange in the Strait of Gibraltar:

The driving force of the exchange through the Strait of Gibraltar is the net loss of freshwater in the Mediterranean Sea, due to the excess of evaporation over precipitation and river runoff. Nevertheless, due to the complexity of the physical processes in this area, there is high variability over the average exchange from tidal to seasonal scale and depending on the position in the Strait, omission of interface movements, etc. It is this factor which is mainly responsible for the wide diversity in the literature sources in respect of not only the water fluxes but also the exchange of biogeochemical substances through the Strait of Gibraltar (Gomez 2003). In this paper, the water fluxes are calculated using the budget proposed by Baschek et al. (2001) based on a tidal inverse model, estimating an average transport of 0.81 Sv for the Atlantic inflow and -0.76 for the Mediterranean outflow (positive flows are defined as those into the Mediterranean Sea). These numbers imply a net water flow of 0.05 Sv towards the Mediterranean. The water transport estimations by Bascket et al. (2001) fall within the range of those reported in studies by Bryden et al. (1994) and Tsimplis and Bryden (2000), but below the older

estimation by Bethoux (1979) that did not take the interface layer into account in the water budgets. The inorganic carbon inflow and outflow will be calculated by multiplying the average concentration for each layer by its corresponding water transport. The estimates of the upper and lower layer volume transports thus depend on the choice of the separating isohaline. Baschek et al. (2001) define the isohaline 38.1 as the one that maximizes the transport in each layer. Therefore, in order to be consistent with the water volume transports used in this study, the DIC concentration has been averaged for waters above and below the isohaline 38.1. The average DIC concentration in the upper layer is 2118.4 μmol kg^{-1} and 2251 μmol kg^{-1} for the deep layer. Due to the shallowness of the sampling (down to 225 m depth) and in order to obtain a more realistic estimation of the transport in the Strait, the DIC values obtained in 2002 by Ait-Ameur and Goyet (2006) for the Mediterranean layer have been used. The resulting estimate of transport yields a total Atlantic input of 5.56 10^{13} mol C yr^{-1} and a total Mediterranean output of 5.70 10^{13} mol C yr^{-1}; this produces a net DIC output to the Atlantic of 1.47 10^{12} mol C yr^{-1}. The net transport represents only 1.3 % of the total transport for the Atlantic or Mediterranean , but this amount plays an important role in the global carbon budgets since it is injected in the Atlantic deep water circulation, as mentioned earlier. The net transport obtained in this study is very close to a recent estimation proposed by Ait-Ameur and Goyet (2006). Previous estimations in the literature for the inorganic carbon exchange at the Strait of Gibraltar results in a wide range of net DIC transport values, which vary from 3.8 - 4.9 10^{12} mol C yr^{-1} (Dafner et al., 2001a) and 0.98 10^{12} mol C yr^{-1} Gomez (2003). The diversity of results found in the literature is due to the particular estimates made of DIC concentration for each layer, as well as to the values for water volume transport used.

With the object of calculating an average flux, it is worth noting the high variability of the water fluxes on different time scales. In this respect, tidal currents produce flow fluctuations whose amplitude reaches up to 4 Sv during spring tides, more than four times greater in magnitude than the average flow (García-Lafuente and Vargas

Dominguez, 2003). In order to asses this variability, Macias et al. (2007) developed a model that coupled hydrodynamical and biogeochemical factors to explore the effects of the strong advection and mixing processes on the biogeochemical exchange and on the pelagic community of the area. In this model, a third intermediate layer has been incorporated and this leads to a significant improvement in the estimation of biogeochemical budgets. The model calibration exercise, carried out for salinity values obtained from an extensive data base, demonstrated the need to include mixing in any model for the Strait. Hence, the application of this model to the inorganic carbon data base obtained in this study allows estimates to be made of the amount of carbon in the outflowing layer that is introduced into the upper layer and therefore recirculated to the Mediterranean Sea. As a result, it has been estimated that, on average, 1.35 % of the outflowing DIC is incorporated into the upper layer, varying between 2.6% at spring tides and 0.5% at neap tides. This means that, on average, 35.7 μmol kg^{-1} of DIC from the deep layer are being injected into the upper layer as a result of the mixing effects and transported again towards the Mediterranean Sea. This recirculation phenomenon by mixing means that the total Atlantic inflow is increased from 5.56 10^{13} to 5.64 10^{13} mol C yr^{-1}. Several direct and indirect estimations have been made for the nutrient recycling (Gomez et al., 2000; Dafner et al., 2003; Macias et al., 2007) to explain the upper layer fertilization in the eastern Section of the Strait; this recirculation has been neglected until now for calculations of the carbon exchange in the Strait of Gibraltar.

Recent investigations (Rios et al., 2001; Alvarez et al., 2005; Bethoux et al., 2005) have drawn attention to the role of the Mediterranean Sea on the sequestration of anthropogenic carbon. The Mediterranean Sea is one of the few areas around the global ocean where the formation of deep water is possible; this is then incorporated into deep water currents through its outflow at the Strait of Gibraltar (Bethoux et al., 2005). Using the data base for oxygen, TA and DIC values, it is possible to estimate the anthropogenic carbon concentration in the Strait of Gibraltar by means of the TROCA approach

(Touratier and Goyet, 2004). The average anthropogenic carbon concentration in the Mediterranean water obtained in this study is 65 μmol kg^{-1}, which represents 3% of the inorganic carbon transported to the Atlantic. This value underestimates the total anthropogenic carbon value in the Mediterranean outflow but it is representative of the upper water column sampled in this study (at 250 m depth). Previous estimates vary in the approach used for its computation, and in the region of the study: values reported range from 50 μmol kg^{-1} (Rios et al., 2001) in the eastern Atlantic region draw-down of the Central Atlantic Water plus Mediterranean Outflow Water, to 111 μmol kg^{-1} for the Mediterranean Outflow Water recently calculated by Ait-Ameur and Goyet (2006), who concluded that the complex circulation in the Gulf of Cadiz leads to a deep penetration of anthropogenic carbon from the Mediterranean Sea to the Atlantic Ocean.

4. Conclusion

Given the key role of the Mediterranean Outflow in the global carbon budget, a better understanding is required of the carbonate system variability as the Outflow passes through the Strait of Gibraltar toward the Atlantic Ocean. The vertical distribution of the inorganic carbon and oxygen are highly dependent both on the position of the interface between the main water bodies interacting in the Strait, and on the intensity of the vertical mixing processes associated with the spring-neap tidal cycle. An increase in DIC and AOU with depth has been clearly identified, resulting from the larger carbon content budget of the Mediterranean water as a consequence of the intense remineralization processes taking place in the Mediterranean basin (Dafner et al., 2001b; Bethoux et al., 2005). Tidal action causes the Strait to behave as a deep water pulsating area, the intensity of which is a function of various fluctuation phenomena, such as the internal hydraulic jump and the arrested internal waves over the Camarinal Sill. As a consequence, the upwelling of deep water on the Camarinal Sill at high water causes an increase in the DIC and AOU in the upper water column; this water is subsequently

advected to the eastern section and causes higher DIC and AOU concentrations in the eastern area. Although several authors (Gomez et al., 2000; Macias et al., 2006) have highlighted the effect of the nutrient input to the upper layer on the enhanced primary production of the eastern section, both the inorganic carbon pool and oxygen present a highly conservative behaviour, suggesting that hydrodynamics rather than biological processes are the main mechanisms involved in its variability. In any case, this carbon recirculation from the deepest to the upper layer must be taken into account to obtain a more realistic estimation of the carbon exchange at the Strait of Gibraltar.

Acknowledgments

This work has been funded by the projects of the Spanish National Research Program REN-2001-2733-C02-02 and by the project CTM 2005-01364/MAR. The authors thank Dr. Miguel Bruno for the technical assistance during the paper elaboration and to Dr. A. Izquierdo who kindly helped with the data processing.

References

Aït-Ameur, N. and Goyet, C., 2006. Distribution and transport of natural and anthropogenic CO_2 in the Gulf of Cadiz. Deep-Sea Research II, 53: 1329-1343.

Alonso del Rosario, JJ., Bruno, M., Vázquez-Escobar, A., 2003. The influence of the tidal hydrodynamics conditions on the generation of lee waves at the main sill of the Strait of Gibraltar. Deep-Sea I 50, 1005-1021.

Alvarez, M., Perez, F.F., Shoosmith, D.R., Bryden, H.L., 2005. Unaccounted role of Mediterranean Water in the drawdown of anthropogenic carbon. Journal of Geophysical Research 110, C09S03.

Armi, L., Farmer, D., 1988. The flow of Mediterranean Water through the Strait of Gibraltar. Progress in Oceanography 21, 41–82.

Baschek, B., Send, U., Garcia-Lafuente, J., Candela, J., 2001. Transport estimates in the Strait of Gibraltar with a tidal inverse model. Journal of Geophysical Research 106 (C12), 31033–31044.

Benson, B. B., and Krause, JR. 1984. The concentration and isotopic fractionation of oxygen dissolved in freshwater and seawater in equilibrium with atmosphere. Limnology and Oceanography 29: 620–632.

Bethoux, J.P., 1979. Budgets of the Mediterranean Sea, their dependence on the local climate and on the characteristics of the Atlantic waters. Oceanologica Acta 2, 157–163.

Bethoux, J.P., El Boukhary, M.S., Ruiz-Pino, D. Morin, P. Copin-Montégut, C, 2005. Nutrient, Oxygen and Carbon Ratios, CO_2 Sequestration and Anthropogenic Forcing in the Mediterranean Sea. In: The Handbooks of Environmental Chemistry, Part K. Springer-Verlag Berlin Heidelberg, pp: 67-86.

Bray, N.A., Ochoa, J., Kinder, T.N., 1995. The role of the interface in exchange through the Strait of Gibraltar. Journal of Geophysical Research 100 (C6), 10755–10776.

Bruno, M., Alonso, J.J., Cózar, A., Vidal, J., Ruiz-Cañavate, A., Echevarría, F., Ruiz, J., 2002. The boiling-water phenomena at Camarinal Sill, the strait of Gibraltar. Deep-Sea Research II 49, 4097–4113.

Bryden, H.L., Candela, J., Kinder, T.H., 1994. Exchange through the Strait of Gibraltar. Progress in Oceanography 33, 201–248.

Copin-Montégut, C., 1993. Alkalinity and carbon budget in the Mediterranean Sea. Global Biogeochemical Cycles 7 (4), 915–925.

Dafner, E.V., González-Dávila, M., Santana-Casiano, J.M., Sempere, R., 2001a. Total organic and inorganic carbon exchange through the Strait of Gibraltar in September 1997. Deep-Sea Research II 48, 1217–1235.

Dafner, E.V., Semp_er_e, R., Bryden, H.L., 2001b. Total organic carbon distribution and budget through the Strait of Gibraltar in April 1998. Marine Chemistry 73, 233–252.

Dafner, E.V., Boscolo, R., Bryden, H.L., 2003. The N:Si:P molar ratio in the Strait of Gibraltar. Geophysical Research Letters 30 (10), 13.1–13.4.

DeGrandpre, M.D., Hammar, T.H., Wallace, D.W.R. and Wirick, C.D., 1997. Simultaneous mooring-based measurement of seawater CO_2 and O_2 off Cape Hatteras, North Carolina. Limnology and Oceanography 42(1): 21-28.

Dickson, A.G., 1990. Standard potential of the reaction: AgCl(s)+ ½ H_2(g)=Ag(s)+HCl(aq), and the standard acidity constant of the ion HSO^{4-} in synthetic seawater from 273.15–318.15 K. Journal of Chemical Thermodynamics. 22, 113–127.

Dickson, A.G., Riley, J.P., 1979. The estimation of acid dissociation constants in seawater media from potentiometric titrations with strong base. I. The ionic product of water — KW. Marine Chemistry. 7, 89–99.

Echevarría, F., García-Lafuente, J., Bruno, M., Gorsky, G., Goutx, M., González, N., García, C.M., Gómez, F., Vargas, J.M., Picheral, M., Striby, L., Varela, M., Alonso, J.J., Reul, A., Cózar, A., Prieto, L., Sarhan, T., Plaza, F., Jiménez-Gómez, F., 2002. Physical biological coupling in the Strait of Gibraltar. Deep-Sea Research II 49 (19), 4115–4130.

García-Lafuente, J., Vargas Domínguez, J.M., 2003. Recent observations of the exchanged flows through the Strait of Gibraltar and their 642 fluctuations at different time scales. Recent Research Development in Geophysics 5, 73–84.

García-Lafuente, J., Vargas, J.M., Plaza, F., Sarham, T., Candela, J., Basheck, B., 2000. Tide at the eastern section of the Strait of Gibraltar. Journal of Geophysical Research 105 (C6), 14197–14213.

García-Lafuente, J., Delgado, J., Vargas, J.M., Vargas, M., Plaza, F., Sarhan, T., 2002. Low frequency variability of the exchanged flows 646 through the Strait of Gibraltar during CANIGO. Deep-Sea Research II 49 (19), 4051–4067.

Gascard, J.C., Richez, C., 1985. Water masses and circulation in the western Alboran Sea and in the Strait of Gibraltar. Progress in Oceanography 15, 157–216

Gómez, F., González, N., Echevarria, F., García, C.M., 2000. Distribution and fluxes of dissolved nutrients in the Strait of Gibraltar and its relationships to microphytoplankton biomass. Estuarine Coastal Shelf Science 51, 439–449.

Gómez, F., Gorsky, G., Striby, L., Vargas, J.M., González, N., Picheral, M., García Lafuente, J., Varela, M., Goutx, M., 2001. Small-scale temporal variations in biogeochemical

features in the Strait of Gibraltar, Mediterranean side - the role of NACW and the interface oscillation. Journal of Marine Systems 30, 207–220.

Gómez, F. 2003. The role of the exchanges trough the Strait of Gibraltar on the Budget of elements in the Western Mediterranean Sea: consequences of human induced modifications. Marine Pollution Bulletin 46, 685-694.

González-Dávila, M., Santana-Casiano, J.M., Dafner, E.V., 2003. Winter mesoscale variations of carbonate system parameters and estimates of CO2 fluxes in the Gulf of Cádiz, northeast Atlantic Ocean (February 1998). Journal of Geophysical Research 108 (C11), 3344.

Lueker, T.J., Dickson, A.G. and. Keeling, C.D., 2000. Ocean pCO_2 calculated from dissolved inorganic carbon, alkalinity, and equations for K_1 and K_2 : validation based on laboratory measurements of CO_2 in gas and seawater at equilibrium. Marine Chemistry., 90 (105-119)

Macías, D., 2006. Efectos biológicos de la mezcla interfacial y de los procesos hidrodinámicos mesoescalares en el Estrecho de Gibraltar. Ph.D. Thesis, University of Cadiz, Cadiz, Spain.

Macías, D., García, C.M., Echevarría, F., Vázquez-Escobar, A., Bruno, M., 2006. Tidal induced variability of mixing processes on Camarinal Sill (Strait of Gibraltar). A pulsating event. Journal of Marine Systems 60, 177–192.

Macías, D. ,Martín, A.P., García-Lafuente , J., García , A. Yool , C.M., Bruno, M., Vázquez-Escobar , A., Izquierdo, A. Sein , D.V., Echevarría, F, 2007. Analysis of mixing and biogeochemical effects induced by tides on the Atlantic–Mediterranean flow in the Strait of Gibraltar through a physical–biological coupled model. Progress in Oceanography 74: 252-272.

Minas, H.J., Coste, B., Le Corre, P., Minas, M., Raimbault, P., 1991. Biological and geochemical signatures associated with the water circulation through the Strait of Gibraltar and in the Western Alboran Sea. Journal of Geophysical Research 96, 8755–8771.

Reid, J.L., 1979. On the contribution of the Mediterranean Sea outflow to the Norwegian-Greenland Sea. Deep-Sea Research 26, 1199–1223.

Ríos, A.F., Perez, F.F. Fraga, F., 2001. long-term (1977-1997) measurement of carbon dioxide in the Eastern North Atlantic: evaluation of anthropogenic input. Deep-Sea Research II 48: 2227-2239.

Santana-Casiano, J.M., González-Dávila, M., Laglera, L.M., 2002. The carbon dioxide system in the Strait of Gibraltar. Deep-Sea Research II 49, 4145–4161.

Sarmiento, J.L., Gruber, N., 2002. Sinks for anthropogenic carbon. Physical Today, 30–36.

Takahashi, T., Sutherland, S.C., Sweeney, C., Poisson, A.,Metzl, N., Tilbrook, B., Bates, N., Wanninkhof, R., Feely, R.A., Sabine, C., Olafsson, J., Nojiri, Y., 2002. Global sea–air CO2 flux based on climatological surface ocean pCO2, and seasonal biological and temperature effects. Deep-Sea Research II 49, 1601–1622.

Touratier, F., Goyet, C., 2004a. Definition, properties, and Atlantic Ocean distribution of the new tracer 'TrOCA'. Journal of Marine Systems 46, 169–179.

Touratier, F., Goyet, C., 2004b. Applying the new 'TrOCA' approach to assess the distribution of anthropogenic CO2 in the Atlantic Ocean. Journal of Marine Systems 46, 181–197.

Tsimplis, M.N., Bryden, H.L., 2000. Estimation of the transports through the Strait of Gibraltar. Deep-Sea Research I 47 (12), 2219–2242

Wu, P. and Haines, K., 1996. Modeling the dispersal of Levantine Intermediate Water and its role in Mediterranean deep water formation. Journal of Geophysical Research, 101 (C3): 6591–6608.

Zeebe, R. E., and D. A. Wolf-Gladrow, CO_2 in Seawater: Equilibrium, Kinetics, Isotopes, 346 pp., Elsevier Sci., New York, 2001.

Seasonal variability of surface fCO_2 in the Strait of Gibraltar (SW Spain)[1]

Mercedes de la Paz*, Abelardo Gómez-Parra and Jesús Forja.

Departamento de Química-Física, Facultad de Ciencias del Mar y Ambientales, Universidad de Cádiz, Campus Río San Pedro s/n, Puerto Real (Cádiz) 11510, Spain

Abstract:

From September 2005 to May 2006 four cruises were performed in the Strait of Gibraltar in order to study the seasonal variability of carbon dioxide at surface waters and the assessment of the air-sea CO_2 fluxes. Continuous underway water measurement of fugacity of CO_2 (fCO_2), temperature and salinity has been performed along the longitudinal and latitudinal axis of the Strait. Additionally, discrete surface water samples were taken to measure dissolved inorganic carbon (DIC) and oxygen. The spatial distribution on surface fCO_2 shows low variability compare to the seasonal scale, with fCO_2 values ranging from 329 μatm in March to 387 μatm in September. The seasonal variability of fCO_2 is assessed and discussed in terms of temperature versus biology effects, being the temperature the main controlling mechanisms. The Strait of Gibraltar is CO_2 undersaturated most of the year, excepting in September, being the annual average CO_2 uptake equal to 0.28 mol C m^{-2} yr^{-1}, then behaving as a discreet sink of CO_2 on an annual scale.

Keywords: Carbon dioxide, air-sea exchange, seasonal variability, continental shelf, Strait of Gibraltar.

INTRODUCTION

Coastal and marginal seas play a key role in the global carbon cycle by linking the terrestrial, oceanic and atmospheric carbon reservoirs. They host strong biological activity and buffer the terrestrial and human impacts before such impacts reach the open ocean systems. In general, the coastal ocean tends to absorb CO_2 in winter, when the water cools, and in spring, as a consequence of the biological processes. In summer and

fall, the processes of warming, respiration of marine organism, and decomposition of organic matter release CO_2 back into the atmosphere (Chen, 2003). Finally, direct and indirect human perturbations to the continental margins (e.g., pollution and eutrophication) are large and have direct consequences for marine ecosystem. Unfortunately, owing to the diversity and therefore complexity of the shelf systems, their precise roles in the carbon cycle have not been quantified yet with any degree of certainty, and although coastal and marginal seas cover only 7% of the world ocean´s surface (Gattuso et al., 1998), their contribution in the exchange of CO_2 with the atmosphere plays a significant role in the global carbon budget (Chen, 2003). The seasonal amplitudes of the air-sea CO_2 gradient can easily be on the order of 100 ppm, with continuous undersaturation in the North Sea (Thomas et al., 2004) or even up to 400 ppm in the Baltic Sea (Thomas and Schneider, 1999). In contrast, in the open ocean regimens of similar latitudes, the seasonal amplitudes are only around 40 ppm (Takahashi et al., 2002). These much higher air-sea CO2 disequilibrium cause higher CO2 uptake from the atmosphere by coastal and continental shelves, and need to be taken into account in the global budgeting efforts.

Several processes transport oceanic properties onto shelves. Coastal upwelling areas are known to show important CO2 oversaturation of CO2 with respect to the atmosphere due to the inputs of CO2-rich deep waters. However the inputs of nutrients from upwelling fuel important primary productions that in turn lower the pCO2 values. Each of these two processes have then an antagonistic effect on the gradient of CO2 across the interface, and so far, it is difficult to assess the role of the coastal upwelling areas either as sources or sinks of atmospheric CO2 (Borges and Frankignoulle, 2002). The typical coastal upwelling follows longer periods between upwelling events and relaxation than the tidal mixing periods found at the Gibraltar Strait, were the mixing processes occur mainly on the tidal scale. The changes in the biogeochemical parameters of waters interacting through the Strait of Gibraltar are largely controlled by hydrodynamic

phenomena. The normal regime in the Strait of Gibraltar consists of two superimposed flows; a shallow Atlantic inflow and a deeper Mediterranean outflow. In turn, these two water masses show very different biogeochemical properties. Atlantic inflow is characterised by lower dissolved inorganic carbon concentrations, inorganic nutrients and AOU content as compared to the Mediterranean deep water (Minas et al., 1991; Santana-Casiano, et al. 2002). Eventually, there exists a third water mass on the upper layer, the North Atlantic Central Water (NACW) with slightly higher DIC content and lower salinity (S<36.2) than the Atlantic water. The long term average flow pattern in the Strait of Gibraltar exhibits large fluctuation at different time scale. Seasonal and subinertial fluctuations (meteorologically-induced) are on the order on 40 to 8 times lower than the tidal variability (Garcia-Lafuente et al., 2002). This fact can be explained by the dramatic bottom topography changes from 900 to 300 depth near the Camarinal Sill. The interaction between mean flows and the topography makes the interface between Atlantic and Mediterranean water change abruptly originating internal hydraulic jumps (Armi and Farmer, 1985) or arrested internal waves (Bruno et al., 2002). Such undulatory processes enhance the interfacial mixing and can inject deep Mediterranean water into the upper Atlantic layer. In addition, the intensity of these undulatory phenomena is related to the tidal amplitude, with a maximum mixing and surface nutrient enrichment at spring tides (Macias et al., 2006). Macias et al. (2007) recently developed a model that couples hydrodinamical and biogeochemical factors with the aim to explore the effects of the strong advection and mixing processes on the biogeochemical exchange and on the pelagic community of the area. These authors found that the short residence times within the channel do not allow phytoplankton communities to grow and proliferate appreciably during their transit. Therefore, all the phenomena co-occurring in the Strait of Gibraltar make very difficult to discern between the different biogeochemical driving mechanisms from tidal to seasonal scale.

The goal of this work is to evaluate the seasonal variability of the sea-surface CO2 and to asses the relative contribution of the physical and biological processes affecting the CO_2 concentration. Finally, it has been evaluate the air-sea CO2 exchanges on an annual scale.

MATERIAL AND METHODS

The data were obtained during four cruises in the Strait of Gibraltar carried out on board the R/V "Amir Moulay Abdellah", covering all the seasons in a consecutive order (7-8 September 2005, 12-13 December 2005, 20-21 March 2006 and 22-23 May 2006). The ship tracks and sampling stations are shown in figure 1. Two crossed tracks were performed for each cruise, one covering the West-East surface distribution including three discrete sampling station (from G1 to G3), and a second North-South track at the Camarinal Section comprising five sampling stations (from C1 to C5). In addition to the continuous underway sampling of the temperature, salinity and pCO_2, discrete samples were taken to measure pH, Total Alkalinity (TA) and dissolved oxygen at each station with the exception of March, when only discrete samples were taken. Underway parameters were sampled with a 30 second frequency from the surface seawater supply of the ship (pump inlet at depth of 3 m). Salinity and temperature were measured with a Seabird thermosalinograph (SBE-45-MicroTSG) before entry into the gas equilibrator. The equilibrator design is a combination of shower and bubble type similar to the system described by Koertzinger et al (1996). The CO2 molar fraction (xCO2) was detected by means of a non-dispersive infrared gas analyzer (Li-Cor 6262), which was calibrated twice per day with CO_2 free synthetic air and a second standard of 523 ppm molar fraction made and certified by Air Liquide (France).

The water saturated CO2 fugacity (fCO2) in the equilibrator was calculated from the xCO2 in dry air, atmospheric pressure and equilibrium water vapour, according to the

protocol described in DOE (1994). The formulation proposed by Takahashi et al. (1993) was employed for the partial pressure corrections to in situ water temperature. The atmospheric pCO_2 data has been obtained from the data measured at Tenerife Atmospheric Observatory (Spain) taken form the World Data Centre for Greenhouse Gases (WDCGS/WMO) air sampling network (available at http://gaw.kishou.go.jp/wdcgg.html). These atmospheric molar fraction CO_2 values were converted to wet air fugacity.

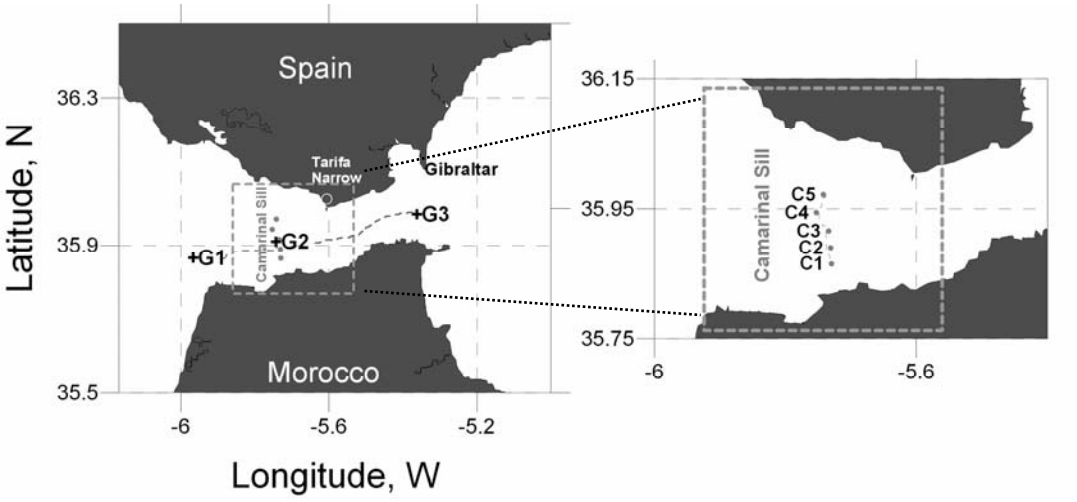

Figure1. Map of the sampling stations and ship-track for the continuous underway measurement.

The pH was measured with a glass combined electrode (Methrom) calibrated in the Free pH Scale (Zeebe and Wolf-Gladrow, 2001). The alkalinity computation was made from the titration curve by means of the Gran Function and taking into account the correction for sulphate and fluoride interaction, using the constants proposed by Dickson (1990) and by Dickson and Riley (1979) respectively. The dissolved inorganic carbon (DIC) were calculated from pCO_2 and TA using the K_1 and K_2 acidity constants proposed by

Lueker et al. (2000) in the Total pH Scale. For the cruise performed in March, in absence of CO_2 underway data, the pH and TA were used for the DIC calculations. The method was validated with reference standards obtained from A. Dickson (Scripps Institution of Oceanography, San Diego, USA) to an accuracy of ±2 μmol kg^{-1}.

The oxygen was fixed in a sealed flask and stored in darkness during 24 h as described by the Winkler method, for later analysis by potentiometric titration (Metrohm 670 Titroprocessor). The Apparent Oxygen utilization (AOU) is defined as departure of oxygen from an O_2 concentration in equilibrium with the atmosphere calculated from the Benson and Krause (1984) solubility equation. Measurements for TA and oxygen were accomplished within 24-48 hours after sampling.

Wind speed data used for the gas exchange calculation were provided by the regional government (Red de estaciones agroclimáticas de la Junta de Andalucía) for the meteorological station located at Vejer (Cádiz, Spain)

RESULTS AND DISCUSSION

Surface seasonal distribution in the Strait of Gibraltar

The surface water properties in the Strait of Gibraltar during the study period are shown in figure 2. In order to study the spatial distribution of fCO_2, the longitudinal and the latitudinal tracks have been separated. For a given cruise, the longitudinal variability of surface salinity, temperature, and fCO_2 is slightly higher than the latitudinal variability. The amplitude of the longitudinal and latitudinal variability for salinity at water surface is very homogeneous both on the spatial scale and on the seasonal scale, with values within the range of the Surface Atlantic Water (SAW). However, the spatial amplitude for temperature varies between 0.3-3.5ºC. Those values are between 20 to 0.5 times lower

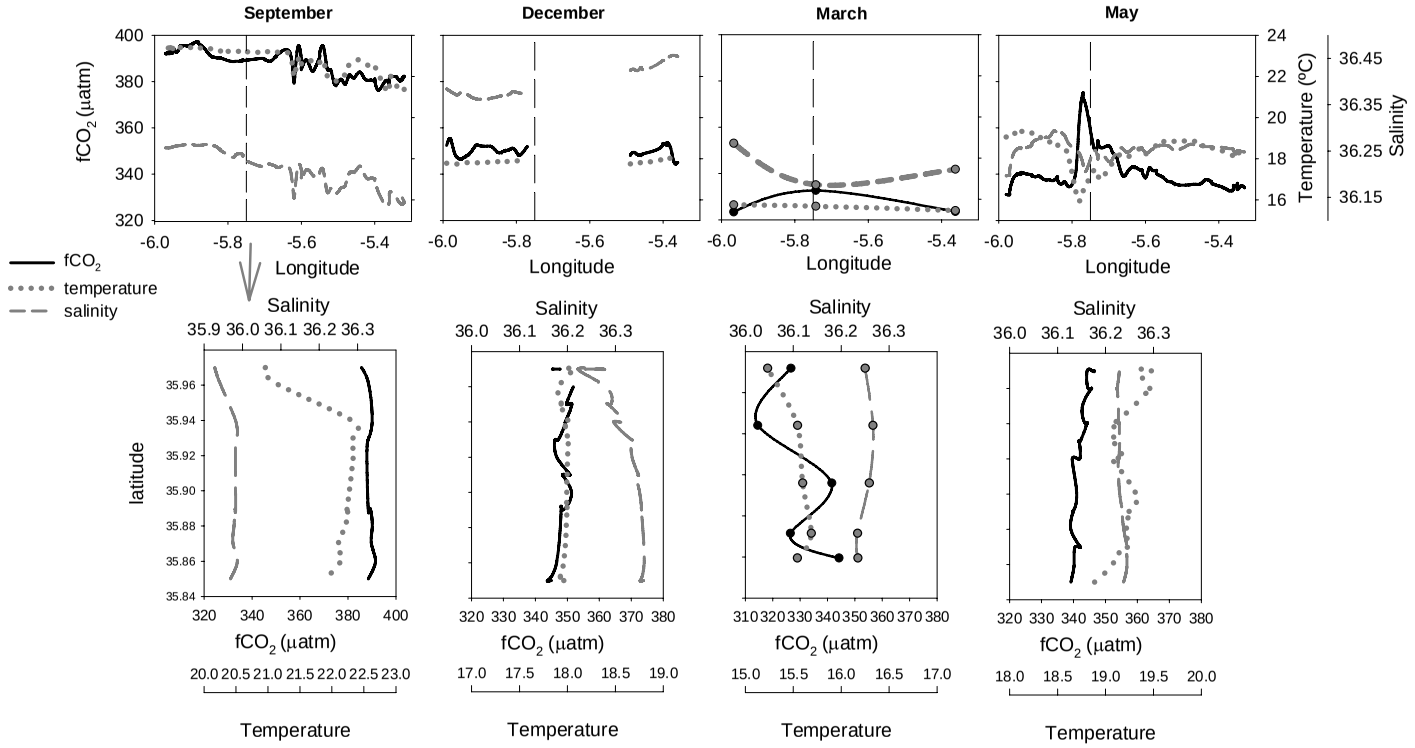

Figure2. Salinity, temperature and fCO2 at surface water for the four sampling performed on 7-8 September 2005, 12-13 December 2005, 20-21 march 2006 and 22-23 May 2006.

than the seasonal amplitude, which is around 6.5ºC, with the minimum temperature reached in March and a temperature maximum detected in September. The spatial amplitude for fCO_2 range between 10-44 μatm, with the maximum recorded in May and with higher variability on the East-West than on the North –South axis, although a reproducible seasonal pattern for spatial distribution does not seem to be noticeable This accounted variability may be explained on the basis of the hydrodynamics of the Strait of Gibraltar, considering also the sampling strategy used in this study. The changes in the biogeochemical parameters of water interacting through the Strait of Gibraltar are largely controlled by hydrodynamic phenomena. Undulatory phenomena, such as the internal hydraulic jumps or arrested internal waves, enhance the interfacial mixing and can inject deep, DIC and nutrient rich water into the upper layer of the Atlantic water and eventually the biochemical imprint arrives to the water surface. The higher interface oscillations are normally found during high tide along the Camarinal Sill (Gascard and Richez, 1985). In this study, the North-South axis was always sampled during low tide, when the interface occurs at the deepest position along the Camarinal Sill. This circumstance would avoid the commented tidal variability and, explaining also the lower variability in comparison to the one observed at a longitudinal axis, which was sampled without taking into account the tidal stage. In May, and throughout the Camarinal Sill, a high increase at surface fCO_2 from 336 μatm up to 375 μatm is accompanied by a temperature decrease (from 18.5ºC to 15.9ºC) as a consequence of the maximum upwelling of deeper water in that area during high tide, coinciding with the sampling time at that particular station.

In order to achieve a better understanding of the fCO_2 variability for each cruise, the thermodynamics effects of temperature on the fCO_2 have been corrected from the in-situ temperature to the annual average temperature measured in the Strait of Gibraltar (18.5ºC), using the expression proposed by Takahashi et al. (1993):

$$fCO_{2\,T\,mean} = fCO_{2\,obs} \exp [0.0423 (T_{mean} - T_{obs})] \qquad (1)$$

where T is the temperature in ºC and the subscripts ''mean'' and ''obs '' indicate the annual average and observed values, respectively. The fCO_2 at the mean temperature will be named hereinafter $fCO_{2\ T\ mean}$. The relationship between $fCO_{2\ T\ mean}$ versus temperature and salinity for the continuous underway data base can be statistically tested by lineal regression: a high lineal correlation for $fCO_{2\,T\,mean}$ versus temperature was obtained for each cruise, with r^2 varying from 0.87-0.86 in May and September respectively and 0.4 in December (in all cases $p<0.01$). The $fCO_{2\ T\ mean}$ versus salinity only showed a good fitting in September with an $r^2 = 0.74$ ($p < 0.01$), while for the rest of cruises the relationship was not statistically significant. The $fCO_{2\,T\,mean}$ versus temperature exhibited a negative slope. Since the thermodynamic effects are corrected for this variable and colder waters are linked to higher fCO_2, it can be suggested than the surface CO_2 variability is related to the influence of deeper water by the hydrodynamic processes explained above. The fact that no correlation between fCO2 and salinity was found, can be justified considering the origin and thermal characteristics of the water. The observed occurrence of colder water was accompanied by a rise in fCO_2, water that could have diverse origins:, either NACW (characterised by both lower salinity and temperature and higher fCO_2), the Mediterranean flow or upwelled interface consequence of the Atlantic flow divergence at the Camarinal sill, coastal water inputs as well as by the surface signal of the propagated internal waves on the eastern section of the Strait (Macías et al., 2007).

The presence of theses surface fCO_2 peaks seems to be in agreement with previous observations reported by Santana-Casiano et al. (2002) in the Strait of Gibraltar in September 1997, who also found episodic upwelling of high DIC and fCO2 in surface waters along the Camarinal Sill and on the eastern section of the Strait, especially evident at the main sill.

Latitudinal and longitudinal variations of DIC in surface waters have been plotted in Figure 3. The differences observed in the surface DIC concentration are similarly to those measured for salinity and temperature, being highly affected by the different mixing and upwelling phenomena, and thereby directly related to the tidal stage at each station during sampling. Maximum DIC values were recorded along the Camarinal Sill (during high tide) in March with 2140.9 μmol kg^{-1} and the minimum was recorded in the same location in May during low tide, with a value of 2044.6 μmol kg^{-1}.

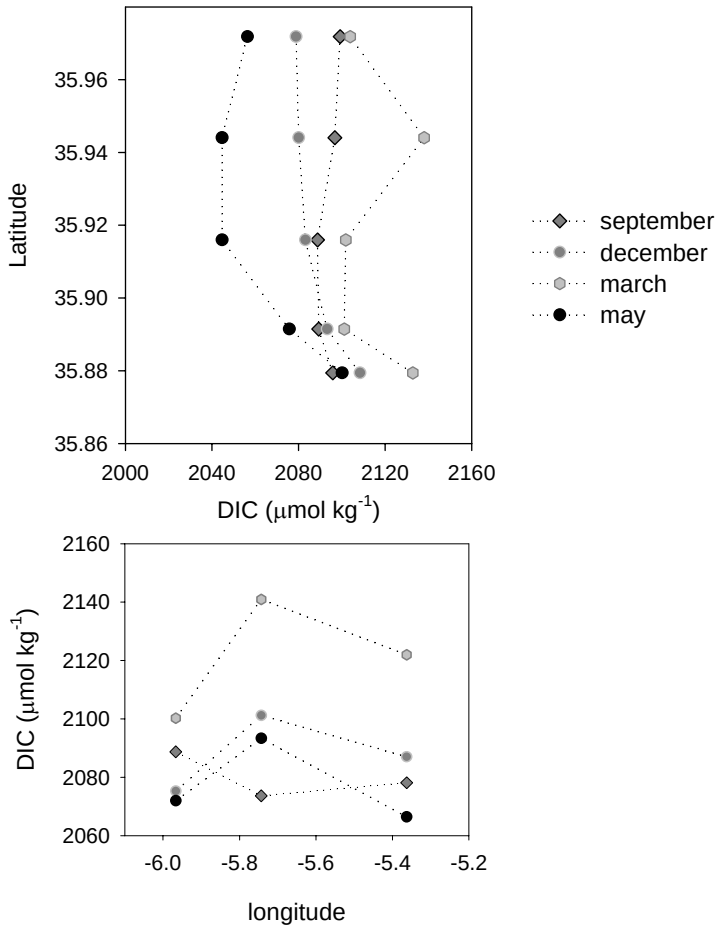

Figure 3. Longitudinal and latitudinal variations of DIC concentrations in the Strait of Gibraltar for each cruise.

There exists slightly higher DIC concentrations on the southern side of the Strait than in the northern side, with the latitudinal DIC amplitude ranging from 10-55 mol kg^{-1}, and although the stations located on the Camarinal section show a deeper bathymetry than the 100 m isobath, these DIC differences could suggest the possible influence of coastal inputs enriched in DIC towards the south. The DIC amplitude found for each cruise comprised between 25 and 55 μmol kg^{-1} is in the same range of the seasonal DIC amplitude of 48 μmol kg^{-1}.In fact, the DIC values obtained in this study are in agreement of those measured previously in surface Atlantic waters in the Strait of Gibraltar (Dafner et al., 2001; Santana-Casiano et al., 2002). These studies were focused on the characterization of the water column variability and coincided than most of the variability in the biogeochemical parameters in the water column were controlled by the complex hydrodynamics of the Strait and related to the short residence time of the water in the channel (12 hours inside the surface layer).

Due to this high variability in both the Mediterranean and Atlantic flows on a tidal time scale in the Strait of Gibraltar, seasonal signals of DIC are significantly difficult to asses and also no studies have been seasonally addresses in this area. Previous seasonal hydrodynamic works carried out by Garcia–Lafuente et al. (2002) showed the existence of an annual cycle of the inflow that peaks in late summer. Its amplitude is 10 % of the mean flow, being related to the annual cycle of the density differences between inflowing and outflowing waters (following the seasonal warming of the Atlantic Water since Mediterranean Outflowing water is not exposed to solar heating). In addition, the interface between both water bodies exhibit an annual cycle that places it deepest position in summer, to subsequently shallow in late winter (February – March). The cycle of the position of the interface only explains 30% of the annual signal of the inflow. The remaining percentage is accounted for by the velocity variations linked to the annual cycle of the density differences. On the other hand, the simultaneous sinking of the interface and the development of a seasonal thermocline will hinder the pumping of

nutrients and other particles to the upper layer (Echevarria et al., 2002). Theses counteracting influences would probably obscure the biological cycle itself, and any reliable description of the seasonal cycle if any, needs of more in-situ data. However, in the present study, shallower position of the interface in the end of winter may explain the maximum surface DIC concentration (2118 μmol kg^{-1}) recorded on March, when the vertical DIC advection is expected to be maximum. Furthermore, in the proximal waters of the Strait, there exists a clear relationship between the zonal winds and upwelling episodes in the Gulf of Cadiz (Huertas et al., 2006) and in the Alboran Sea (Macias, 2006). Nevertheless, these wind-induced upwellings are not expected to be so relevant in the channel of the Strait, due to the orientation of the geographical borders and to the mainly one-dimensional character of the flow in the Strait of Gibraltar characterized by very high advection velocities.

Temperature versus biological control on fCO_2

In order to identify and quantify the temperature and "net biology" effects on the surface fCO_2 variability the method proposed by Takahashi et al. (2002) has been applied, which assumes the fCO_2 to be controlled by temperature and biological drawdown. As defined by these authors, the "net biology effect" includes all the biogeochemical processes acting on net CO_2 utilization (primary production, respiration), and other processes also governing the CO_2 such as riverine inputs, changes on DIC by advection or air-sea CO_2 fluxes, are inherently attributed to the biological signal. The effect of biology on the surface water fCO_2 in a given area $(\Delta fCO_2)_{bio}$, is represented by the seasonal amplitude of fCO_2 values corrected to the mean annual temperature (fCO_2 at T_{mean}), values computed using the equation (1).

$$(\Delta fCO_2)_{bio} = (fCO_{2\,T\,mean})_{max} - (fCO_{2\,T\,mean})_{min} \qquad (2)$$

where the subscripts "max" and "min" indicate the seasonal maximum and minimum values.

The effects of temperature changes on the mean annual fCO_2 value (equal to 352 μatm in the Strait of Gibraltar) $(\Delta fCO_2)_{temp,}$ is represented by the seasonal amplitude of fCO_2 at T_{obs} values computed using the equation:

$$fCO_{2\ T\ obs} = \text{mean annual } fCO_2 * \exp\ [\ 0.0423\ (T_{obs} - T_{\ mean}\ )] \qquad (3)$$

where the mean annual temperature of 18.5ºC has been used. The changes in fCO_2 related to temperature effects follow then as:

$$(\Delta fCO_2)_{temp} = (fCO_{2\ T\ obs})_{max} - (fCO_{2\ T\ obs})_{min} \qquad (4)$$

The relative importance of each effect may be expressed in terms of the ratio either differences between the temperature effects (T) and biological effects (B):

$$T / B = (\Delta fCO_2)_{temp} / (\Delta fCO_2)_{bio} \qquad (5)$$

In areas with high seasonal variability of the biological activity the ratio (T/B) would be less than one whereas in regions with weaker or annually rather constant biology, the (T/B) ratio would be larger than one. Besides Takahashi et al. (2002), this method has been widely used by others authors to asses the role of temperature versus biological control in continental shelves (Thomas et al., 2005, Padin et al., 2007, Schiettecatte et al., 2007).

Figure 4 shows the seasonal variations on the experimental fCO_2 and the biological and temperature effects represented by $fCO_{2\ T\ mean}$ and $fCO_{2\ T\ obs}$. The seasonal evolution of the observed fCO_2 exhibited a minimum in March and progressively increased during summer to subsequently decrease in early winter. This fCO_2 follows the same pattern than temperature and $fCO_{2\ Tobs}$, which present minimum values in March and maximum

in September, corresponding also with the minimum (15.5ºC) and maximum (21.7ºC) temperatures respectively. May and December are nearly in equilibrium, being the observed fCO_2 values very similar to the annual average concentration (352 μatm).

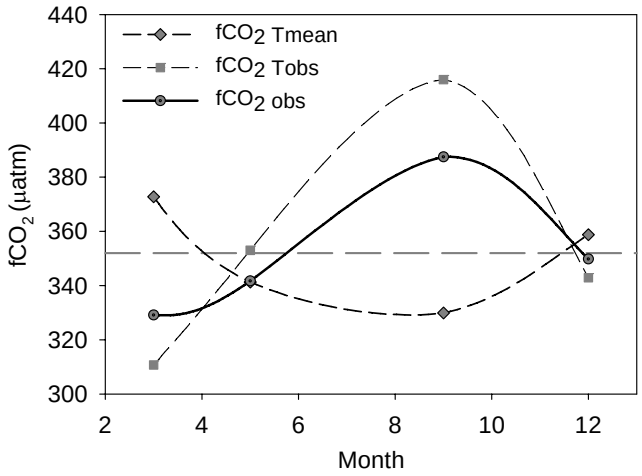

Figure 4. Seasonal variations on the observed $fCO_{2\ obs}$, and the biological and temperature effects represented in $fCO_{2\ T\ obs}$ and $fCO_{2\ T\ mean}$.

The fCO_2 differences encountered between the observed fCO_2 and the $fCO_{2\ T\ obs}$ are counterbalanced by the biology effect ($fCO_{2\ T\ mean}$), which decreases towards spring and summer. Unlike the temperature effect, the seasonal amplitude is significantly lower. Taking into account the data base, the annual ratio T/B is equal to 2.4, indicating than temperature is the main controlling mechanism of the seasonal fCO_2 variability, with an amplitude $(\Delta fCO_2)_{temp}$ of 105 μatm. Regarding the net biological effects on the seasonal cycle of fCO_2, the amplitude of the $(\Delta fCO_2)_{bio}$ is 43 μatm, which is relatively low in relation to other European continental shelves studied and compared by Borges et al. (2006).

As mentioned above, the method used assumes the vertical mixing processes and lateral inputs to be inherently included into the biological signal. In order to achieve a

better understanding of the seasonality on the biological signal, the AOU values were considered. Figure 5a shows the relationship found between DIC and AOU for all the discrete sample data. It can be observed that negative AOU values corresponded to March, possibly as a consequence of a higher biological primary production in the area whereas maximum positive AOU values were reached in September, most likely due to the organic matter remineralization processes. The negative relationship between DIC and AOU may indicate that the DIC seasonal variability is more related to vertical mixing inputs than to the net biological effect. In fact, a DIC versus observed fCO_2 graph (Fig. 5b) des not match the expected positive relationship, since on a seasonal scale and as above mentioned, fCO_2 is controlled by the temperature annual cycle. Hence, the minimum fCO_2 observed in March can be a combination of a temperature decrease and in a less extent a biological consume. During this month the $fCO_{2\ T\ mean}$ was maximum although this could be probably overestimated because of maximum DIC inputs by vertical mixing, which can be inherently attributed to the biological signal computed by the method. The AOU values above cero observed in December and May also match with the equilibrium situations between temperature and biological effects accounted by the method of Takahashi et al. (2002).

Then, assuming that TA is affected neither by seasonal change of temperature nor biology, and considering than biological change on DIC follows the classical Redfield ratio on oceanic thermocline waters (Redfield, 1963), equal to ΔO_2: Δ DIC = 138:-106, it is possible to revaluate the seasonal amplitude of the fCO_2 due to net biological processes. The seasonal amplitude for AOU is 49.2 $\mu molO_2\ kg^{-1}$, which is equivalent to 37.8 μmolC kg^{-1}. Using the k_1 and k_2 dissociation constant proposed by Luecker et al. (2000), this change on DIC yields a change on fCO_2 equal to 63 μatm. Such a change is larger than the resulting amplitude of the $fCO_{2\ T\ mean}$ obtained by the Takahashi et al (2000) method.

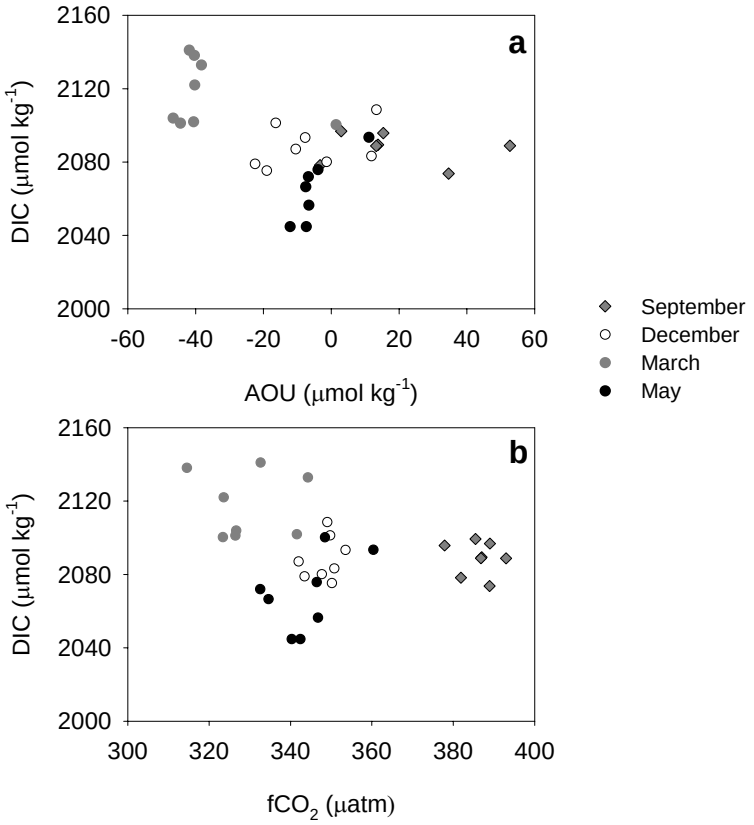

Figure 5. DIC vs. AOU and fCO_2 vs AOU for all the stations and cruises.

Furthermore, if the ratio T/B is recalculated using this new $(\Delta fCO_2)_{bio}$ the resulting value computes 1.7. Considering this new T/B ratio, temperature continues being the key factor controlling fCO_2 seasonality, although in a much lesser extent.

Other surface fCO_2 values found in the area are those determined by Santana-Casiano et al. (2002) in February, March and September, with a very similar range to the ones reported in this study. These authors observed in May a fCO_2 equal to 327.6 μatm (at 17.4 º), lower than the 341.7 μatm (at 18.7ºC) obtained in this study, which can be

probably explained by the temperature difference. Nevertheless, the highest differences between both studies have been found in September, since the previous study showed an average surface fCO_2 of 356.6 μatm quite lower in comparison to 387.5 μatm observed in our study at very similar temperature (21.7ºC).

Borges et al. (2006), in a recent review of the european coastal waters comparing the seasonal cycle of five temperate european continental shelves, encountered that four of them, meso- and eutrophic ecosystems, exhibited a springtime decrease of the $fCO_{2\ obs}$ $fCO_{2\ T\ mean}$ due to phytoplankton spring blooms and then a decrease until late summer or early autumn, when heterotrophic processes increase the fCO_2. The exception to this seasonal biology control is the oligotrophic Bay of Angels in the Mediterranean Sea, where the fCO_2 follows the annual temperature cycle with a progressive rise in fCO_2 towards the summer months and a subsequent fCO_2 decrease as winter cooling begins. The net biological effect ($\Delta fCO_{2\ bio}$) accounted in these continental shelves ranges from 569 μatm in the Gotland Sea to 68 μatm achieved in the Bay of Angels, that is the one showing more similarities on the seasonality of fCO_2 to the Strait of Gibraltar, where the amplitude of the net biological effects is 63 μatm.

Air-sea CO_2 exchange

The air-sea CO_2 exchange ($F\ CO_2$) was calculated using the equation:

$$F\ CO_2 = k\ S\ (fCO_{2\ sea} - fCO_{2\ air}) \qquad (6)$$

where k is the gas transfer velocity, S is the CO_2 solubility and $fCO_{2\ sea}$ and $fCO_{2\ air}$ are the seawater and atmospheric CO_2 fugacity. Seawater solubility has been calculated using the expression proposed by Weiss (1974). The k has been computed using the k

parameterization for long term wind speed given by Wanninkhof (1992) and the monthly average wind speed data. Negative fluxes indicate air to sea gas transfer.

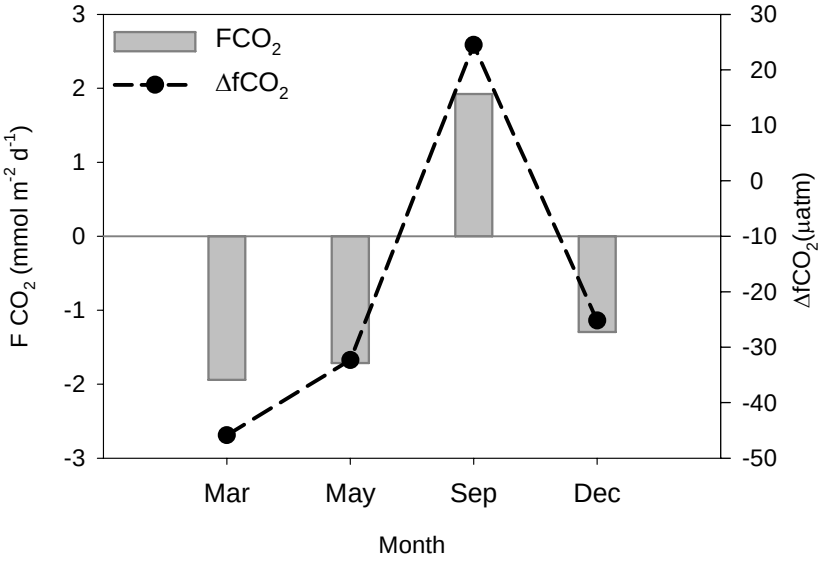

Figure 6. Seasonal variability of the air-sea CO_2 fluxes

Figure 6 shows the seasonal variability of the air-sea CO_2 fluxes. The CO_2 fluxes ranged from -1.9 to 1.9 mmol m^{-2} d^{-1}, with the maximum uptake in March and maximum outgassing in September. The calculated fluxes showed a clear seasonality following the CO_2 air-sea gradient (ΔfCO_2) seasonal variability. Wind speed average values used for the k calculations were very homogeneous ranging from 3.7 to 5.1 m s^{-1} in March and September respectively. According to these data, during most of the year, the Strait of Gibraltar behaves as a moderate sink for atmospheric CO_2 except in summer, following the temperature and biology cycle described in the previous section (3.2). The resulting mean annual CO_2 flux in the Strait of Gibraltar was -0.28 mol m^{-2} y^{-1} (-0.76 mmol m^{-2} d^{-1}), indicating than the area acts as a net sink on annual basis. This sink behaviour is in agreement with the results obtained by Santana-Casiano et al. (2002), who estimated an

annual average CO2 flux of -2.5 mmol m^{-2} yr^{-1} considering only the September and February CO2 data as extreme seasonal situations. The differences in the magnitude of the uptake, besides of the shorter temporal coverage, may derive mainly from the wind speed used for the k calculations, which were systematically much greater in the study of Santana-Casiano et al. (2002), with wind speeds ranging from 8 to 15 m s^{-1}. These high wind speeds yield a CO2 flux of -19 mmol m^{-2} d^{-1} in February and -5.5 mmol m^{-2} d^{-1} in May, up to three times higher than the one obtained in this study.

Seasonal studies of surface water CO_2 dynamics and air-sea CO_2 fluxes are rather scarce in the Strait as well as in adjacent waters. Huertas et al. (2006) carried out a 12 months study about the inorganic carbon dynamics in the Gulf of Cadiz, concluding than the annual cycle of phytoplankton biomass, nutrients riverine inputs and the fluctuation of local temperature (influenced by coastal wind-induced upwellings) control the surface pCO_2 variability. The Gulf of Cadiz remains CO_2 undersaturated most of the year with respect to atmospheric equilibrium, excepting the oversaturation observed in late summer, behaving as a net CO2 sink of atmospheric CO2 on an annual scale, with fluxes ranging between 0.8 mmol m^{-2} d^{-1} in summer and -2.0 mmol m^{-2} d^{-1} in October. The mean annual air-sea CO_2 flux in the Gulf of Cadiz is about -0.4 mmol C m^{-2} yr^{-1} (Borges et al., 2006 based on data of Huertas et al., 2006) slightly higher than the net annual CO2 flux -0.28 mmol C m^{-2} yr^{-1}- obtained in this study for the Strait of Gibraltar, indicating a slightly higher uptake capacity than the adjacent Strait of Gibraltar.

Taking into consideration that the total surface area of the Strait of Gibraltar delimited by Cape Spartel to the West and Point Almina to the East, is around 1500 km^2, the total CO_2 uptake by the Strait of Gibraltar would be 0.5 10^{-3} TgC yr^{-1} (4.2 10^8 mol C yr^{-1}), amount that can be integrated into the total uptake estimated by Borges et al. (2006) for European continental shelves of -68.1 TgC yr^{-1}, which constitutes a high significant CO_2 sink equivalent to the carbon sink of the terrestrial biosphere.

In summary, the present study reports and discuss surface fCO_2 data obtained in surface waters of the Strait of Gibraltar, whose seasonal sequence is characterised by a minimum concentration observed in March 2006 equal to 329 μatm and a progressive increase in concentration caused by the water warming until reaching a maximum concentration in September, coinciding with the maximum temperature of the system. Surface waters in the Strait remains undersaturated most of the year, excepting in September, when the warming of surface waters leads to oversaturation in CO_2, although the study area behaves as a discrete net sink on annual scale. The high intensity of the mixing processes in a tidal scale, masks the seasonal variability of the DIC and the assessment of the biological seasonal cycle in the Strait.

REFERENCES:

Armi, L., D.,Farmer, 1985. The internal hydraulics of the Strait of Gibraltar and associated sill and narrows. Oceanologica Acta 8 (1): 37– 46.

Benson, B. B., and JR. Krause, 1984. The concentration and isotopic fractionation of oxygen dissolved in freshwater and seawater in equilibrium with atmosphere. Limnology and Oceanography 29: 620–632.

Borges, A.V. and M.Frankignoulle, 2002. Distribution of surface carbon dioxide and air sea exchange in the upwelling system off the Galician coast. Global Biogeochemical Cycles 16 (2): 1020. doi:10.1029/2000 GB001385.

Borges, A.V., L.-S., Schiettecatte, G., Abril, B., Delille and F., Gazeau, 2006. Carbon dioxide in European coastal waters. Estuarine Coastal and Shelf Science 70(3): 375-387.

Bruno, M., J.J., Alonso, A., Cózar, J., Vidal, A., Ruiz-Cañavate, F., Echevarría, J., Ruiz, 2002. The boiling-water phenomena at Camarinal Sill, the strait of Gibraltar. Deep-Sea Research II 49: 4097–4113.

Chen, C.T.A., K.K., Liu, R., Macdonald, 2003. Continental margin exchanges. In: Fasham, M.J.R. (Ed.), Ocean Biogeochemistry: A Synthesis of the Joint Global Ocean Flux Study (JGOFS). Springer-Verlag, Berlin, pp. 53-97.

Dafner, E.V., M., González-Dávila, J.M., Santana-Casiano, R., Sempere, 2001. Total organic and inorganic carbon exchange through the Strait of Gibraltar in September 1997. Deep-Sea Research II 48: 1217–1235.

Dickson, A.G., 1990. Standard potential of the reaction: AgCl(s)+ ½ H_2(g)=Ag(s)+HCl(aq), and the standard acidity constant of the ion HSO^{4-} in synthetic seawater from 273.15–318.15 K. Journal of Chemical Thermodynamics. 22, 113–127.

Dickson, A.G., J.P., Riley, 1979. The estimation of acid dissociation constants in seawater media from potentiometric titrations with strong base. I. The ionic product of water — KW. Marine Chemistry 7:89–99.

DOE, 1994. Handbook of methods for the analysis of various parameters of carbon dioxide in seawater; version 2. In: Dickson, A.G., Goyet, C. (Eds.), ORNL/CDIAC-74.

Echevarría, F., J., García-Lafuente, M., Bruno, G., Gorsky, M., Goutx, N., González, C.M., García, F., Gómez, J.M., Vargas, M., Picheral, L., Striby, M., Varela, J.J., Alonso, A., Reul, A., Cózar, L.,Prieto, T., Sarhan, F., Plaza, F., Jiménez-Gómez, 2002. Physical biological coupling in the Strait of Gibraltar. Deep-Sea Research II 49 (19): 4115–4130.

García-Lafuente, J., J., Delgado, J.M.,Vargas, M., Vargas, F., T., Plaza, Sarhan, 2002. Low frequency variability of the exchanged flows 646 through the Strait of Gibraltar during CANIGO. Deep-Sea Research II 49 (19): 4051–4067.

Gascard, J.C., C., Richez, 1985. Water masses and circulation in the Western Alboran Sea and in the Strait of Gibraltar. Progress in Oceanography 15: 157–216.

Gattuso, J.-P., M., Frankignoulle, and R., Wollast, , 1998. Carbon and carbonate metabolism in coastal aquatic ecosystems. Annual Review Ecology Systematics, 29: 405-433.

Huertas, E., G., Navarro, S. Rodríguez-Galvez, and L.M., Lubián, 2006. Temporal patterns of carbon dioxide in relation to hydrological conditions and primary production in the northeastern shelf of the Gulf of Cadiz (SW Spain). Deep-Sea Res. PT II, 53:1344-1362.

Körtzinger, A., H., Thomas, B., Schneider, N., Gronau, L., Mintrop, J.C., Duinker, 1996. At-sea intercomparison of two newly designed underway pCO_2 systems - Encouraging results. Marine Chemistry 52:133-145.

Lueker, T.J., A.G., Dickson, and. C.D., Keeling, 2000. Ocean pCO_2 calculated from dissolved inorganic carbon, alkalinity, and equations for K_1 and K_2 : validation based on laboratory measurements of CO_2 in gas and seawater at equilibrium. Marine Chemistry 90: 105-119

Macías, D., C.M., García, F., Echevarría, A., Vázquez-Escobar, M., Bruno, 2006. Tidal induced variability of mixing processes on Camarinal Sill (Strait of Gibraltar). A pulsating event. Journal of Marine Systems 60: 177–192.

Macías, D. , A.P., Martín, J., García-Lafuente , C.M.,García , A., Yool , M.,Bruno, A., Vázquez-Escobar , A. Izquierdo, D.V., Sein , F, Echevarría, 2007. Analysis of mixing and biogeochemical effects induced by tides on the Atlantic–Mediterranean flow in the Strait of Gibraltar through a physical–biological coupled model. Progress in Oceanography 74: 252-272.

Minas, H.J., B., Coste, P., Le Corre, M., Minas, P., Raimbault, 1991. Biological and geochemical signatures associated with the water circulation through the Strait of Gibraltar and in the Western Alboran Sea. Journal of Geophysical Research 96: 8755–8771.

Padin, X.A., M., Vázquez-Rodríquez, A.F., Ríos, F.F, Pérez, 2007. Surface CO_2 measurements in the English Channel and Southern Bight of North Sea using voluntary observing ships. Journal of Marine Systems 66:297-308.

Redfield, A.C., B.H., Ketchum, F.A., Richards, 1963. The influence of organisms on the composition of sea-water. pp. 26–77. in M.N. Hill (Ed.) The Sea. Vol. 2, pp. 554. John Wiley & Sons, New York. 50

Santana-Casiano, J.M., M., González-Dávila, L.M., Laglera, 2002. The carbon dioxide system in the Strait of Gibraltar. Deep-Sea Research II 49: 4145–4161.

Schiettecatte L-S., H., Thomas, Y., Bozec , A.V., Borges, 2007. High temporal coverage of carbon dioxide measurements in the Southern Bight of the North Sea. Marine Chemistry: 106:106-173.

Takahashi, T., J., Olafsson, J., Goddard, D.W., Chipman, S.C., Sutherland, 1993. Seasonal variation of CO2 and nutrients in the high latitude surface oceans: a comparative study. Global Biogeochemical Cycles 7: 843–878.

Takahashi, T., S.C., Sutherland, C., Sweeney, A., Poisson, N., Metzl, B., Tilbrook, N., Bates, R., Wanninkhof, R.A., Feely, C., Sabine, J., Olafsson, Y., Nojiri, 2002. Global sea–air CO2 flux based on climatological surface ocean pCO2, and seasonal biological and temperature effects. Deep-Sea Research II 49: 1601–1622.

Thomas, H., B., Schneider, 1999. The seasonal cycle of carbon dioxide in Baltic Sea surface waters. Journal of Marine Systems 22 (1): 53-67.

Thomas, H., Y., Bozec, K., Elkalay, H., De Baar, 2004. Enhanced open ocean storage of CO2 from shelf sea pumping. Science 304: 1005–1008.

Thomas, H., Y., Bozec, H.J.W., De Baar, K., Elkalay, M., Frankignoulle, L.-S., Schiettecatte, A.V., Borges, 2005. The carbon budget of the North Sea. Biogeosciences 2 (1): 87-96.

Wanninnkhof, R., 1992. Relationship between wind speed and gas exchange over the ocean. J. Geophys. Res., 97 (C5): 7373-7382.

Weiss, R.F., 1974. Carbon dioxide in water and seawater: the solubility of a non-ideal gas. Mar. Chem., 2:203–215.

Zeebe, R. E., and D. A. Wolf-Gladrow, 2001. CO_2 in Seawater: Equilibrium, Kinetics, Isotopes, 346 pp., Elsevier Sci., New York.

Acknowledgments: Thanks to E. Huertas and S. Rodriguez who coordinates the work related to the cruises, especially to E. Huertas, by the usefully revision and suggestions to improve the manuscript. Thanks also to the crew of the R/V “Amir Moulay Abdellah” for the collaboration during the sampling task. Thanks to X.A. Padin by the assistance in the data processing. This work has been supported by the Spanish CICYT under the contract CTM2005-01364/MAR and by the European CARBOOCEAN IP (511176 GOCE).

Capitulo 5

Síntesis y Conclusiones

5.1 Síntesis

En este último capítulo se realiza una comparación de los resultados obtenidos en los tres sistemas estudiados, que poseen características batimétricas e hidrodinámicas muy distintas (Tabla 6.1). En el estuario del Guadalquivir, el flujo neto de agua tiene su origen en la descarga del río, la cual es muy irregular en función de la época del año. Entre el 2000 y el 2003, el caudal medio fue de 70.7 m^3 s^{-1}, mientras que la descarga más frecuente (utilizada para el calculo del tiempo de residencia) es de 36 m^3 s^{-1}. El Río San Pedro es un caño de marea que no presenta ningún efluente de agua dulce, y por tanto un flujo neto de agua nulo, siendo la marea el mecanismo encargado del intercambio con el agua exterior de la Bahía de Cádiz. De forma puntual, en época de lluvias percibe aportes de agua dulce procedente de escorrentías, y que son responsables de que la salinidad disminuya hasta valores de 20 en el periodo de estudio. El estrecho de Gibraltar a diferencia del estuario del Guadalquivir y el Río San Pedro, es un sistema profundo donde la columna de agua llega a alcanzar en algunos puntos más de 900 m de profundidad. Está caracterizado por un flujo bicapa, con una entrada neta de agua atlántica en superficie y una salida profunda de agua mediterránea. La superficie, profundidad y flujo neto de agua del Estrecho de Gibraltar son dos órdenes de magnitud

mayores que en el estuario del Guadalquivir y el Río San Pedro. A su vez, el gradiente de salinidad en cada uno (Tabla 6.1) recoge información a cerca del grado de influencia de las aguas continentales en cada sistema, lo que ayuda a interpretar el origen del carbono inorgánico en las zonas de estudio.

Tabla 5.1. Superficie y profundidad medias, flujo de agua e intervalo de temperatura y salinidad característicos de cada sistema. ([1]), datos medio de caudal del río medido en Alcalá del Río (Sevilla) datos suministrados por la Confederación Hidrográfica del Guadalquivir; ([2]) Bascket et al. (2001)

	Superficie (km^2)	**Profundidad media (m)**	**Temperatura agua (ºC)**	**Salinidad**	**Flujo agua ($m^3\ s^{-1}$)**
Guadalquivir	38.6	3	15 - 25	2.2 – 36.3	70.7 [1]
Río San Pedro	1.85	3	12 - 32	20 – 41	0
Gibraltar	1500	600	15 - 22	36.3 – 38.3	50000 [2]

En el estuario del Guadalquivir, las mayores concentraciones de carbono inorgánico son observadas aguas arriba del estuario, siendo los aportes continentales el origen de las altas concentraciones de CID observadas (Tabla 6.2). Este hecho es debido fundamentalmente a la geología de la cuenca de drenaje del río Guadalquivir. En el Río San Pedro, las concentraciones medias de CID en el interior del caño son similares a las encontradas en el Guadalquivir. En este caso las fuentes del CID al caño son los aportes de procedentes de la granja acuícola, junto con los procesos in-situ de remineralización de la materia orgánica que tienen lugar tanto en la columna de agua como en el sedimento del caño. En tercer lugar, el estrecho en el Estrecho de Gibraltar la influencia de sus márgenes en la concentración de CID es muy limitada debido al volumen de agua y a la intensidad del intercambio entre las masas de agua atlántica y mediterránea. El agua atlántica de naturaleza oligotrófica, presenta bajas concentraciones de CID en comparación con el agua mediterránea profunda, con mayores valores de AOU y carbono

inorgánico a consecuencia de los procesos de remineralización que experimenta en su tránsito por la cuenca mediterránea. Por tanto, se puede decir que el estuario del Guadalquivir es el que tiene una mayor influencia terrestre o continental, el Río San Pedro presenta una mayor presión antropogénica y por ultimo el Estrecho de Gibraltar presenta unas características más oceánicas. A pesar de estas diferencias, el principal mecanismos que explica las variaciones temporales de las concentraciones de CID son los procesos de mezcla debido a la mareas.

Tabla 6.2. Intervalo de concentraciones observadas para las distintas variables de estudio en cada sistema. ([1]) Se han seleccionado en Macías (2006) los datos correspondientes a la misma campaña realizada en Noviembre 2003.

	CID (μmol kg^{-1})	**AOU (μmol kg^{-1})**	**pH**	**pCO_2 (μatm)**	**Chl-a (μg L^{-1})**
Estuario Guadalquivir	2250 - 4890	8 - 66	7.7 – 8.2	581 - 1617	1.5 – 15.1
Río San Pedro	2330 - 3200	-27.8 – 128.7	7.31 – 8.16	383 - 3763	0.8 – 14.5
Estrecho Gibraltar	2013 - 2341	-1.9 – 91.9	7.86 – 8.01	331 - 397	0 – 2[1]

En lo que respecta al pH, las diferencias encontradas entre los tres sistemas son debidas a las mismas causas que explican el origen del carbono inorgánico, es decir, la mayor acidez de las aguas continentales en el Guadalquivir, la influencia de los aportes de la granja piscícola en el Río San Pedro y la mayor mineralización de la materia orgánica la masa de agua mediterránea.

Para la comparación de los valores de pCO_2 entre los tres sistemas, sólo se ha utilizado los valores obtenidos en continuo en aguas superficiales, y por tanto, no se incluyen la información obtenida en los muestreos de invierno del Guadalquivir, dónde se estimaron a partir de medidas de pH y AT. De esta forma, solo se dispone de información sobre las variaciones estacionales de pCO_2 en el Río San Pedro y en el Estrecho de Gibraltar. Los valores máximos se han registrado en el Río San Pedro, poniendo de

manifiesto la intensidad de lo procesos de mineralización de la materia orgánica tanto dentro como fuera de la granja. De esta forma, aunque las concentraciones de CID son similares en el Río San Pedro y en la parte interna del estuario del Guadalquivir, lo valores máximos de pCO_2 son mas del doble que los encontrados en el Guadalquivir. Los resultados obtenidos en los capítulos anteriores indican que la variabilidad estacional de pCO_2 en el agua superficial del Estrecho de Gibraltar y Río San Pedro está directa e indirectamente ligada a la temperatura. Así pues, el ciclo anual de la temperatura afecta a la solubilidad del CO_2 (una variación de 1ºC supone una variación media de un 4% en el valor de la pCO_2), pero a su vez también modula las tasas de los procesos metabólicos, y por tanto el balance respiración-producción. En el caso del Estrecho de Gibraltar los resultados obtenidos muestran que es mayor el control termodinámico sobre la estacionalidad del CO_2, mientras que en el Río San Pedro, éste es poco significativo en comparación con los procesos de respiración y remineralización de la materia orgánica.

Tanto el estuario del Guadalquivir como el caño del Río San Pedro presentan una elevada disponibilidad de nutrientes (Ponce et al., 2003; Tovar et al., 2000) siendo el factor limitante del crecimiento de la biomasa planctónica los altos valores de turbidez característicos de estos dos sistemas, influidos también en el caso del Río San Pedro por el tiempo de residencia del agua en el caño. Sin embargo, los valores de clorofila en estos dos sistemas son de hasta siete veces mayores que en el Estrecho, debido a las características oligotróficas de la masa de agua atlántica. Los recientes estudios realizados acerca de la comunidad fitoplanctónica en el Estrecho sugieren que a pesar de los episodios de fertilización por nutrientes del agua superficial inducida por la marea (mezcla interfacial), el reducido tiempo de residencia de las aguas en el Estrecho no permite su asimilación por parte del fitoplancton (Macías et al., 2007).

Con el fin de evaluar la magnitud del intercambio de carbono inorgánico en los sistemas costeros con sus compartimentos adyacentes nos remitimos a los valores

calculados para los flujos a la atmósfera y la exportación de carbono en cada uno de los sistemas.

En lo que respecta al flujo de CO_2 a la atmósfera, los valores observados en la tabla 6.3 para el caso de estudio del Guadalquivir corresponden a los datos disponibles en julio teniendo en cuenta la superficie de cada una de las zonas en las que se puede subdividir el estuario en función del gradiente de salinidad (externa, media e interna). Para el Río San Pedro y el Estrecho de Gibraltar, la base de datos disponible permite hacer una media anual, que permite obtener una imagen más representativa del papel de cada sistema como sumidero o fuente de CO_2 a la atmósfera. Como ya se ha explicado en varios puntos de esta Tesis, los flujos a la atmósfera son una función del gradiente de concentraciones de CO_2 entre agua y atmósfera, y en segundo lugar de la velocidad de transferencia (k). Esta velocidad de transferencia es la que introduce una mayor incertidumbre en el cálculo de los flujos. Aunque en los trabajos I, II y V de esta Tesis, la elección de una u otra expresión para k se ha adaptado a las características hidrodinámicas de cada sistema, en esta síntesis se ha unificado el criterio para intentar minimizar las fuentes de discrepancia, y se han calculado los flujos a la atmósfera a partir de la expresión propuesta por Wanninkhof (1992). Debido a que las concentraciones en el agua son siempre mayores que en la atmósfera tanto para el Guadalquivir como para el Río San Pedro, estos dos sistemas siempre actúan como fuente de CO_2 a la atmósfera con unos flujos medios de 72.2 y 32.8 mmol m^{-2} d^{-1} respectivamente. A pesar de que el gradiente agua-atmósfera de CO_2 en el Río San Pedro es casi el doble que en Guadalquivir, esta diferencia en la magnitud de los flujos reside en los distintos valores de velocidad de viento en la época de estudio, mucho mayores para el Guadalquivir. El estrecho de Gibraltar se encuentra infrasaturado en CO_2 la mayor parte del año excepto Septiembre, lo que implica que a nivel anual, el flujo neto sea de la atmósfera al agua, actuando esta zona como sumidero de CO_2. Se puede observar que los flujos de CO_2 en las zonas afectadas por aportes continentales o derivados de la actividad humana son

mucho mayores que en una zona de características más oceánicas, como es el Estrecho de Gibraltar. En el caso del Guadalquivir, a pesar de tener una extensión del orden de 40 veces menor que el Estrecho de Gibraltar, las emisiones de CO_2 son el doble de la capacidad de captación en el Estrecho. Sin embargo en el Río San Pedro, a pesar de los elevados valores medios de pCO_2 que se alcanzan en sus aguas (1300 μatm), los flujos de CO_2 a la atmósfera son menores que en el Guadalquivir, aunque esta diferencia se debe a la influencia de la velocidad de viento.

La exportación de carbono inorgánico hacia el océano Atlántico es de 9.7 10^6 mol C d^{-1} para el Guadalquivir frente a los 2.4 10^6 mol C d^{-1} en el caso del Río San Pedro. Esta diferencia se debe fundamentalmente a la existencia de una descarga neta en el río Guadalquivir, y muestra que el flujo neto de agua en el Río San Pedro es nulo. Estos valores de exportación son poco significativos si se comparan con la tasa neta de intercambio en el Estrecho de Gibraltar, del orden de 4 10^9 mol C. d^{-1}, y que es consecuencia del mayor flujo de agua.

Si se evalúa la relación entre el C intercambiado con la atmósfera y el C exportado, se llega a la conclusión de que las emisiones en el Guadalquivir son muy significativas, y alcanzan el 22 % del intercambio neto de C (suma de exportación y flujo a la atmósfera), mientras que en el Río San Pedro sólo suponen el 2.5 %, y en el Estrecho es casi despreciable, con un valor para este ratio de 0.03 %.

Si los flujos de CO_2 a la atmósfera en el Río San Pedro se extrapolan a la superficie afectada por la acuicultura en la Bahía de Cádiz (29.2 10^6 m^2 ; Márquez et al., 1996) la emisión neta es de 10^6 mol C d^{-1}, dato que se aproxima mucho a la capacidad de captación de toda el área del Estrecho de Gibraltar. Esto pone de manifiesto la importancia de cuantificar el impacto que tienen las actividades humanas en las zonas costeras a la hora de evaluar el papel que pueden tener en el ciclo global del carbono.

Tabla 5.3. Gradiente de pCO_2 agua-atmósfera (Δ pCO_2), flujos medios de CO_2 agua-atmósfera, exportación neta por unidad de superficie de CID, exportación neta de CID, y emisión/captación de CO_2 en cada sistema. El signo en las emisiones y en los flujos de CO_2 indica el sentido del intercambio, el criterio que se ha tomado en positivo desde el agua hacia la atmósfera y negativo, de la atmósfera al agua. ([1]) Se ha incluido la extensión de la granja (Tovar et al., 2000).

	Δ pCO_2 (μatm)	**Flujo CO_2 (mmol m^{-2} d^{-1})**	**Exportación CID (mmol C m^{-2} d^{-1})**	**Exportación CID (10^6 mol C d^{-1})**	**emisión / captación CO_2 (10^6 mol C d^{-1})**
Estuario Guadalquivir	448	72.2	251	9.7	2.8
Río San Pedro	919	32.8	839[1]	2.4	0.06
Estrecho Gibraltar	-19.7	-0.76	2684.9	4030	-1.14

5.2 Conclusiones

La alta concentración de carbono inorgánico en el río Guadalquivir, con un valor medio de 3780 μmol kg^{-1} , es la principal característica que determina su dinámica en el estuario. Constituye uno de esos estuarios atípicos, donde los procesos de mezcla con el agua de mar responden a un comportamiento prácticamente conservativo, y que presenta un gradiente negativo de carbono inorgánico al acercarse al mar. Por esta razón, intensificada por las escorrentías en épocas de lluvia, el Guadalquivir exporta a la costa atlántica una cantidad próxima a 9.7 10^6 mol C d^{-1}. El estuario del Guadalquivir también se comporta como una fuente de CO_2 a la atmósfera durante todo el año, con un flujo medio de 85.2 mmol m^{-2} d^{-1}. La información disponible permite considerar que otros procesos biogeoquímicos, tales como la respiración de la materia orgánica y la disolución de carbonato cálcico en el tramo final del río, explican la conservatividad aparente del sistema a pesar de estos elevados flujos de CO_2 a la atmósfera.

En el Río San Pedro existe una marcado gradiente longitudinal de carbono inorgánico, con valores próximos a 3040 μmol kg^{-1} en su parte interna, próxima a los efluentes de una piscifactoría con un régimen de producción intensivo de *Sparus aurata*. La dinámica del carbono inorgánico en este sistema es consecuencia del grado de mezcla del agua del bahía de Cádiz con las aguas internas enriquecidas por los procesos de mineralización de la materia orgánica (piensos y heces fundamentalmente), tanto en el interior de la piscifactoría como en el caño. La linealidad de las variaciones de carbono inorgánico con la salinidad muestra que las mareas son el principal mecanismo de transporte, responsable de una exportación neta de 2.4 **10^6 mol C d^{-1}** mol C d^{-1} a la bahía de Cádiz.

Los valores de la concentración de carbono inorgánico y pCO_2 presentan importantes variaciones diarias en el Río San Pedro acopladas a los ciclos de marea: los valores máximos corresponden a situaciones de bajamar, con una mayor influencia de los vertidos de la piscifactoría y de la mineralización en el interior del caño, y valores mínimos en pleamar, asociados a una mayor proporción de aguas exteriores que provienen de la bahía de Cádiz. La amplitud de estas variaciones de carbono inorgánico y pCO_2 se encuentra modulada por el ciclo quincenal de mareas vivas/muertas, de forma que las mayores diferencias se observan en mareas de un elevado coeficiente. No obstante, los valores de pCO_2 experimentan un aumento en el interior del caño durante mareas muertas, consecuencia de la menor dilución del efluente de la piscifactoría y del mayor tiempo de residencia en el sistema, que genera una mayor influencia de los procesos degradativos de la materia orgánica. A una escala temporal mayor, se produce una intensa variación estacional con valores de pCO_2 en bajamar superiores a 3760 μatm durante los meses de verano, y que es consecuencia de la intensificación de los procesos metabólicos con la temperatura y de la actividad acuícola. El Río San Pedro presenta una sobresaturación de CO_2 durante todo el año, con un flujo medio a la atmósfera de 46.2 mmol m^{-2} d^{-1}.

La dinámica del carbono inorgánico en el Estrecho de Gibraltar es consecuencia de la complejidad hidrodinámica que caracteriza este sistema. La masa de agua mediterránea, situada en la capa más profunda, posee mayores AOU y concentraciones de carbono inorgánico, con valores medios de 47.74 µmol kg^{-1} y 2238.5 µmol kg^{-1} respectivamente. Para el agua superficial atlántica, lo valores medios observados son 19.27 µmol kg^{-1} para la AOU y 2016.2 µmol kg^{-1} para el carbono inorgánico. La distribución vertical de estos parámetros presenta una alta variabilidad mareal, que dependen en gran medida tanto de las fluctuaciones verticales de la posición de la interfase de separación entre las aguas mediterránea y atlántica como de la intensidad de los procesos de mezcla, relacionada con los ciclos de mareas vivas y muertas.

A pesar de que existe un flujo neto de agua del Atlántico al Mediterráneo, las mayores concentraciones en el agua mediterránea profunda provoca un transporte neto del orden de 4 10^9 mol C d^{-1} hacia el Atlántico. Este balance depende en última medida de los valores utilizados para el flujo neto de agua entre las dos cuencas, así como a la profundidad a la que se defina la interfase de separación entre las dos masas de agua. Dada la intensidad de los procesos de transporte en la zona, las variaciones estacionales responden principalmente al efecto de la temperatura sobre la solubilidad del CO_2. Los flujos con la atmósfera varían a lo largo del año, con valores extremos que corresponden a captaciones de -1.9 mmol m^{-2} d^{-1} en marzo y emisiones de 1.9 mmol m^{-2} d^{-1} en septiembre. El flujo medio observado a lo largo del año es de -0.76 mmol m^{-2} d^{-1}, indicando que el Estrecho de Gibraltar actúa como un sumidero moderado de CO_2.

Bibliografía

Baschek, B., Send, U., García-Lafuente, J., Candela, J., 2001. Transport estimates in the Strait of Gibraltar with a tidal inverse model. Journal of Geophysical Research 106 (C12), 31033–31044.

Macías, D., 2006. Efectos biológicos de la mezcla interfacial y de los procesos hidrodinámicos mesoescalares en el Estrecho de Gibraltar. Tesis Doctoral. Universidad de Cádiz.

Macías, D. ,Martín, A.P., García-Lafuente , J., García , A. Yool , C.M., Bruno, M., Vázquez-Escobar , A., Izquierdo, A. Sein , D.V., Echevarría, F, 2007. Analysis of mixing and biogeochemical effects induced by tides on the Atlantic–Mediterranean flow in the Strait of Gibraltar through a physical–biological coupled model. Progress in Oceanography 74: 252-272.

Márquez, C., Narváez, A., Pérez, M. C. y Ruiz, J. (1996) In Estudios para la Ordenación, Planificación y Gestión Integradas en las Zonas Húmedas de la Bahía de Cádiz, ed. J. M. Barragán, pp. 303-323. Oikos-tau, Barcelona.

Ponce, R., Ortega., T., de la Paz, M., Gómez-Parra y Forja, J.M., 2003 Dinámica del Carbono Inorgánico y sales nutrientes en el estuario del río Guadalquivir.2003. En: Contaminación por metales pesados en el estuario del Guadalquivir. Eds: Servicio de publicaciones de la Universidad de Cádiz.pp: 127-163.

Tovar, A., Moreno, C., Manuel-Vez, M.P. y García-Vargas, M., 2000a. Environmental impacts of intensive aquaculture in marine waters. Water Res. 34, 334–342.

Wanninnkhof, R., 1992. Relationship between wind speed and gas exchange over the ocean. J. Geophys. Res., 97 (C5): 7373-7382.